T.R.
GEBZE TECHNICAL UNIVERSITY
GRADUATE SCHOOL

THE NETWORK BETWEEN POLYP, LON PROTEASE AND SECONDARY METABOLITE PRODUCTION IN STREPTOMYCES COELICOLOR A3(2)

NAGİHAN GENEL

A THESIS OF DOCTORATE
DEPARTMENT OF MOLECULAR BIOLOGY AND GENETICS

ADVISOR: PROF. DR. SEDEF TUNCA GEDİK

JANUARY 2025

T.R.

GEBZE TECHNICAL UNIVERSITY

GRADUATE SCHOOL

THE NETWORK BETWEEN POLYP, LON PROTEASE AND SECONDARY METABOLITE PRODUCTION IN STREPTOMYCES COELICOLOR A3(2)

NAGİHAN GENEL

A THESIS OF DOCTORATE

DEPARTMENT OF MOLECULAR BIOLOGY AND GENETICS

ADVISOR: PROF. DR. SEDEF TUNCA GEDİK

JANUARY 2025

T.C.
GEBZE TEKNİK ÜNİVERSİTESİ
LİSANSÜSTÜ EĞİTİM ENSTİTÜSÜ

STREPTOMYCES COELİCOLOR A3(2)'DE POLİP, LON PROTEAZ VE SEKONDER METABOLİT ÜRETİMİ ARASINDAKİ İLİŞKİ

NAGİHAN GENEL

DOKTORA TEZİ
MOLEKÜLER BİYOLOJİ VE GENETİK
ANABİLİM DALI

DANIŞMAN: PROF. DR. SEDEF TUNCA GEDİK

OCAK 2025

DOCTORATE JURY APPROVAL FORM

A thesis submitted by Nagihan GENEL, defended on 22 / 01 / 2025 before the jury formed with the 13 / 01 / 2025 date and 2025 / 05 numbered decision of the GTU Graduate Administration Board, has been accepted as a DOCTORATE thesis in the Department of Department of Molecular Bialogy and Genetics.

JURY

MEMBER
(THESIS ADVISOR) : Prof. Dr. Sedef TUNCA GEDİK

MEMBER : Prof. Dr. Nuri ÖZTÜRK

MEMBER : Prof. Dr. Tunahan ÇAKIR

MEMBER : Prof. Dr. Ayten YAZGAN KARATAŞ

MEMBER : Prof. Dr. Gamze TORUN KÖSE

APPROVAL

Gebze Technical University Graduate Administration Board

…..…/…..…/..…… date and ……/…….. numbered decision.

SIGNATURE/SEAL

First of all, I would like to express my profound gratitude to my esteemed supervisor, Sedef TUNCA GEDLIK, who has played a pivotal role in introducing me to the scientific community and facilitating my involvement in this valuable process. I would also like to acknowledge the unwavering support and assistance provided to me by my family members throughout this journey. In addition, I would like to express my deepest gratitude to the STG laboratory team, my colleagues in the Gebze Technical University Molecular Biology department, and my dear housemate Callie, who provided me with invaluable support and solace during my academic struggles.

ABSTRACT

The bacterial stringent response is a global regulatory process that can be triggered by amino acid deprivation or energy limitation. Guanosine tetra- and penta-phosphates (ppGpp and pppGpp), also known as alarmones, are the effector molecules of the stringent response. The RelA is primarily responsible for producing these alarmones, with some contribution from the SpoT. An increase in alarmone concentration results in the accumulation of polyP, which is an inorganic phosphate polymer synthesized by polyphosphate kinase (PPK). In *Escherichia coli*, this polymer forms a complex with the ATP-dependent Lon protease under stringent conditions. The complex is involved in the degradation of ribosomal proteins to obtain the amino acid pool.

Previous studies have shown that overexpression of the *lon* gene and deletion of the *ppk* gene significantly increased actinorhodin (ACT) production in *Streptomyces coelicolor* A3(2) (SCO). In this study, we simulated a recombinant SCOΔ*ppk-lon* cell expressing the extra *lon* gene in *ppk*-deficient strain using a modified *in silico* model, ecSco-GEM. The results have confirmed the negative effect of PPK on actinorhodin production. The ensemble modelling results have indicated that NADH dehydrogenase/complex-I, Beta-ketoacyl-[acyl-carrier-protein] synthase III, glycine cleavage system and superoxide dismutase are enzymes that have a positive role in ACT production.

The *in silico* results were validated by *in vitro* experiments. *lon* gene was integrated into the genome of SCOΔ*ppk* strain and antibiotic production was determined. It is important to note that overexpression of *lon* converted the wild-type strain into a hyper-antibiotic producer, but this effect was not observed in the SCOΔ*ppk* strain, demonstrating the significance of PPK in cellular metabolism. The accuracy of the ensemble modelling results was verified by measuring superoxide dismutase activity. This study suggests that GEMs can be a reliable starting point for *in vitro* studies of *Streptomyces*.

Keywords: *Streptomyces coelicolor* A3(2); ATP-dependent Lon protease; enzymatically constrained model; actinorhodin production; ensemble modelling

ÖZET

Sınırlandırılmış (stringent) cevap, amino asit açığı veya enerji eksikliği ile tetiklenebilen global bir düzenleyici süreçtir. Alarmonlar olarak da bilinen guanozin tetra- ve penta-fosfatlar (ppGpp and pppGpp), sınırlandırılmış cevabın efektör molekülleridir. RelA ve SpoT proteinleri bu alarmonların üretilmesinden birincil olarak sorumludur. Alarmon konsantrasyonundaki artış, polifosfat kinaz (PPK) enzimi tarafından sentezlenen inorganik bir fosfat polimeri olan polifosfatın (poliP) birikmesine neden olur. *Escherichia coli*'de sınırlandırılmış cevap koşullarında bu polimer, ATP'ye bağlı Lon proteaz ile bir kompleks oluşturur. Bu kompleks, eksik olan amino asit havuzunu doldurmak için var olan ribozomal proteinlerin parçalanmasında rol oynar.

Önceki çalışmalar, *lon* geninin aşırı ekspresyonunun ve *ppk* geninin silinmesinin *Streptomyces coelicolor* A3(2)'de (SCO) aktinorhodin (ACT) üretimini önemli ölçüde artırdığını göstermiştir. Bu çalışmada, modifiye edilmiş bir *in silico* model olan ecSco-GEM kullanarak *ppk* geni silinmiş olan hücrelerde *lon* genini fazla ifade eden rekombinant SCOΔ*ppk-lon* hücresi simüle edilmiş ve PPK'nın aktinorhodin üretimi üzerindeki olumsuz etkisi doğrulamıştır. Ensemble modelleme sonuçları ise, NADH dehidrojenaz/kompleks-I, Beta-ketoasil-[açil-taşıyıcı-protein] sentaz III, glisin parçalama sistemi ve süperoksit dismutazın ACT üretiminde olumlu rolü olan enzimler olduğunu göstermiştir.

In silico sonuçlar *in vitro* deneylerle doğrulanmıştır. *lon* geni SCOΔ*ppk* suşunun genomuna entegre edilmiş ve antibiyotik üretimi ölçülmüştür. İlginç bir şekilde *lon*'un aşırı ekspresyonu vahşi tip suşu hiper-antibiyotik üreticisine dönüştürürken, bu etki SCOΔ*ppk* suşunda gözlenmemiştir. Bu da PPK'nın hücresel metabolizmadaki önemini göstermektedir. Ensemble modelleme sonuçlarının doğruluğu ise süperoksit dismutaz aktivitesi ölçümüyle gerçekleştirilmiştir. Bu çalışma, GEM'lerin *Streptomyces'*in *in vitro* çalışmaları için güvenilir bir başlangıç noktası olabileceğini göstermektedir.

Anahtar Kelimeler: *Streptomyces coelicolor* A3(2); ATP bağımlı Lon proteaz; enzimatik olarak kısıtlanmış model; aktinorhodin üretimi; ensemble modelleme

ACKNOWLEDGEMENTS

I would like to express our gratitude to Prof. Rainer Breitling and Dr. Francesco Del Carratore for their invaluable support during the ensemble modelling.
I would like to express our sincere gratitude to Prof. Tunahan ÇAKIR and Prof. Nuri ÖZTÜRK for their invaluable critical feedback and suggestions provided during the thesis process. This research was supported by a research grant (BAP-2023-A-102-01) from Gebze Technical University in Turkey.

TABLE OF CONTENTS

LIST OF SYMBOLS AND ABBREVIATIONS

ACT	: Actinorhodin
ACP	: Acyl Carrier Protein
APR	: Apramycin
ATP	: Adenosine Triphosphate
COBRA	: Constraint-based Reconstruction and Analysis
ecGEM	: Enzymaically Constrained Genome Scale Model
ETC	: Electron Transport Chain
ETS	: Electron Transport System
FBA	: Flux Balance Analysis
GEM	: Genome Scale Metabolic Model
GPR	: Gene Protein Reaction
KN	: Kanamycin
KS	: Ketosynthase
LB	: Luria Broth
NA	: Nalidixic Acid
NOS	: Reactive Nitrogen Species
PCD	: Programmed Cell Death
PCR	: Polymerase Chain Reaction
PKS	: Polyketide Synthase Pathway
PLS	: Partial Least Squares Regression
PolyP	: Polyphosphate
PpGpp	: Guanosine Tetraphosphate
PPK	: Polyphosphate kinase
PppGpp	: Guanosine Pentaphosphate
PPX	: Exopolyphosphatase
RED	: Undecylprodigiosin
ROS	: Reactive Oxygen Species
SCO	: *Streptomyces coelicolor* A3(2)
SEM	: Scanning Electron Microscope
SOD	: Superoxide Dismutase
STR	: Streptomycin
TE	: Thioesterase
Δ	: Delta (deficiency)

LIST OF FIGURES

LIST OF TABLES

1. INTRODUCTION

Streptomycetes are gram-positive, filamentous bacteria that live in soil and belong to the large family of *Actinobacteria.* They are the main producers of bioactive molecules with a wide range of applications in the industrial and medical fields. Naturally, *Actinomycetes* produce secondary metabolites on a small scale, which cannot meet industrial and medical demands. Therefore, new strategies must be developed to obtain higher quality strains that produce the desired molecules in large quantities. *Streptomyces coelicolor* is a *de facto* model organism for the production of secondary metabolites, especially antibiotics. The production of secondary metabolites depends on environmental factors such as pH, temperature, and nutrient availability and type. Stringent response is a stress defence mechanism activated in response to nutrient and energy deprivation and was first observed in *Escherichia coli* during amino acid starvation. The stringent response is stimulated by alarmones [(p)ppGpp] and promotes survival by modulating transcription. During the stringent response, the synthesis of transfer RNA (tRNA) and ribosomal RNA (rRNA) is halted, protein degradation is initiated, and the production of amino acids are stimulated [Traxler et al., 2008].

In *Streptomyces spp.* the production of secondary metabolites starts at the end of the exponential phase and continues during the stationary phase of the developmental cycle. The depletion of nutrients in the surrounding environment and the subsequent deceleration of cellular growth serve as the impetus for the production of secondary metabolites [Bibb, 2005]. Nevertheless, the precise relationship between stringent response and secondary metabolite production in *Streptomyces spp*. remains to be fully elucidated.

In *E. coli*, the accumulation of inorganic polyphosphate (polyP) molecules within the cell is triggered by the inhibition of the exopolyphosphatase (PPX) enzyme which is responsible from the degradion of polyP. Than polyP molecules and the ATP-dependent Lon protease forms a complex, which targets free ribosomal proteins [Kuroda, 2006]. In our preceding studies, our laboratory focused on the PPK protein, which is responsible for polyP synthesis in the cell. We have reported that *ppk*-deficient *S. coelicolor* A3(2) (SCO-Δ*ppk*) cells produce 5 times more actinorhodin

than the wild type [Yalim Camci et al., 2012]. Furthermore, the effect of ATP-dependent Lon protease on secondary metabolite production was investigated by integrating an additional copy of the *lon* gene into the *S. coelicolor* A3(2) genome. The results demonstrated that the recombinant strain (SCO-pRA*lon*) exhibited significantly enhanced production of actinorhodin and undecylprodigiosin, specifically 34 and 9 times higher, respectively, compared to the wild-type strain.

In this study, the relationship between ATP-dependent Lon protease, polyP and secondary metabolite production in *Streptomyces coelicolor* A3(2) was investigated using a combination of computational and molecular genetic approaches.

2. PURPOSE OF THE STUDY

Lon protease, which plays very fundamental roles in cellular metabolism, is a conserved enzyme in both eukaryotic and prokaryotic cells. The relationship between ATP-dependent Lon protease and polyP was first demonstrated in *E. coli* by Kuroda et al. (2006). Under stringent response conditions, the polyP accumulates inside the cell and forms a complex with Lon protease, helping this enzyme to degrade ribosomal proteins and thus contributing to the acquisition of amino acids needed to synthesize the proteins required under these hard conditions.

Studies conducted in our laboratory on the ATP-dependent lon protease and PPK of *S. coelicolor* have shown that PPK has a negative effect on antibiotic production, while lon protease has the opposite positive effect. The aim of the present study is to investigate the relationship between ATP-dependent Lon protease, polyP and secondary metabolite production in *Streptomyces coelicolor* A3(2) by using a combination of *in silico* and *in vitro* approaches. This work has the potential to provide strategies for the high-scale production of secondary metabolites of industrial importance.

3. BACTERIAL ATP-DEPENDENT PROTEASES

Bacterial ATP-dependent proteases are responsible for the lysis of intracellular proteins under certain conditions. ATP-dependent proteases are classified as members of a vast family of proteins known as AAA+ proteases. In *E. coli*, there are five defined AAA+ proteases, ClpAP, HslUV, ClpXP, FtsH, 26S proteasome and Lon. AAA+ proteases have a barrel-like shape (Fig. 3.1) and consist of two domains: ATPase and protease. ClpAP, HslUV and ClpXP comprise separate ATPase and peptidase domains, whereas FtsH and Lon contain both domains in a single polypeptide [Gur et al., 2013]Proteolysis is initiated by the protease's recognition of the substrate. The ATPase unfolds the substrate and transfers it to the protease cavity (Fig. 3.1). Recognition and degradation are ATP-independent, but unfolding and translocation of the target peptide are ATP-dependent processes.

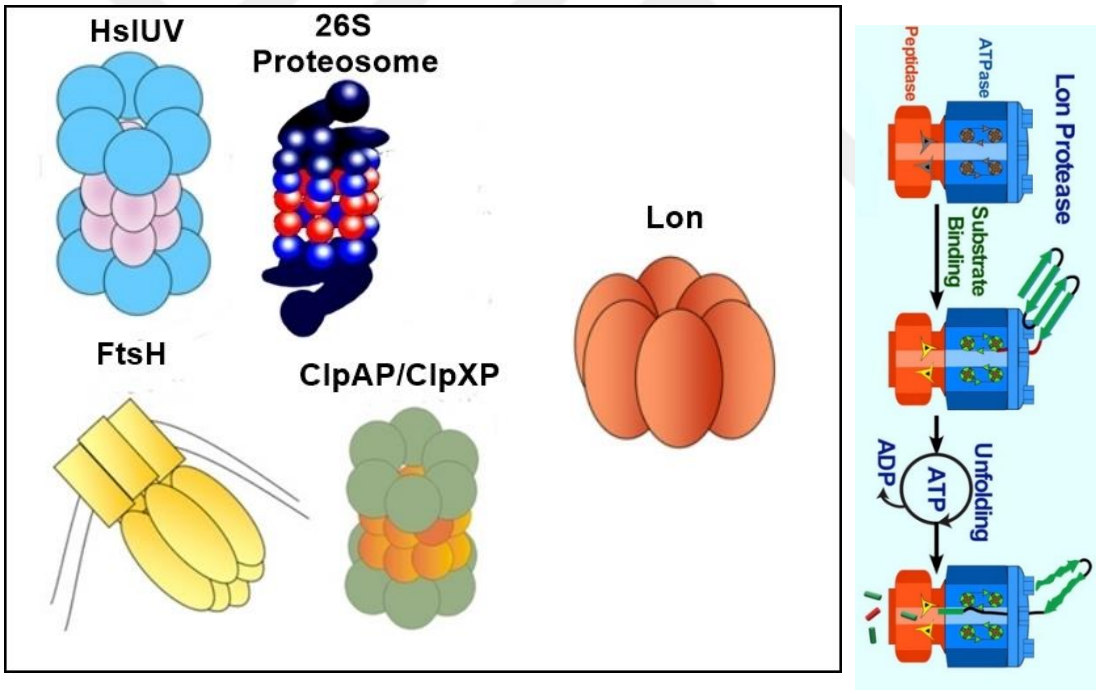

Figure 3.1: AAA+ proteases (left) and schematic illustration of AAA+ protease activity (right).

The ATP-dependent Lon protease (Endopeptidase La) was first identified in *E. coli* in 1981 [C. H. Chung & Goldberg, 1981]. It acts as a global regulator protein for both eukaryotic and prokaryotic cells, controlling vital functions in cellular metabolism, including cell division, DNA replication and repair [Burby & Simmons, 2020,Jonas et

al., 2013], DNA methylation [Calmann & Marinus, 2003], the SOS response [Breidenstein et al., 2012], virulence and motility [Clemmer & Rather, 2008], sporulation [Serrano et al., 2001a], secondary metabolite production [Demir et al., 2019], heat shock response [Omnus et al., 2023], the toxin-antitoxin system and bacterial persistence [Maisonneuve & Gerdes, 2014], and other stress responses [Serrano et al., 2001b].

The ATP-dependent Lon protease consists of homo-hexamers and three subunits: N-terminal, ATPase, and C-terminal. The ATPase unit is involved in cellular activities and the C-terminal consists of a peptidase domain, a unique serine-lysine hydrolase. The Lon protease family comprises three major subfamilies: LonA, LonB and LonC. Lon A is found in archaea, bacteria and eukaryotes. It is involved in protein quality control and is therefore important for cell homeostasis. Lon B is mainly found in bacteria and is structurally similar to LonA, but differs in its ATPase and proteolytic domains. Like LonA, LonB is involved in protein quality control. The LonC subfamily is a group of Lon-like proteases. It is less studied than LonA and LonB. Of all the subfamilies, LonA is the well-studied protease subfamily. The cryo-EM structure of *E. coli* Lon protease (LonA) was determined by Botos et al. [Botos et al., 2019] (Fig. 3.2).

The ATP-dependent Lon protease of *S. coelicolor* was identified in the 2000s [Bentley et al., 2002]. It is a member of the LonA protease family (Fig. 3.3). The 3D structure has not yet been experimentally characterised. For now, the 3D simulation of Alphafold PDB is available (Fig. 3.3).

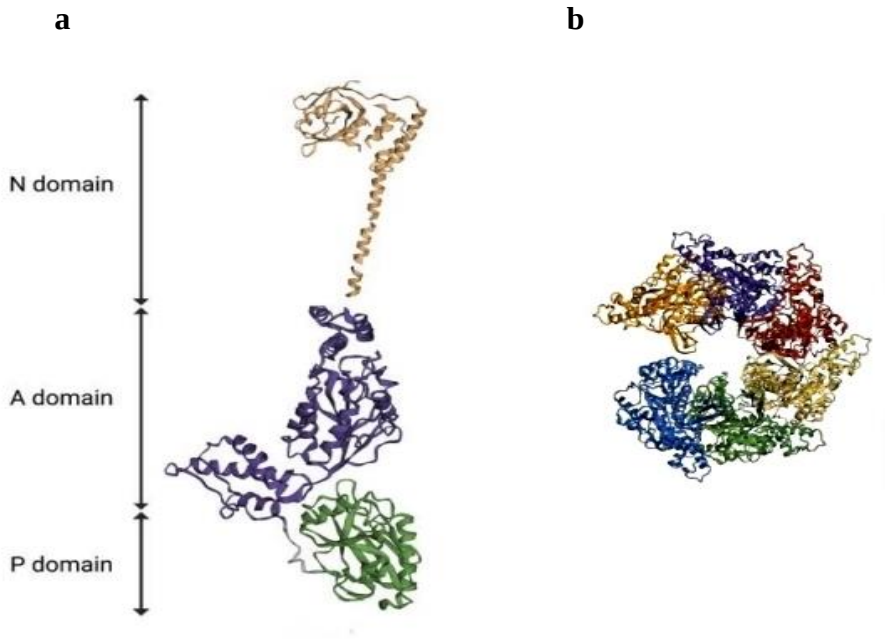

Figure 3.2: Three dimensioanal structure of *E. coli* LonA. 3D model of single protomer (a) and Cryo-EM structure of *E. coli* LonA (PDB:6U5Z) (b).N domain: N terminal, A domain: ATPase, P domain: Protease.

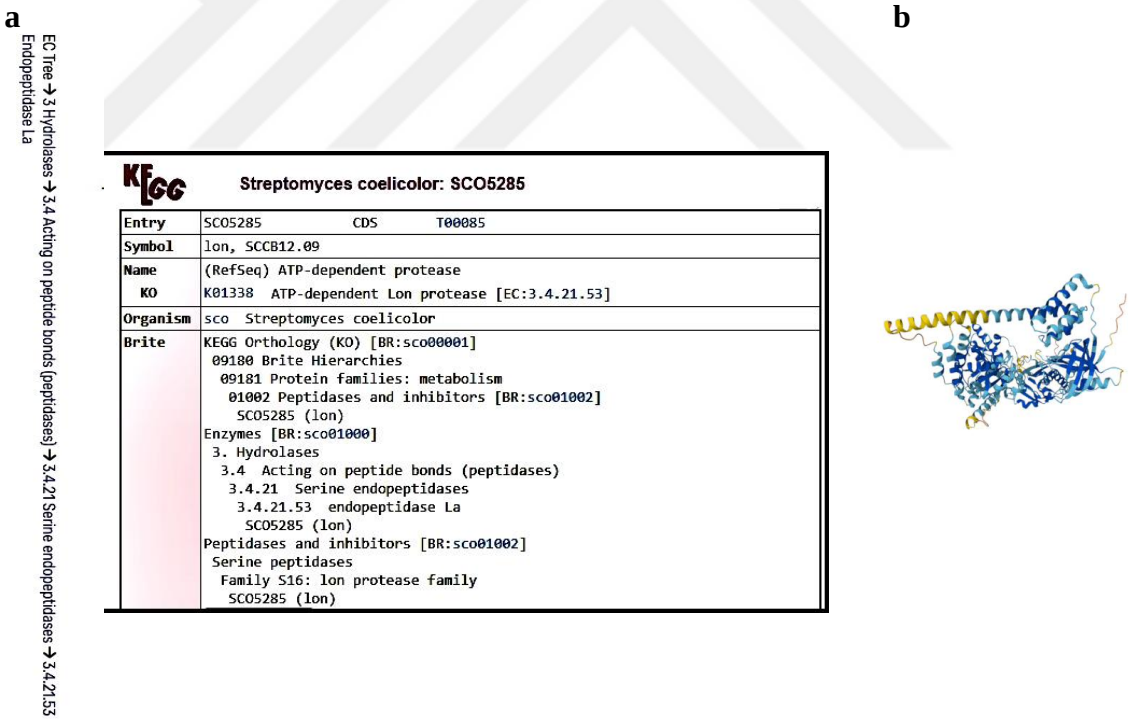

Figure 3.3: *S. coelicolor* ATP-dependent Lon protease. EC tree (Brenda database) and general information of *S. coelicolor* ATP-dependent Lon protease (KEGG database) (a). The 3D illustration of *S. coelicolor* ATP-dependent Lon protease (Alphafold PBD accession: AF-Q9EVK2-F1-v4) (b).

4. INORGANIC POLYPHOSPHATE

Inorganic polyphosphates (polyP) are linear chains comprising ten to hundreds of orthophosphate (Pi) residues linked by high-energy phosphoanhydride bonds (Fig. 4.1). PolyP is universally present in bacteria, protists, archaea, algae, fungi, protists, insects, mammals, and plants (Fig. 4.2). Inorganic PolyP play a pivotal role in cellular maintenance, functioning as a phosphate reserve, integrating into cell structures [Reusch, 1989], serving as an alternative to ATP [Kornberg et al., 1999], Metin girmek için buraya tıklayın veya dokunun.chelating metal ions [Andreeva et al., 2013, 2014], and influencing motility and pathogen virulence [Ogawa et al., 2000; Rashid et al., 2000].

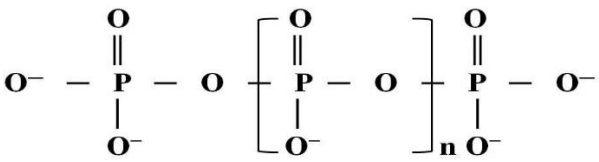

Figure 4.1: Linear inorganic polyphosphate chain.

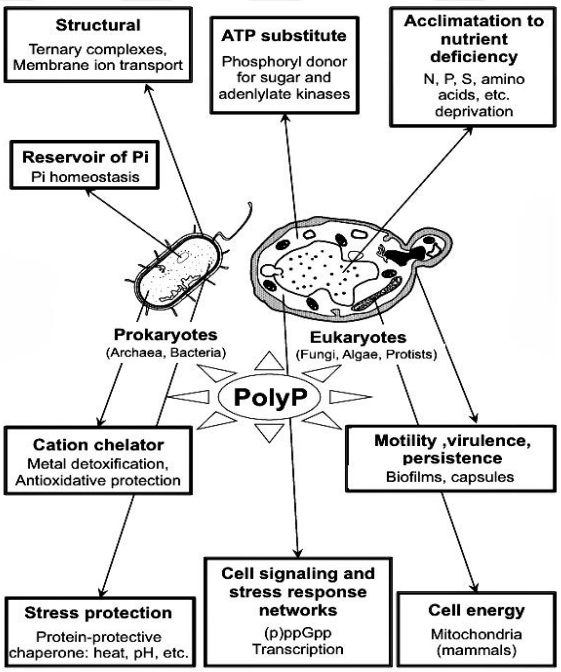

Figure 4.2: PolyP roles in prokaryotic and eukaryotic cells.

4.1. PolyP Cycle and Regulation

Two distinct polyphosphate kinases, PPK1 and PPK2, have been identified in bacteria as the primary enzymes responsible for synthesising inorganic polyP. PPK1 is primarily responsible for synthesising polyphosphate (polyP) from ATP [Barreiro & Martínez-Castro, 2019]. In contrast, PPK2 displays a high degree of versatility in its ability to utilise both GTP and ATP for the synthesis of polyP, and it exhibits a particular proficiency in the hydrolysis of polyP, whereby it generates nucleotide triphosphates (Zhang et al., 2002). The hydrolysis of polyphosphate to inorganic phosphate is achieved by the action of exopolyphosphatase (PPX) enzyme [Akiyama et al., 1993].

In *Escherichia coli*, starvation stress triggers the synthesis of (p)ppGpp by RelA and SpoT [Rao et al., 1998]. This (p)ppGpp inhibits PPX without affecting PPK activity. Under the stringent conditions polyP accumulate inside the cell. PolyP synthesis relies on RpoN, RpoE, DksA, and PhoB transcription factors. However, none of these factors have been identified as activators of the *ppk* gene (Fig. 4.3). The precise functioning of this mechanism remains to be elucidated.

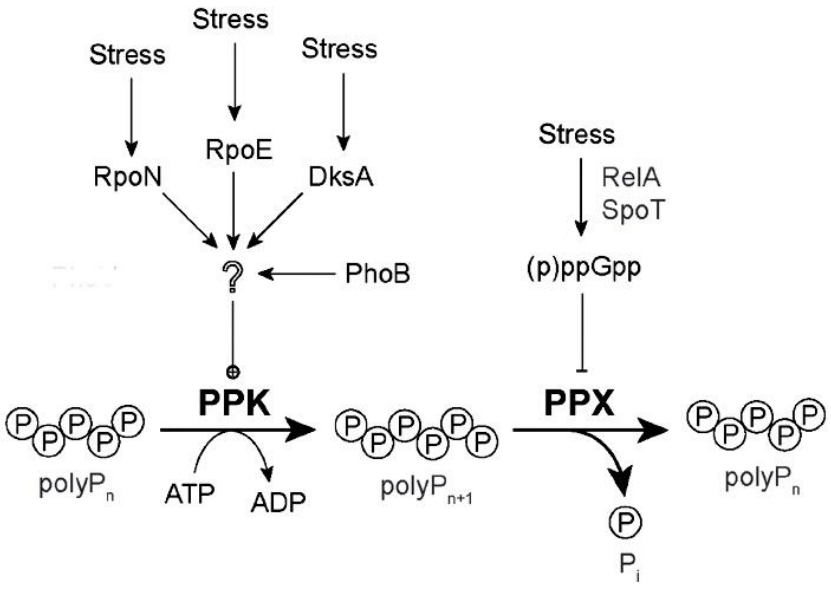

Figure 4.3: Regulation of polyP synthesis. The standard arrows indicate activation, and the dashed arrows indicate inhibition[Bowlin & Gray, 2021].

4.2. Cellular Role of PolyP and ATP-dependent Lon protease in Nutrient Limiting Conditions

In the early 2000s, a hypothesis was proposed suggesting that polyP promotes Lon protease, which in turn cleaves ribosomal proteins [Kuroda et al., 2001]. In 2006, Kuroda developed a model that addresses the stringent response mechanism in *E. coli*. According to Kuroda's model, the SpoT and RelA proteins synthesise (p)ppGpp molecules in an amino acid-starved cell. The accumulation of (p)ppGpp inhibits PPX activity and does not affect PPK. Consequently, polyP accumulation occurs within the cell. The polyP molecules form a complex with Lon protease, which subsequently degrades the ribosomal proteins, thereby releasing free amino acids into the cell (Fig. 4.4). Free amino acids play a crucial role in cellular maintenance, providing essential building blocks that facilitate cell' resilience in the face of stress.

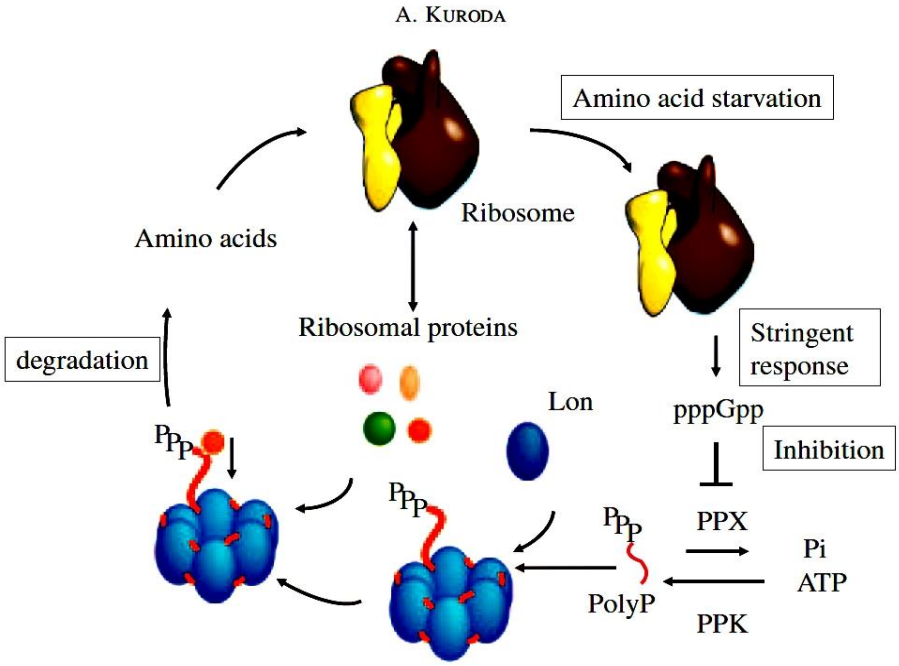

Figure 4.4: Kuroda's polyP-Lon complex model [Kuroda et al., 2001]**.**

5. STREPTOMYCES

The genus *Streptomyces* comprises gram-positive, soil-dwelling, spore-forming bacteria with a high GC content of the genome. *Streptomyces spp.* are filamentous bacteria that form a gridded mycelium. *Streptomyces spp.* the primary source of 70-80% of the antibiotics used in clinical and medical fields. They are considered a valuable source of diverse natural products. The natural products derived from *Streptomyce*s have the potential to be used in a variety of ways, including as antimicrobial, antiviral, immunosuppressive, antitumour, antidiabetic, insecticidal agents, and so forth [Nguyen et al., 2020,Sharma et al., 2021]. The secondary metabolites are encoded in biosynthetic gene clusters (BGCs), which are between 20 and 30. Most BGCs remain cryptic and have yet to be discovered, opening up a new realm of possibilities.

The *Streptomyces* family boasts remarkable species, including *Streptomyces coelicolor*, *Streptomyces avermitilis* and *Streptomyces griseus*. *S. coelicolor* is a model organism for the investigation of *Streptomyces* genetics. It has been the subject of extensive study due to its capacity to produce two distinct pigments: the blue-pigmented antibiotic actinorhodin (ACT) and the red-pigmented undecylprodigiosin (RED) (Gyun Kang et al., 1998). *S. avermitilis* is the natural source of avermectin, a powerful compound used to treat parasitic infections in humans and animals [Omura & Shiomi, 2007]. *Streptomyces griseus* is renowned for its capacity to produce streptomycin, the first antibiotic to be proven effective against tuberculosis[Newman et al., 2000,Wainwright, 1991].

5.1. Streptomyces Life Cycle

Streptomycetes' development is characterised by a high degree of sophistication, encompassing multicellular and mycelial growth and morphological differentiation. These processes are coordinated with various physiological mechanisms, demonstrating a complex and integrated development.

In a solid culture, the *Streptomyces* spore undergoes germination within a compartmented early substrate mycelium. Some of the early substrate mycelium cells undergo PCD (programmed cell death) and develop into multinucleated hyphae where

secondary metabolites are produced. Subsequently, the cells undergo differentiation, developing into aerial hyphae. Then, at the end of the cycle, the second PCD takes place, and the cells develop into mononucleated spores (Fig. 5.1) [Manteca & Yagüe, 2018].

In liquid culture, in the majority of species, the formation of aerial mycelia and sporulation does not occur. In contrast, hyphae differentiate into pellets and clumps. The central region of the pellet is populated by substrate mycelial cells that are undergoing programmed cell death (PCD). Secondary metabolite-producing cells are situated in the peripheral region of the pellet (Fig. 5.1) [Manteca & Yagüe, 2018].

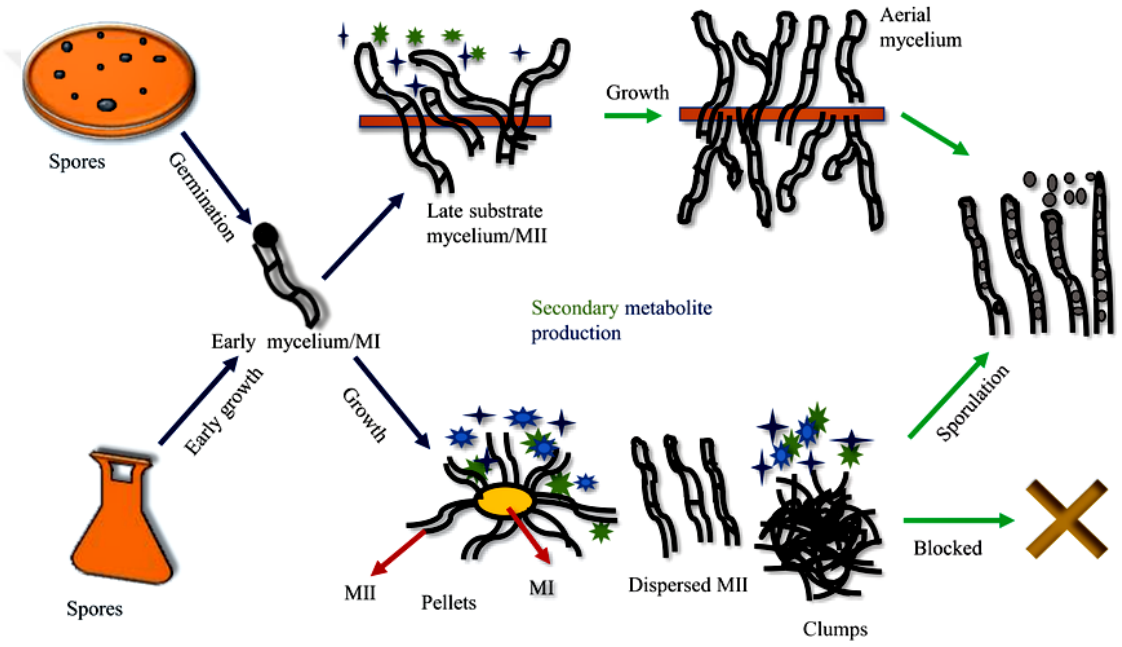

Figure 5.1: *Streptomyces* life cycle schema. Secondary metabolites are illustrated by blue/green symbols clustered around hyphae[Khushboo et al., 2022]**.**

5.2. Secondary Metabolite Production in *Streptomyces*

Microorganisms produce primary metabolites (Fig. 5.2a), essential for growth, during the log phase of development (Fig. 5.2b). It is well-established that microbial bioactive and complex molecules are produced in the late log or stationary phase of growth in secondary metabolite-producing microorganisms (Fig. 5.2b). Nevertheless, in *Streptomyces*, the production of secondary metabolites occurs during the late logarithmic, stationary, and even death phases [Harir et al., 2018a].

The primary and secondary metabolite pathways are interconnected by precursors and building blocks [Krysenko & Wohlleben, 2024a](Fig. 5.2c). As the organism transitions to the stationary phase, precursors and building blocks derived from primary metabolic pathways are redirected towards secondary metabolite production. Six distinct pathways are responsible for the production of secondary metabolites in *Streptomyces*: the shikimate pathway, peptide pathway, β-lactam synthase pathway, non-ribosomal synthase pathway, polyketide synthase pathway and hybrid synthase pathway (Fig. 5.3)[Harir et al., 2018b]. Actinorhodin is a type II polyketide, a product of the polyketide synthase pathway (PKS). The production of actinorhodin begins with malonyl-CoA, which is derived from central carbon metabolism (Fig. 5.3). Following a series of reactions catalysed by enzymes encoded by 22 genes (SCO5071-SCO5092) in the actinorhodin biosynthetic cluster, the actinorhodin is synthesised (Fig. 5.3).

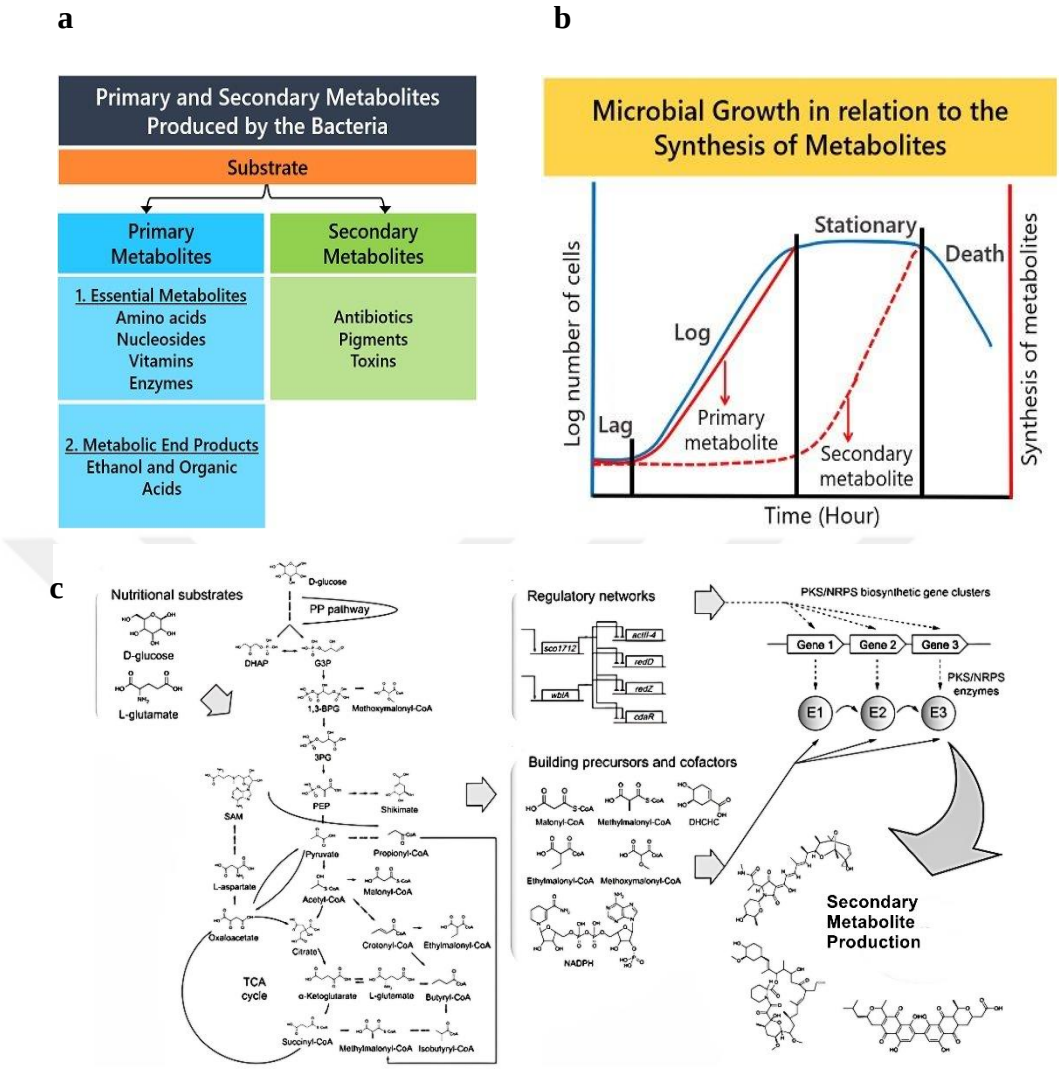

Figure 5.2: Microbial growth and primary and secondary metabolite production. Primary and secondary metabolites in microorganisms (a), microbial growth (b) and secondary metabolite production in *S. coelicolor* (c) were illustrated.

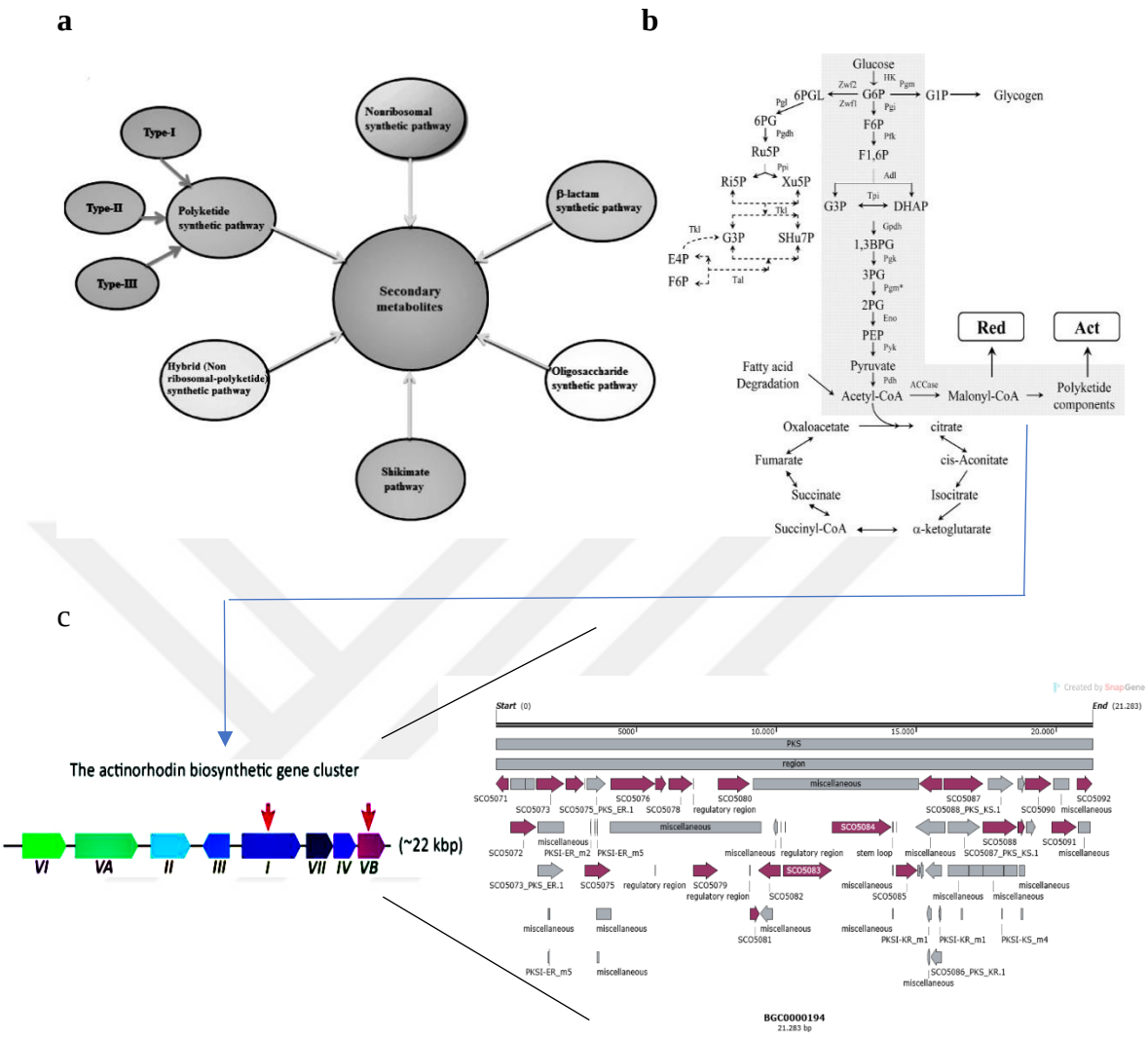

Figure 5.3: Six pathways in *Streptomyces* involving the secondary metabolite production pathway (a); the central carbon metabolism of actinorhodin production (b); the actinorhodin biosynthetic gene cluster, and the actinorhodin BGC representation from the MIBiG (Minimum Information about a Biosynthetic Gene cluster) database, referenced as BGC0000194 (https://mibig.secondarymetabolites.org/repository/BGC0000194.5/index.html#r1c1) (c), were shown. The BGC0000194 map was created using the SnapGene software tool.

5.2.1. The Chemistry of Actinorhodin Production

Type II polyketide synthases (PKSs) are primarily responsible for producing aromatic polyketides, which frequently encompass multiple benzene rings and other aromatic characteristics. The synthesis steps are as follows: The initial step involves the loading

of acetate onto acyl carrier protein (ACP), forming acyl-ACP (1). Subsequently, the ketosynthase (KS) domain catalyses the decarboxylative Claisen condensation reaction, whereby two-carbon units, typically malonyl-CoA, are added to the expanding polyketide chain (2). Subsequently, cyclisation occurs, an intramolecular process whereby the polyketide chain is catalysed by thioesterase (TE) to form aromatic rings (3). Modification is an optional step, whereby some polyketide chains can be altered by adding domains (4-1). Dimerisation is the formation of covalent or non-covalent bonding between two polyketide molecules (4-2). The dimerisation step is also optional, as is the modification step. Both steps are undertaken to enhance the activity of the end product. The termination process involves releasing the polyketide from the enzyme complex through hydrolysis (5). The synthesis of actinorhodin commences with the presence of one acetyl-CoA and seven malonyl-CoA molecules. Thereafter, the carbon skeleton undergoes a cyclisation process. This is followed by modifications and dimerisation (Fig. 5.4).

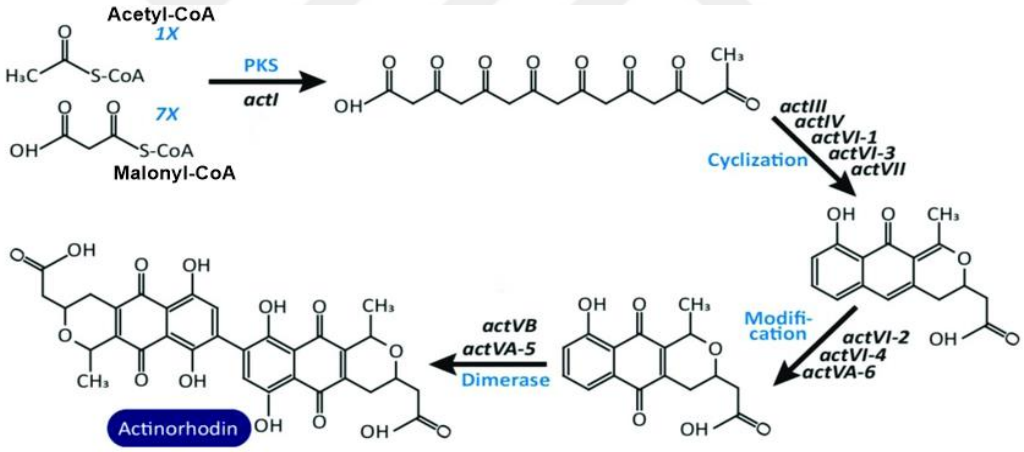

Figure 5.4: Enzymatic actinorhodin production process and the genes involved. The process starts with 1 acetyl-CoA and 7 malonyl-CoA. The carbon chain then goes in through cyclisation, modification and dimerization. The *act*-I, *act*-III, *act*-V, *act*-VI-1, *act*-VI-3, *act*-VII, *act*-VI-2, *act*-VI-4, *act*-VA 6, *act*-VB, *act*-VA-5 are the genes encoding enzymes involved in the process in the scheme.

5.2.2. Regulation of Actinorhodin Production

The production of secondary metabolites depends on numerous genetic and environmental factors, including pleiotropic or pathway-specific regulators [Xia et al.,

2020,Yan & Xia, 2024], nutrient depletion [Wentzel et al., 2012], oxygen availability, pH [Krysenko & Wohlleben, 2024b], signalling factors [Kong et al., 2019], and small regulator molecules (cAMP, purines, etc.) [Sivapragasam & Grove, 2019].

In *S. coelicolor* A3(2) cells, actinorhodin production is limited to the stationary phase because the actII-ORF4 promoter is only activated in this phase [Gramajo et al., 1993a]. The following factors achieve the transcriptional regulation of actinorhodin: ActII-1 and ActI-4, components of the actinorhodin BGC, stimulate actinorhodin synthesis [Malpartida & Hopwood, 1986]. Conversely, XdhR, a member of the TetR family of transcriptional regulators, inhibits the activity of both ActII-1 and ActI-4. [Fu et al., 2017].

The interconnection between primary and secondary metabolites has been a persistent focus in this thesis and the existing literature on the subject. While the genes mentioned above are of particular significance in the synthesis of secondary metabolites, particularly actinorhodin synthesis, the production of actinorhodin in *S. coelicolor* A3(2) is contingent upon the interplay of all factors entering and leaving the cell [Krysenko & Wohlleben, 2024c,Romero-Rodríguez et al., 2018]. To illustrate, genes implicated in the processing of glucose (GlcP, Pho-P, etc.), phosphate (phoS, phoP, etc.), and nitrogen (AfsQ1, AfsQ2, etc.) are, in a manner of speaking, indirectly accountable for the production of actinorhodin (Fig. 5.5). Moreover, numerous additional factors and genes remain to be identified. On the other hand, in contrast to the availability of nutrients, in the stationary phase, a reduction in the concentration of nutrients in the growth medium (carbon, phosphate, nitrogen) results in a decline in the growth rate, the onset of a stringent response and alterations in pH and oxygen availability. This results in the stimulation of actinorhodin production in *S. coelicolor* A3(2) [Gramajo et al., 1993b].

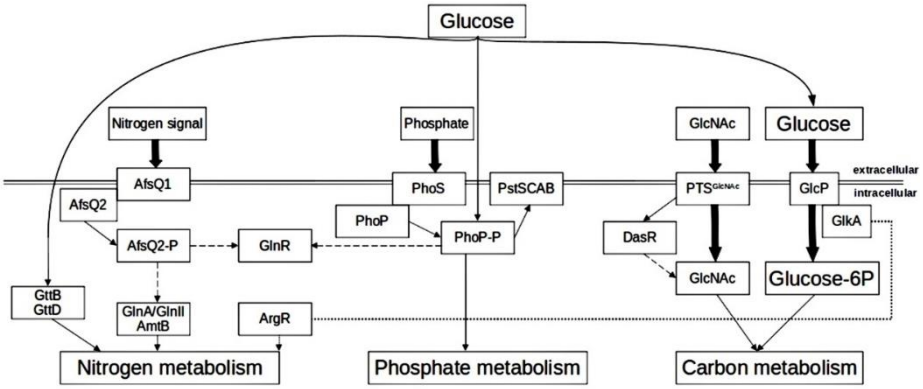

Figure 5.5: The schematic representation of phosphate, carbon and nitrogen metabolism of *S. coelicolor* A3(2). The bold arrows indicate negative effects, the dashed arrows indicate uncharacterised or indirect effects, and the remaining arrows indicate positive effects.

6. METABOLIC NETWORK MODELING

Metabolic Network Modeling is a computer-based approach developed to analyse and simulate metabolic networks within an organism. Metabolic network modelling has a wide range of applications. These include researching the underlying causes of disease and developing targeted medicines [Kell & Goodacre, 2014], increasing crop yields [Dersch et al., 2016], elucidating plant-microbe interactions [Kumar et al., 2016], and increasing the production of the desired metabolite through strain optimisation and metabolic engineering approaches [Shen et al., 2019].

6.1. Genome-Scale Metabolic Models

Genome-scale metabolic Models (GEMs), in simple terms, are computational representations of gene-protein-reaction (GPR) interactions in any organism. The use of these models is predicated upon their capacity to predict metabolic fluxes and thereby facilitate a more profound comprehension of the organism's metabolism under varying conditions. The fundamental component of GEMs is the stoichiometric matrix (S), which provides a quantitative framework for metabolic reactions (Fig. 6.1). The rows of the stoichiometric matrix show the metabolites and the columns show the reactions. The matrix entries are stoichiometric coefficients, showing the number of molecules consumed or produced.

The metabolic models for *S. coelicolor* are listed as follows: iIB711[Borodina et al., 2005], iMA789 [Alam et al., 2010] , iMK1208 [Kim et al., 2014], iKS1317 [Sulheim et al., 2019], Sco4 [Wang et al., 2018a],iAA1259 [Amara et al., 2018] , and Sco-GEM & ecSco-GEM [Sulheim et al., 2020].

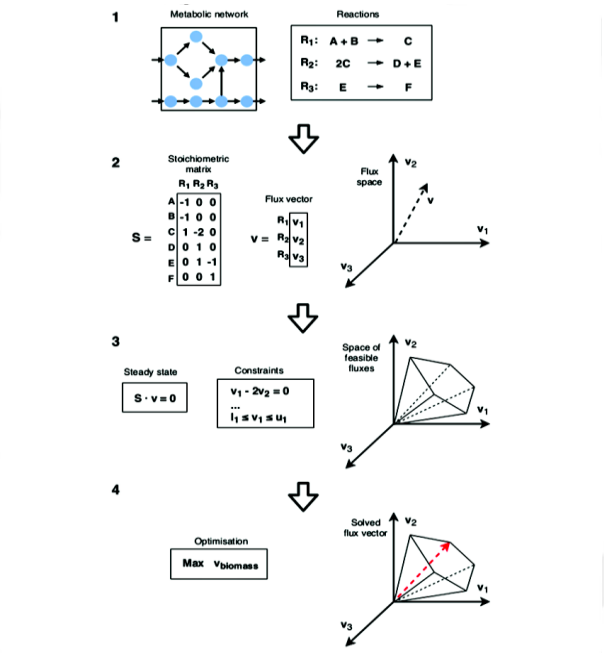

Figure 6.1: Genome-scale metabolic model construction & FBA.

6.2. Constraint-based Genome-Scale Metabolic Models

Constraint-based GEMs represent a distinct category of GEMs, whereby mathematical constraints are employed to simulate and analyse the metabolic network's behaviour under varying conditions. In constraint-based metabolic models, various data types can be incorporated as constraints to enhance the model's accuracy and relevance. These data types include nutrient availability, indicating what nutrients and substrates the organism can use. Reaction directionality is based on thermodynamics, and enzyme capacities like turnover rates (k_{cat}) and enzyme concentrations are also considered. Gene expression data from omics studies are used to estimate the levels of metabolic enzymes, while proteomics data reflects the actual levels of enzymes in the cell. Metabolomics data provides concentrations of metabolites that can set constraints on metabolite levels and physiological constraints are based on conditions such as pH, temperature, and oxygen levels. By incorporating these diverse constraints, the models can more accurately simulate and predict the metabolic network's behaviour under varying conditions.

Enzymatically constrained ec-GEMs are a currently developed metabolic model in which the enzyme constraints, such as concentrations and turnover rates (kcat), are

incorporated into the metabolic network (Fig. 6.2) . The development of the model has been driven by the necessity of providing more realistic predictions than standard GEMs. As a result, there is an increasing demand for these models, and their applications are expanding.

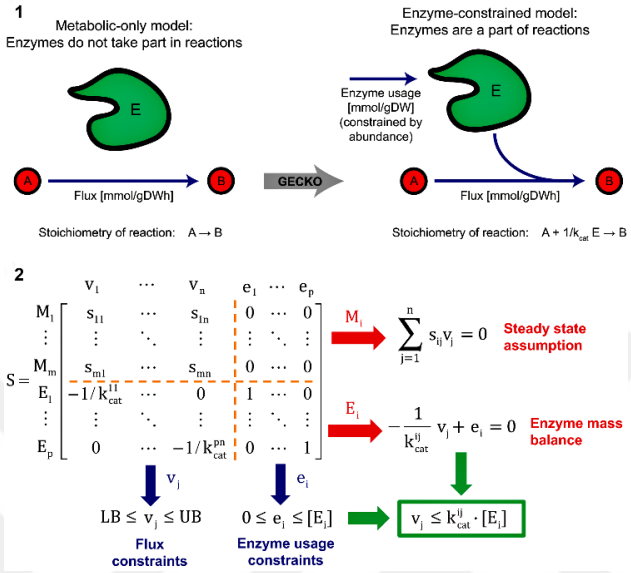

Figure 6.2: Enzymatically constrained GEM.

6.3. Flux Balance Analysis (FBA)

Flux balance analysis (FBA) is the most popular method for analysing constraint-based GEMs. In the FBA method, the S matrix is formulated as steady-state reactions and an objective function is assigned. This methodology is thus employed to calculate the optimum results (Fig. 6.1). The most popular toolbox for studying GEMs is the Constraint-based Reconstruction and Analysis (COBRA) Toolbox, which involves model reconstruction, optimisation, FBA, and omic data integration into the model.

6.3. Genome-scale Enzyme Constraint Kinetics (GECKO) Approach

Standard metabolic models are characterised by an emphasis on reaction stoichiometry and are further constrained by the availability of nutrients and reaction directionality.

However, these models generally do not account for the dynamics of enzyme kinetics and enzyme concentrations. The GECKO (Genome-scale Enzyme Constraint Kinetics) is a *de novo* technique used in metabolic modelling to improve genome-scale metabolic models (GEMs) by incorporating enzyme constraints. The method integrates kinetic parameters, such as kcat, and enzyme mass constraints. The incorporation of constraints derived from enzyme kinetics and omics data enables the GECKO approach to consider the availability and activity of enzymes within the cell. The method involves the allocation of enzymes from a total protein pool or the utilisation of measured protein levels from experimental data. These constraints allow GECKO models to enhance their predictive capabilities regarding metabolic flux distributions, thereby facilitating the understanding of phenomena such as overflow metabolism and metabolic switches. The GECKO approach is implemented as a toolbox, often in MATLAB, providing a range of tools for reconstructing, simulating, and analysing enzyme-constrained metabolic models.

6.3. Ensemble Modeling

Ensemble modelling is a recent approach used to improve the accuracy of GEMs, specifically ec-GEMs for this study. The methodology applied in this study for ensemble modelling is based on the protocol developed by Tsigkinopoulou et al. [Tsigkinopoulou et al., 2018]. This protocol involves randomly varying the k_{cat} values of the enzymes involved in the reactions of interest, thereby providing multiple possibilities for the optimum result.

In the context of the aforementioned information, the objective of this study was to investigate the relationship between ATP-dependent Lon protease, polyP and secondary metabolite production in *S. coelicolor* A3(2) from both a genetic and metabolic perspective, employing *in vitro* and *in silico* approaches.

7. MATERIAL AND METHODS

7.1. Materials

The complete list of strains, plasmids and other materials used in this study is provided in Table 7.1-Table 7.7.

Table 7.1: *Streptomyces* strains used in this study.

Streptomyces Strains	Characteristics	References
SCO	Prototropic wild-type	Hopwood, 1999
SCO-Δ*ppk*	*ppk* deficient *S. coelicolor* A3(2) strain	Yalim Camci et al., 2012
SCO + pRA*kn*	SCO carrying pRA*kn* plasmid	This study
SCO + pRA*knlon*	SCO carrying pRA*knlon* plasmid	This study
SCO-Δ*ppk*+ pRA*apr/strlon*	SCO-Δ*ppk* carrying pRA*apr/strlon* plasmid	This study
SCO-Δ*ppk*+ pRA*apr/str*	SCO-Δ*ppk* carrying pRA*apr/str* plasmid	This study
SCO + pRA*apr/str*	SCO carrying pRA*apr/str* plasmid	This study

Table 7.2: *E. coli* strains used in this study.

E. coli Strains	Characteristics	References
E. coli DH5α	F– *rec*A1, *end*A1, *gyr*A96, *thi*-1, *hsd*R17 (rK–, mK+), *sup*44, *rel*A1λ, (σ80 dL*ac*ZAM15), D (*lac*ZYA-*arg*F) U169	Hanahan, 1983
E. coli ET12567	*dam, dcm, hsdS, cat, tet*	Macneil et al., 1992
E. coli ET12567/pUZ8002	*dam, dcm, hsdS, cat, tet /tra, neo,* RP4	Kieser et al., 2000; Gust et al., 2002
E. coli DH5α + pRA^{apr}*lon*	*E. coli* DH5α carrying pRA^{apr}*lon* plasmid	Demir et al., 2019

Table 7.2: *E. coli* Strains used in this study (continued)

E. coli Strains	Characteristics	References
E. coli DH5α+pRA^{kn}	*E. coli* DH5α carrying pRA^{kn} plasmid	This study
E. coli ET12567(pUZ8002) + pRA^{kn}	*E. coli* ET12567(pUZ8002) carrying pRA^{kn} plasmid	This study
E. coli DH5α+pRA^{kn}*lon*	*E. coli* DH5α carrying pRA^{kn}*lon* plasmid	This study
E. coli ET12567(pUZ8002) + pRA^{kn}*lon*	*E. coli* ET12567(pUZ8002) carrying pRA^{kn}*lon* plasmid	This study
E. coli DH5α + pRA$^{apr/str}$*lon*	*E. coli* DH5α carrying pRA$^{apr/str}$*lon* plasmid	This study
E. coli ET12567(pUZ8002) + pRA$^{apr/str}$*lon*	*E. coli* ET12567(pUZ8002) carrying pRA$^{apr/str}$*lon* plasmid	This study
E. coli DH5α+pRA$^{apr/str}$	*E. coli* DH5α carrying pRA$^{apr/str}$ plasmid	This study
E. coli ET12567(pUZ8002) + pRA$^{apr/str}$	*E. coli* ET12567(pUZ8002) carrying pRA$^{apr/str}$ plasmid	This study

Table 7.3: Plasmids used in this study.

Plasmids	Characteristics	References
pRA^{apr} (5769 bp)	Integrative and conjugative vector derived from pSET152	Pérez-Redondo et al., 2010
pSK*desA*Kn	pSK plasmid carrying *kn* gene	Tunca et al., 2007
pIJ778*str* (4377 bp)	pIJ778 plasmid carring *aadA* gene	Gust et al., 2002
pUZ8002	*tra, neo, RP4*	Paget et al., 1999
pRA^{apr}*lon* (9166 bp)	pRA^{apr} carrying *lon* gene	Demir et al., 2019
pRA^{kn} (7289 bp)	pRA$^{apr/str}$ carrying *aad*A and *aac*(3)IV genes	This study
pRA^{kn}*lon* (10686 bp)	pRA$^{apr/str}$ carrying *lon* gene	This study

Table 7.3: Plasmids used in this study (continued).

Plasmids	Characteristics	References
pRA$^{apr/str}$*lon* (10577 bp)	pRA$^{apr/str}$ carrying *lon* gene	This study
pRA$^{apr/str}$ (7180 bp)	pRA$^{apr/str}$ carrying *aad*A and *aac*(3)IV genes	This study

Table 7.4: The list of restriction endonuclease and other enzymes used in this study.

Enzymes &	Buffers
*Nde*I (BioLabs)	CutSmart
*Spe*I (BioLabs)	CutSmart
*Eco*RI (Thermo Fisher) *Eco*RI (Thermo Fisher)	R Buffer Tango Buffer
*Eco*RV (Biolabs)	CutSmart
*Pst*I (Roche)	Sure/Cut Buffer
*Xba*I (Roche)	Sure/Cut Buffer
*Sph*I (Thermo Fisher)	Tango Buffer
*Hind*III (Thermo Fisher)	R Buffer
*Xho*I (Thermo Fisher)	R Buffer
NcoI (Thermo Fisher)	Tango Buffer
Lysozyme	-
RNase	-

Table 7.5: The list of antibiotics used in this study.

Antibiotics	Stock Solution	CAS Number
Apramycin Sulfate (Biosynth corbosynth)	50 mg/ml 0.5 g Apramycin Sulfate was dissolved in 10 ml dH_2O and filtered.	65710078
Ampicillin	50 mg/ml 0.5 g Ampicilin Sodium Salt was dissolved in 10 ml dH_2O and filtered.	69-52-3
Chloramphenicol (Sigma)	25 mg/ml 0.25 g Chloramphenicol Sulfate was dissolved in 10 ml 95 % Ethanol and filtered.	56-75-7
Nalidixic Acid (Sigma)	30 mg/ml 0.3 g Nalidixic Acid was dissolved in 10 ml 300 mM NaOH and filtered.	33705-8

Table 7.5: The list of antibiotics used in this study (continued).

Antibiotics	Stock Solution	CAS Number
Kanamycin (Vetaş-Kanovet) 250 mg/ml	50 mg kanamycin was diluted to 50 mg/ml and filtered.	-
Streptomycin Sulfate (Applichem)	50 mg/ml 0.5 g Streptomycin Sulfate was dissolved in 10 ml dH_2O and filtered.	3810-74-0

Table 7.6: The list of media used in this study.

<table>
<tr><th>Media</th><th>Contents</th></tr>
<tr><td>R2YE (1 L)</td><td>R2YE (800 ml)

103 g Sucrose, 0.25 g K_2SO_4, 10.12 g $MgCl_2$, 10 g Glucose, 5 g Yeast Extract, 0.1 g Casamino acids were dissolved in 800 ml dH_2O and autoclaved. 4.4 g agar was added into the 200 ml media for R2YE agar.

The following substances were added to the R2YE media in order before using it.
<table>
<tr><td>5 % KH_2PO_4</td><td>10 ml</td></tr>
<tr><td>3.68 % $CaCl_2.2H_2O$</td><td>80 ml</td></tr>
<tr><td>20 % L-Proline</td><td>15 ml</td></tr>
<tr><td>5.73 % TES Buffer (pH 7.2)</td><td>100 ml</td></tr>
<tr><td>1 N NaOH</td><td>5 ml</td></tr>
<tr><td>Trace Elements

-200 mg $ZnCl_2$
- 1000 mg $FeCl_3.6H_2O$
- 50 mg $CuCl_2.2H_2O$
- 50 mg $MnCl_2.4H_2O$
- 50 mg $Na_2B_4O_7.10H_2O$
-50 mg $(NH_4)_6Mo_7O_{24}.4H_2O$

https://actinobase.org/index.php/R2YE</td><td>2 ml</td></tr>
</table></td></tr>
<tr><td>2xYT (1 L)</td><td>16 g Peptone, 10 g Yeast Extract, 5 g NaCl
were dissolved in 1000 ml dH_2O and autoclaved.</td></tr>
</table>

Table 7.6: The list of media used in this study.

Media	Contents
LB (1 L)	10 g Peptone, 5 g Yeast Extract, 10 g NaCl were dissolved in 1000 ml dH_2O and autoclaved.
TSB (1 L)	30 g TSB was dissolved in 1000 ml dH_2O and autoclaved.
CRM (1L)	Glucose 10 g Sucrose 103 g $MgCl_2.6H_2O$ 0.12 g Trypticase Soy Broth 15 g Yeast Extract 5 g

Table 7.7: The list of chemicals used in this study.

Chemicals	Contents
20x SSC	3 M NaCl 0.3 M Sodium Citrate adjusted to pH 7.0
Depurination Solution	0.25 M HCl
Denaturation Solution	1.5 M NaCl 0.5 M NaOH
Neutralization Solution	1.5 M NaCl 0.05 M Tris-HCl pH 7.2 1 mM EDTA
Prehybridization Solution	5x SSC % 1 Blocking Reagent % 0.1 Sarcosine % 0.02 SDS
Probe Solution	Probe 20 ml Prehybridization Solution
Washing Buffer I	2x SSC % 0.1 SDS
Washing Buffer II	0.1x SSC % 0.1 SDS
Maleic Acid Solution	0.1 M Maleik asit 0.15 M NaCl adjusted to pH 7.5
Maleic Acid Washing Buffer	0.1 M Maleik asit 0.15 M NaCl % 0.3 Tween 20 adjusted to pH 7.5

Table 7.7: The list of chemicals used in this study.

Chemicals	Contents
10x Blocking Reagent	20 ml Maleic Acid Solution 2 g Blocking Reagent
Antibody Solution	1x Blocking Solution 2 µl Anti-Digoxigenin-AP Conjugate
Detection Buffer	0.1 M Tris-HCl 0.1 M NaCl adjusted to pH 9.5
Color Substrate Solution	10 ml Detection Buffer 200 µl NBT/BCIP
P (-) Buffer	Sucrose 103 g K_2SO_4 0.25 g $MgCl_2.6H_20$ 2.02 g Trace element solution 2 ml Distilled water to 800 ml
P (+) buffer	P (-) Buffer 80 ml KH_2PO_4 (0.5%) 1 ml $CaCl_2.2H_20$ (3.68%) 10 ml TES buffer (5.73%, adjusted to pH7.2) 10 ml
Electroporation Buffer	% 30 PEG 1000 % 10 Glycerol % 6.5 Sucrose
TfbI Solution (4 ^oC)	30 mM KAc 100 mM KCl 10 mM $CaCl_2$ 50 mM $MnCl_2$ % 15 Glycerol adjusted to pH 5.8 using acetic acid filtered with 0.22 µm filter
TfbII Solution (4 ^oC)	10 mM Na–MOPS (pH 7.0) 75 mM CaCl2 10 mM KCl % 15 Glycerol adjusted to pH 6.5 using KOH filtered with 0.22 µm filter
Transfection Strong Solution (4 ^oC)	% 10 PEG 8000 % 5 DMSO 50 mM $MgCl_2$

Table 7.7: The list of chemicals used in this study.

Chemicals	Contents
Solution I	25 mM Tris (pH 8) 10 M EDTA (pH 8) 50 mM Glucose
Solution II	0.2 N NaOH % 1 SDS
Solution III	% 60 5 M Potassium Acetate % 11.5 Glacial Acetic Acid
STET Solution	% 8 Sucrose % 5 Triton x-100 50 mM EDTA (pH 8) 50 mM Tris-HCl (pH 8)
CTAB/NaCl Solüsyonu	% 10 CTAB 0.7 M NaCl
TES Buffer (1 L)	50 ml 1 M Tris-HCl(pH:8) 50 ml 0.5 M EDTA 20 ml 500 mM Sucrose
Riboflavin 10 mM	0.0376 g Riboflavin + 10 ml dH_2O
0.1 % NBT	0.002 g NBT + 2 ml dH_2O
TES Buffer	0.05 M Tris-HCl 0.01 M EDTA 10 mM Sucrose

7.2. Methods

7.2.1. Ensemble Modeling

Enzyme k_{cat} values were retrieved from the BRENDA database, and to generate log-normally distributed k_{cat} data for each enzyme, the protocol developed by Tsigkinopoulou et al. (2018) was followed. Log-normally distributed 10,000 random values between the maximum and minimum k_{cat} of each enzyme were obtained, and these random values were converted into stoichiometric coefficients ($-1/k_{cat}$) for each enzyme. In the context of ensemble modelling for a single enzyme, coefficients were randomly assigned to the target enzyme, and the ACT flux estimate of the model and the k_{cat} values of each feasible model were recorded. For the modelling of enzymes as a group, the $-1/k_{cat}$ values for each enzyme were randomly assigned to each enzyme as

new coefficients, and the ACT generation of the model and the k_{cat} values at which the model worked were recorded. These coefficients were randomly converted from the log-normal values for each enzyme in the ensemble modelling for the enzyme as a group and assigned to the target enzyme as a new coefficient. The ACT flux prediction of the model and the k_{cat} values of each feasible model were recorded. The k_{cat} obtained were scored for ACT change using PLS analysis to identify potential effects on ACT production.

7.2.2. Gurobi Optimization

The Gurobi Optimization was used for Flux Balance Analysis (FBA) because its advanced algorithms and parallelised computations deliver fast and accurate solutions to the complex optimisation problems in FBA.

7.2.3. Gene Inactivity Moderated by Metabolism and Expression (GIMME) Approach

To integrate the transcriptomic data of SCO and SCOΔppk into necSco-GEM, we used the GIMME approach, which is the best choice for bacterial models because it integrates transcriptomic data and provides insights into gene expression levels under specific conditions. This improves the prediction of bacterial metabolism, enabling researchers to understand how bacteria adapt to different environments, optimise metabolic pathways for biotechnological applications and design effective metabolic engineering strategies. The GIMME was performed with a cut-off 0.25*mean(mean(RNASEQData)) and the obj-frac was 0.8.

7.2.4. Partial Least Squares Regression (PLS) Analysis

Partial least squares regression is an algorithm for modelling the relationship between independent and dependent variables, especially when there are many interrelated independent variables. The PLS analysis was performed utilising the MATLAB 'PLSregress' function. The 'response' variable was assigned as the prediction of ACT production, and the 'predictor(s)' variable(s) were assigned as enzymes to be determined to ascertain their effect on ACT production.

7.2.5. Preparation of *E. coli* Competent Cells

The preparation of *E. coli* competent cells was undertaken by modifying the method of Sanders Laboratory (Sanders, 2011).*E. coli* cells were cultivated overnight in 10 ml LB (containing 25 µg/ml chloramphenicol for *E. coli* ET12567 cells and 25 µg/ml chloramphenicol and 50 µg/ml kanamycin for ET12567/pUZ8002 cells). These precultures were then inoculated at a ratio of 1:100 into 50 ml of LB medium containing the appropriate antibiotics. Cultures were then incubated at 37 °C with 180 rpm agitation until an OD_{600} of 0.4 was reached. The culture was then subjected to centrifugation at 4000 rpm for 10 min. at 4 °C. Thereafter, 20 ml of TfbI solution was added to the pellet, which was then kept on ice for a further 10 min. The cell suspension was subjected to a second round of centrifugation at 4 °C, 4000 rpm, and the resulting pellet was placed on ice. 1 ml of TfbI solution was added to the pellet aliquoted in 100 µl volumes and stored at -80 °C.

An alternative second method was also followed for the preparation of *E. coli* competent cells. The *E. coli* cells were grown overnight in 10 ml LB (containing 25 µg/ml chloramphenicol for *E. coli* ET12567 cells and 25 µg/ml chloramphenicol and 50 µg/ml kanamycin for ET12567/pUZ8002 cells). These precultures were then inoculated at a ratio of 1:100 into 10 ml of LB medium containing the appropriate antibiotics. The cultures were then incubated at 37 °C with 180 rpm agitation until an OD600 of 0.4 was reached. The culture was then subjected to a centrifugation process at 4 °C, 4000 rpm, for 10 min. Following this, 1 ml of TSS (transfection-strong solution) was added to the resulting pellet, which was then aliquoted into 100 µl volumes. The aliquots were then stored at -80 °C.

7.2.6. Standard Transformation Method

The transfer of DNA into *E. coli* competent cells were achieved by the chemical transformation method as described by Sambrook et al. (1989). A volume of 100 µl of *E. coli* competent cells and 8-10 µl of the recombinant plasmid were mixed on ice and left to chill for 30 min. Following this, the cells were placed in a heat block at 42 °C for 45 seconds. Thereafter, the cells were returned to ice for two min. Following this, 900 µl of LB was added to the cell-DNA mixture and the contents were incubated for

one hour at 37°C, 180 rpm. The cells were then spread on LB agar (containing the necessary antibiotic/s).

7.2.7. Plasmid Isolation from *E. coli* Cells

Two different methods were used for plasmid isolation from *E. coli* cells.

7.2.7.1. Maxiprep Plasmid Isolation

The maxiprep plasmid isolation method used in this study was developed by Sambrook et al. (1989). The *E. coli* cell was cultivated overnight in 50 ml of LB (containing the requisite antibiotic/s). Following centrifugation at 4000 rpm for 15 min., the resulting pellet was dissolved in 600 µl of solution I. After incubation of 5 min., solution II was added to the suspension, which was then kept on ice for a further 5 min. Following this, solution III was added to the mixture and the resultant solution was placed back on ice. The mixture was then subjected to a centrifugation process at 4 °C, 13000 rpm, for 30 min. Thereafter, 0.6 volume of isopropanol was added to the remaining mixture and left at room temperature for 1 h. The isopropanol-supernatant mixture was then subjected to a further round of centrifugation at room temperature, at 13000 rpm, for 30 min. The pellet was then dissolved in 100 µl dH_2O. RNase (10 mg/ml) was then added to this suspension and the mixture was incubated at 37°C for 1 h. The plasmid DNA was then purified using MN PCR clean-up and gel extraction kit.

7.2.7.2. Miniprep Plasmid Isolation

The miniprep plasmid isolation method applied in this study was developed by Holmes et al. [1981]. The *E. coli* cell was cultivated overnight in 1 ml of LB (containing the required antibiotic/s). Following centrifugation at 13000 rpm for 15 min., the cell pellet was dissolved in 250 µl of STET solution. The suspension was then subjected to heating at 100°C for 10 min. The suspension was then subjected to a second centrifugation step at 4 °C, 13000 rpm, for 30 min. The liquid phase was then transferred to a new eppendorf tube, after which 250 µl of isopropanol was added. Following a one-hour waiting period, the mixture was subjected to a second centrifugation at 13000 rpm for 30 min. Thereafter, the pellet was allowed to dry. Following this, the pellet was dissolved in 20 µl dH_2O.

7.2.8. Ligation

In this study, the ratio of insert and vector in all ligation reactions was calculated according to the formula given in equation 7.1, where "ng" represents nanogram and "kb" kilobases. All ligation reactions were performed with T4 DNA ligase (BioLabs). Each ligation sample (maximum volume of 10 µl) was maintained at 16°C for 16 hours, after which it was transferred to the appropriate cell.

$$ng(insert) = \frac{ng(vektör) * kb(insert)}{kb(vektör)} \quad (7.1)$$

7.2.9. Chromosomal DNA Isolation from *S. coelicolor* A3(2)

The isolation of chromosomal DNA from *S. coelicolor* A3(2) was undertaken using a modification of the standard method developed by Hopwood et al. (1999). 100 µl of the spore solution was inoculated in 50 ml of YEME medium and incubated for 48 h at 30 °C, 220 rpm. These precultures were then inoculated at a ratio of 1:10 into 50 ml of YEME medium and incubated for a further 48 hours at 30 °C with agitation at 220 rpm. Following this, the cultures were subjected to a centrifugation process at 4000 rpm for 15 min. at room temperature. The resultant pellet was then dissolved in 8.5 ml of TE buffer containing 2 mg/ml of lysozyme. Subsequently, 500 µl of 20% SDS and 500 µl of RNase (10 mg/ml) were added to the suspension and incubated at 37 °C for 1 h. Following this, 1500 µl of NaCl and 1200 µl of CTAB/NaCl (65 °C) were added to the suspension and kept at 65 °C for 15 min. The suspension was then cooled to room temperature. An equal volume of CIA (24:1) solution was added and the mixture was subjected to centrifugation at room temperature (4500 rpm) for 15 min. The upper phase was then treated with phenol: CIA (25:24:1) solution and the process of centrifugation was repeated. Subsequently, 0.6 volumes of isopropanol were added to the upper phase. Following a 15-minute isopropanol treatment, the sample was subjected to a 30-minute centrifugation process at 4500 rpm. Thereafter, the resultant pellet was dried for 3 min. and dissolved in 2 ml of TE buffer. Subsequently, 1 ml of a phenol: CIA (25:24:1) solution was added to each 1 ml sample, and the samples were then subjected to a 15-minute centrifugation process at 13000 rpm. Thereafter, an equal volume of CIA (24:1) solution was added to the upper phase and subjected to a further round of centrifugation at room temperature (13000 rpm) for five min.

Subsequently, 3 volumes of 100% ethanol were added to the upper phase and stored at -20 °C overnight. The next day, the sample was subjected to a final round of centrifugation at 4 °C (13000 rpm) for 15 min. Following this, the pellet was washed with 70% ethanol, dried, and dissolved in 50 µl dH_2O. The obtained chromosomal DNA was purified using MN PCR clean-up and gel extraction kit.

7.2.10. Klenow Fragment Reaction

The Klenow Fragment reaction was performed in the process of obtaining the pRA$^{apr/str}$*lon* plasmid. The sticky ends of the DNA formed after *Eco*RI cleavage were converted into blunt ends by the Klenow Fragment reaction. The subsequent klenow reaction was carried out by the following procedure given in Table 7.8.

Table 7.8: Klenow fragment reaction

Reaction Contents	Reaction Conditions
80 µl pRA*lon* (Restricted using *Eco*RI)	Incubation for 15 min at 37 °C Inhibition for 15 min at 75 °C
10 µl Tango Buffer (Thermo Scientific)	
2 µl (10 mM) dNTP	
2 µl Klenow Fragment (Merck)	

7.2.11. Plasmid Transfer by Conjugation to *S. coelicolor* A3(2)

Conjugation was performed by the protocol developed by Gust et al. (2002). *E. coli* ET12567/pUZ8002 cells containing the recombinant plasmid were cultivated overnight at 37 °C in 10 ml LB containing kanamycin (25 µg/ml), and chloramphenicol (25 µg/ml) and the antibiotic the recombinant plasmid carrying. 100 µl from each overnight culture was then inoculated into fresh 10 ml of LB, containing the aforementioned antibiotics, and the cultures were grown at 37 °C until an OD_{600} value of 0.4 was reached. The cells were then washed twice with 10 ml of LB and resuspended in 1 ml of LB. 10^8 *S. coelicolor* spores (SCO-Δ*ppk*, SCO-A3(2)) were treated with heat shock at 50 °C in 500 2xYT broth for 10 min. and subsequently cooled. Subsequently, 0.5 ml of *E. coli* ET12567/pUZ8002 (+recombinant plasmid) cell suspension and 0.5 ml of heat-shocked SCO spores were mixed and spun at 13000 rpm for one minute. The majority of the upper layer was decanted, and the pellet was resuspended in 50 µl of liquid. Serial dilution was performed at the rates of 10^{-2}, 10^{-4},

10^{-6}, $10^{-}8$, totalling 100 µl dH_2O. Each dilution was then cultivated on R2YE agar (devoid of antibiotics) at 30°C for 16-20 hours. The incubation was then continued by overlaying with 1 ml of dH_2O containing the antibiotics so that the final concentration in the R2YE agar medium was 25 µg/ml nalidixic acid (NA), 50 µg/ml apramycin, and 50 µg/ml streptomycin (to select recombinant SCO) or 50 µg/ml kanamycin (to select recombinant SCO). Single colonies were then plated on R2YE replica plates containing 25 µg/ml NA, 50 µg/ml apramycin, and 50 µg/ml streptomycin or 50 µg/ml kanamycin. This step was repeated 2-3 times to ensure the removal of *E. coli* cells. Single SCO colonies were subsequently plated on R2YE replica plates containing 50 µg/ml apramycin, 50 µg/ml streptomycin, or 50 µg/ml kanamycin.

7.2.12. Southern Blot Analysis

Southern blot analysis was performed by the method developed by Sambrook et al. (1989). Samples were digested with restriction endonucleases, and the resulting DNA fragments were subjected to electrophoresis on a 1.1% agarose gel. After this, DNA fragments were transferred to the membrane using the blotting system (Amersham Biosciences). The membrane was then washed with 2xSSC and the gel-membrane system was vacuumed at 40-50 mbar. Depurination, denaturation and neutralisation solutions were added to the surface of the agarose gel for 45-45-30 min., respectively. Thereafter, 20xSSC was added to the membrane surface for a further 90 min. The DNA samples transferred to the membrane were then fixed to the membrane by exposure to 100% UV for 4 min. The membrane was then washed with 2xSSC.

7.2.12.1. Hybridization

The membrane was transferred to hybridisation bottles and the pre-hybridisation solution was heated to 47 ^{o}C. The solution was poured into the bottle with the membrane was present and incubated in the hybridisation oven at 37 ^{o}C for 2 hours. The prehybridisation solution was discarded and the membrane was incubated in the probe solution at 47 ^{o}C overnight. After hybridisation, the membrane was washed twice at room temperature with Wash Buffer I for 15 min. and twice with Wash Buffer II at 42°C for 25 min., rinsed in Maleic Acid Wash Buffer for 5 min. and incubated in 70-80 ml of 1x blocking solution for 30 min. The blocking solution was discarded and

the membrane was incubated in 10-20 ml antibody solution at room temperature for 2 hours. The antibody solution was discarded and the membrane was washed in 100 ml maleic acid wash buffer twice for 15 min. and incubated in 20 ml detection buffer for 5 min. The membrane was transferred to a clean container and left in the dark to develop colour by adding colour substrate solution.

7.2.12.2. Probe Preparation

The target gene was amplified and the target gene probe was created following the DIG DNA labelling kit (Roche) protocol. The *kn* and *aadA* probes were prepared by following the kit protocol. The efficiency of the *kn* (Fig.7.1) and *str* (Fig.7.2) probes was tested.

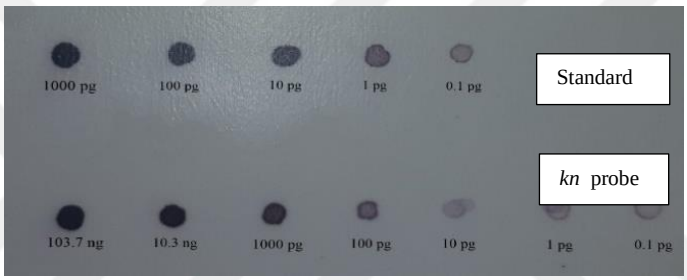

Figure 7.1. The labelling efficiency of *kn* probe . Standard concentrations 1 ng/µl, 100 pg/µl, 10 pg/µl, 1 pg/µl and 0.1 pg/µl. str probe concentrations 103 ng/µl, 10 ng/µl, 1 ng/µl, 100 pg/µl, 10 pg/µl, 1 pg/µl and 0.1 pg/µl. M represents marker.

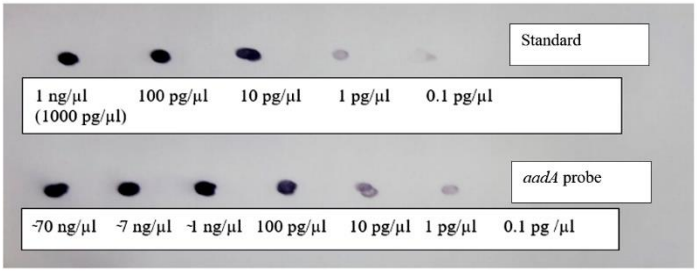

Figure 7.2. The labelling efficiency of *aadA* probe. Standard concentrations 1 ng/µl, 100 pg/µl, 10 pg/µl, 1 pg/µl and 0.1 pg/µl. str probe concentrations 70 ng/µl, 7 ng/µl, 1 ng/µl, 100 pg/µl, 10 pg/µl, 1 pg/µl and 0.1 pg/µl.

7.2.13. Preparation of *Streptomyces* Protoplasts

SCO-Δ*ppk* spore cells were inoculated in TSB and incubated for 48 hours at 30 °C. Subsequently, 5 ml of the preculture was inoculated into 50 ml of YEME containing 5 mM $MgCl_2.6H_2O$, 0.5% glycine and 50 µg/ml apramycin. A 10-ml aliquot of sterile cold 10.3% sucrose was added to the 24 h culture pellet, which was then subjected to centrifugation. The mixture was subjected to a further round of centrifugation at 4500 rpm for 20 min. at 4 °C, after which it was re-treated with sucrose. Thereafter, 5 ml of lysozyme solution was added to the pellet and the mixture was incubated at 30 °C for 90 min. The mixture was then filtered with the aid of a 5 ml pipette tip, loosely filled with cotton, to separate the protoplasts from their mycelles. The filtrate was then subjected to a centrifugation process at 3000 rpm for 7 min. The pellet was then washed in 10 ml of P (+) buffer and subjected to a subsequent centrifugation step at 3000 rpm for 7 min. 1 ml of P (+) buffer was then added to the pellet, which was aliquoted into 50 µl volumes, and stored at -80 °C on ice overnight.

7.2.13.1. Protoplast Transformation of *Streptomyces*

Protoplast transformation was carried out by the polyethylene glycol-mediated method [Gust et al., 2002]. 50 µl of SCO-Δ*ppk* protoplasts were taken from -80°C, kept in tap water and quickly thawed and placed on ice. 5 µl of a DNA solution (isolated from *E. coli* ET2567+ pRA^{aadA}*lon* cells) was then added to the protoplast. 200 µl of P (+) buffer (containing 25% PEG1000) was added to the mixture. The protoplast suspension (100-200 µl) was then inoculated onto R2YE agar (without antibiotics). The plates were then incubated at 30 °C for 20 hours, after which they were flooded with apramycin and streptomycin to select the desired phenotype. After 3-5 days, single colonies were selected and inoculated on R2YE agar containing 50 µg/ml apramycin and 50 µg/ml streptomycin.

7.2.14. Electroporation of *Streptomyces* Cells

The protocol obtained by modifying the Pigac and Schrempf (1995) and Kieser et al. (2000) protocols for electroporation of *Streptomyces* cells was followed. SCO-Δ*ppk* cells were cultivated for 24 hours at 30 °C in 100 ml of CRM medium containing 50 µg/ml apramycin. The culture was then subjected to a centrifugation process at 4 °C,

4500 rpm, for 10 min. Thereafter, the cells were dissolved in 100 ml of cold 10% sucrose. The suspension was then subjected to a second round of centrifugation at 4500 rpm for 10 min at a temperature of +4 °C. The resulting pellet was then dissolved in 10 ml of 15% glycerol, which also contained 100 µg/ml of lysozyme. The mixture was then incubated at 37 °C for 30 min. The cells were then washed with 10 ml of cold (4 °C) 15% glycerol. The pellet was dissolved in 1-5 ml of electroporation buffer and stored at -80 °C as 50 µl aliquots. For transformation, 50 µl of cells thawed at room temperature were placed on ice, and 0.01-1 µg (1-2 µl) of plasmid DNA was added to the cell solution. The cell suspension was transferred to an ice-cold 2 mm gapped electroporation cuvette (VWR) and subjected to a 1 kV electric pulse (5 kV cm-1) from a Gene Pulser (Bio-Rad), connected to a Pulse Controller (25 µF capacitor~ parallel resistance 400 Ohm). The pulsed mycelium was then immediately diluted with 0.75 ml of ice-cold CRM and incubated for 3 hours at 30 °C on a shaker. Following the completion of the three-hour incubation period, the cells were then plated on R2YE agar, which contained a combination of 50 µg/ml apramycin and 50 µg/ml streptomycin.

7.2.15. Sporulation of *Streptomyces spp.*

Wild-type and recombinant cells were cultivated in 50 ml R2YE broth, with the appropriate antibiotic being added for each cell type. The cells were then subjected to a centrifugation process at 3500 rpm for a duration of 20 min. The majority of the resultant supernatant was then discarded, and the pellet was suspended in the remaining liquid. Than 300 µl of the cell suspension (or determined wet weight of cells) was then plated on TBO agar and incubated at 30 °C for 7-10 days.

7.2.16. Quantitative Real-Time PCR Analysis

7.2.16.1. Storing Cell Samples for RNA Isolation

Cell pellets were sampled at 24-hour intervals and frozen by treatment of liquid nitrogen. These pellet samples were then stored in a -80°C freezer until RNA isolation. Subsequently, 200 µl of a Tris-EDTA solution (10 mM/1 mM) and 70 µl of a lysozyme

solution (10 mg/ml) were added to each pellet sample, and the samples were then incubated at 37 °C for 90 min.

7.2.16.2. qPCR Analysis

Livak & Schmittgen [2001] 500 µl of cell samples were collected at 60 and 72 hours of fermentation, washed with a Tris-EDTA (pH 8.0) solution and stored at –80°C. The isolation of RNA was performed using the MN NucleoSpin® RNA Plus kit. The RNA samples were treated with a DNase (NEB) for 105 min (see Table 7.9). The absence of DNA in RNA samples was tested by performing PCR using HrdB primers (Table 7.10). The primers were designed using the online Primer3 tool (Untergasser et al., 2012). The melting temperature, ΔG and the possibility of hairpin and heterodimer structures were analysed by OligoAnalyzer™ Tool. cDNA synthesis was performed using iScript™ cDNA Synthesis Kit (BioRAD). Subsequently, quantitative PCR (qPCR) was performed using the Stepone software for 40 cycles of 5 min. at 25°C, 60 min. at 46°C, and 5 min. at 85°C. The relative expression values ($2^{-\Delta\Delta CT}$) were then calculated by following the method developed by Livak & Schmittgen [2001]. The statistical significance of changes in expression levels was determined by conducting a t-test in MATLAB software, with a p-value threshold of 0.05.

Table 7.9: cDNA synthesis reaction cycle workflow

DNase Reaction Cycle		Reaction Content
37.1 °C	90:00	300 ng RNA 1 µl 10x$MgCl_2$ 1 µl Deoxyribonuclease + dH_2O (variable)
37.1 °C	15:00	
4 °C	60:00	

cDNA Reaction	
25.0 °C	05:00
46.0 °C	60:00
85.0 °C	05:00
4.0 °C	20:00

Pre-cDNA Reaction	
70.0 °C	05:00
4.0 °C	10:00

7.2.17. Confocal Laser Scanning Microscope and Scanning Electron Microscope Analysis

1 ml cell pellet was subjected to two washes with dH_2O and subsequently subjected to centrifugation using a microspin. The pellets were then subjected to staining using the LIVE/DEAD™ BacLight™ Bacterial Viability Kit. The discrimination of live and dead cells was then facilitated by using a ZEISS LSM 880 confocal laser scanning microscope at 488 and 543 nm laser wavelength, respectively.

7.2.18. Antibiotic Measurement

5 ml of each fermentation sample was collected at 24-hour intervals until the 120^{th} hour, with 1 ml of the sample being stored at -20 °C for antibiotic measurement. 4 ml of sample were washed with dH_2O twice and then stored at -20 °C. The measurement of actinorhodin antibiotic was conducted by the spectrophotometric method that was developed by Keiser et al. (2000). To this end, 250 µl of 5M KOH was added to 1 ml of the sample, which was then incubated overnight at +4 °C. The mixture was then subjected to centrifugation at 14000 rpm for a duration of 20 min. The resulting upper layer was then analysed to measure the concentration of actinorhodin present using a spectrophotometer at a wavelength of 640 nm. The molarities of each sample were calculated using the $Abs = \varepsilon \times [M]$ equation. The extinction coefficient (ε) value was assigned as 25230. The specific activity was calculated by dividing the antibiotic concentration (nmol) by the dry weight (mg). Samples stored at -20 °C were thawed and dissolved in 1-1.5 ml dH_2O, then dried at 70 °C to calculate the dry weight values.

7.2.19. Superoxide Dismutase Activity Test

Cells were cultivated in R2YE for 72 hours. Subsequently, 4 ml of cell suspension was subjected to centrifugation at 4500 rpm for 15 min. The resultant pellet was then resuspended in 1 ml of TES Buffer (pH:7.6) and sonicated at 30% amplitude and pulses of 20s:30s. Thereafter, 75 µl of cell suspension was added to 3 ml of TES Buffer, and 150 µl of 0.1% NBT and 50 µl of 10 nM Riboflavin were added to the mixture in a dark place. The mixture was incubated for five min. under the light source. The colour of the samples was then measured at 540 and 560 nm. SOD activity was determined using the equation 7.2.

$$deltaA = \frac{\text{Absorbance final} - \text{Absorbance initial}}{\text{time}} \quad (7.2)$$

$$\%\ Inhibition = \frac{\text{Blank Absorbance} - \text{deltaA}}{\text{Blank Absorbance}}$$

7.2.20. HPLC Analysis

1 ml samples were passed through a 0.22 RC filter. The measurement was performed on the organic acid column (Benson Polymeric BP-800 H4+) under the following conditions: flow rate: 0.6 ml/min, injection volume: 15 µl, column temperature: 65°C, run time: 25 min and mobile phase: 5 mM H_2SO_4.

8. RESULTS

Genome-scale models (GEM) are computational descriptions of protein-gene-reaction associations in the metabolic system of a living organism. GEMs are used to predict the metabolic flux distribution of the organism to guide new strategies and to engineer strains which produce the desired target molecules in higher amounts. *Streptomyces*, as promising industrial hosts for many bioactive metabolites, have been repeatedly targeted by systems biologists, and for the most widely used laboratory model strain of *Streptomyces*, *Streptomyces coelicolor*. Eight generations of increasingly detailed and reliable models have been developed: iIB711[Borodina et al., 2005], iMA789 [Alam et al., 2010], iKS1317 [Sulheim et al., 2019], Sco4 (Wang et al., 2018).iAA1259 (Amara et al., 2018) , and Sco-GEM & ecSco-GEM (Sulheim et al., 2020). In our study, we aimed to elucidate the network between ATP-dependent Lon protease, polyphosphate kinase (PPK) and secondary metabolites (in particular actinorhodin) using ecSco-GEM as a starting point.

8.1. Proving the Negative Effect of *ppk* gene on Actinorhodin Production with Ensemble Modeling Approach

The metabolite and reaction content of the models iKS1317, Sco4, iAA1259, Sco-GEM and ecSco-GEM models were compared. To develop a new model that is stronger in secondary metabolite production 27 reactions and 21 metabolites were added to ScoGEM (template model). Duplicate or erroneous reactions were excluded. And 2 reactions related to the actinorhodin pathway were found in the ScoGEM model and these reactions were also excluded. ecM145 (ecScoGEM) is a derivative model of ScoGEM reported to have been constructed using the GECKO approach, which has an expanded stoichiometric matrix by adding rows specifying enzymatic turnover numbers (k_{cat}) for each enzyme in the system (Sulheim et al., 2020). The reactions and metabolites added to the Sco-GEM model were also added to the enzymatically constrained model (ecM145). This resulted in necSco-GEM.

Ensemble modelling was performed for each enzyme separately to determine the effect of enzymes involved in the stringent response mechanism on actinorhodin (ACT) production. The k_{cat} values of the proteins involved in the stringent response

(Q9KZV6-Ppk/ EC2.7.4.1, P52560-RelA/ EC2.7.6.5, Q9X8H1-Uncharacterized protein SCO3348/Ppx/ EC3.6.1.40, O69970-Kinase/phosphohydrolase/SpoT, Q9ZBH7-tRNA synthetase/ EC6.1.1.10) were obtained from the BRENDA database. The log-normal distributions of the obtained kinetic parameters were calculated following the ensemble modelling protocol [Tsigkinopoulou et al., 2018]. We have found that the enzyme EC2.7.4.1 has large k_{cat} values that do not give feasible results (Fig. 8.1). For the kcat data of the enzyme EC2.7.4.1, a specific range of 720-2240 1/h was identified where the model has a high potential to give feasible results (Fig. 8.2). Even EC3.6.1.40 seems to have an excellent negative correlation with actinorhodin, but this result is not considered reliable as actinorhodin values clustered between 0.016-0.017 g/DW/h (Fig. 8.3). The k_{cat} values for the remaining proteins gave feasible results in the model. However, they did not show a significant correlation with actinorhodin.

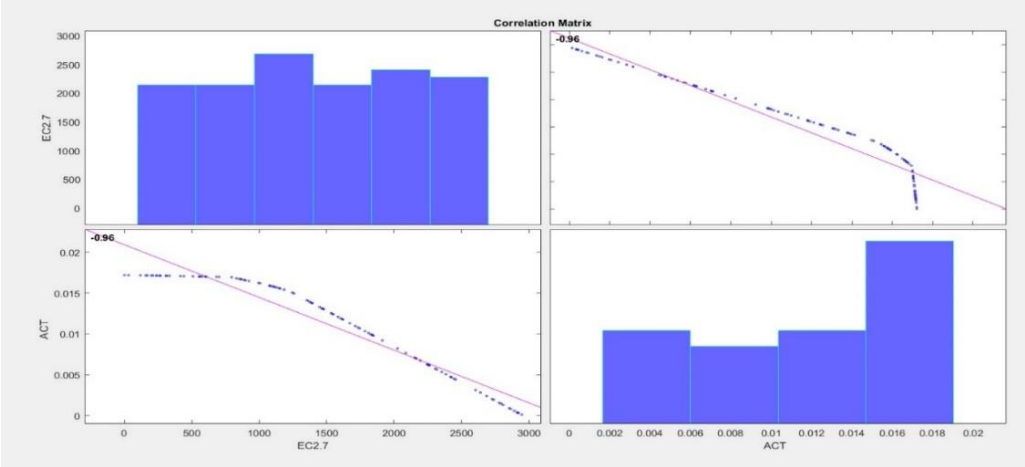

Figure 8.1: Ensemble modelling correlation graphs of EC2.7.4.1 and actinorhodin production. Correlation graph obtained performing ensemble modelling by random kcat values.

a **b**

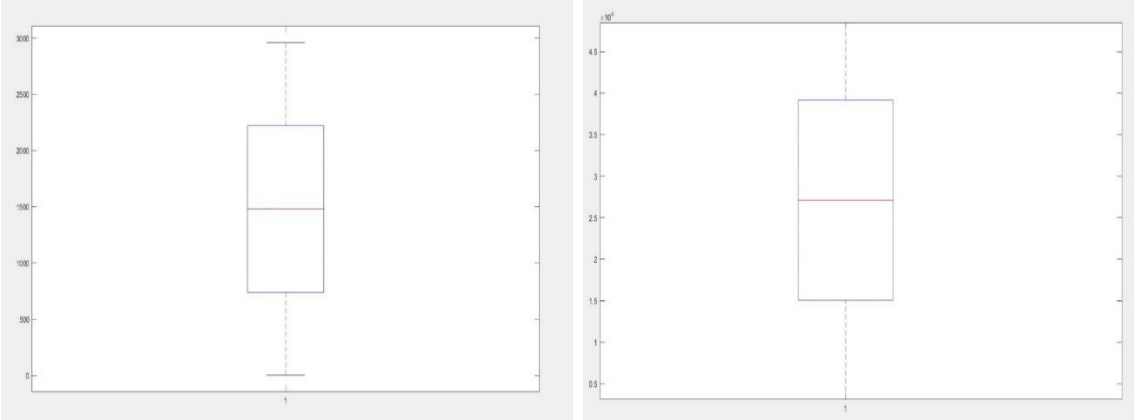

Figure 8.2: Boxplot of feasible (a) and infeasible (b) EC2.7.4.1 k_{cat} data. The graphs show the k_{cat} range in which the model gives feasible and infeasible results.

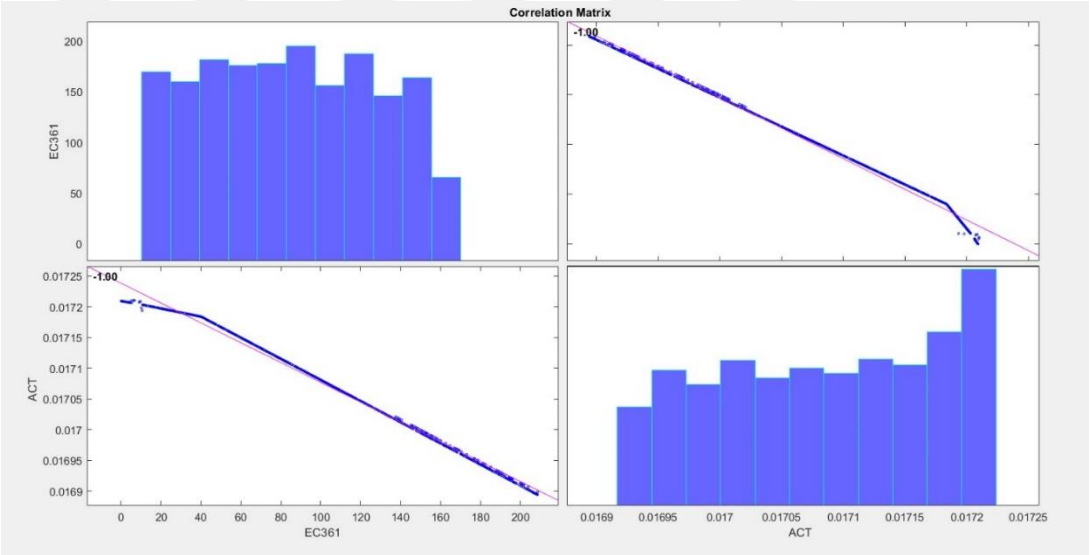

Figure 8.3: Ensemble modelling correlation graphs of EC3.6.1.40 and actinorhodin production. The correlation graph was obtained by performing ensemble modelling with random k_{cat} values.

To investigate the effect of the stringent response pathway on actinorhodin production. Flux balance analysis (FBA) was performed in 8 different running conditions (Table 8.1). In the FBA analysis, the fluxes of the enzymes P52560, Q9X8H1 and O69970 were found to be "0". To add these reactions to the model flux, the method used by Sulheim et al. was modified and used as follows (Sulheim et al., 2020). Initially, since the integration of 24-hour transcriptomic data into the model is planned for the remainder of this study, the running conditions were modified to 21-hour conditions,

the closest period to 24 hours. The normalized 21 h proteomic data (unit: g/gDW/h) (Sulheim et al., 2020), were converted to units of mmol/gDW/h and the enzyme reactions were bounded using the calculation given in equation 8.1, where μ_i is mean, σ_i is standard deviation and e_i is concentration. Since the O69970 protein doesn't have any proteomic data at 21h and has the same reactions as P52560, this protein was excluded from the analysis. The reconstructed model was then used in ensemble modelling to determine the impact of a stringent response mechanism on ACT production. The kcat values of the proteins involved in the stringent response mechanism were obtained from the BRENDA database. The log-normal distributions of the obtained kinetic parameters were calculated according to the ensemble modelling protocol (Tsigkinopoulou et al., 2018). The log-normal distribution for the enzyme Q9KZV6-Ppk/ EC2.7.4.1 was assigned taking into account the range in which it will give feasible results. To perform ensemble modelling under 21 h running conditions, enzyme constraints were calculated by converting the 21 h proteomic data to units of mmol/gDW/h. Glucose, l-glutamate exchange and biomass production values (maximum biomass under 21 h conditions *0.5) were fixed to conditions that allowed the model to produce actinorhodin (Table 8.2). The objective function that has been selected is the maximisation of actinohodin production. It is imperative to note that all simulations conducted throughout the study incorporate these modifications. In the model, the P52560 enzyme was assigned two different reactions with two different kcat values, depending on the substrate usage. Therefore, the P52560 reactions were divided into two groups and designated as RGtp and RGdp in our analyses. Randomly selected kinetic parameters (k_{cat}) were assigned to the reactions involved in the stringent response (Q9KZV6-Ppk/ EC2.7.4.1, P52560-RelA/ EC2.7.6.5 (RGtp & RGdp), Q9X8H1-Uncharacterised protein SCO3348/Ppx/, Q9ZBH7-tRNA synthetase/ EC6.1.1.10). The kcat values, resulting in feasible results, were analysed by Partial least squares regression (PLS) analysis. To perform the PLS analysis, the k_{cat} data were log-transformed and the unit variance was scaled for each variable according to equation 8.2. Mean and variance values were calculated by considering log-normal distributions of each variable (stringent response-related proteins). We obtained PLS plots, which are bar charts of the β coefficients of the variables. The variable with a large β coefficient plays a key role in the model, with negative coefficients indicating a negative relationship and positive coefficients indicating a positive relationship. A simplistic PLS equation was given in equation 8.3.

x represents predictor variables (k_{cat} values in this case) and y represents response variables (actinorhodin production in this case). The results are clear: all stringent response-related proteins except EC2.7.6.5GTP show a negative correlation with actinorhodin production. Notably, the enzyme EC2.7.4.1 exhibits a more pronounced negative correlation with actinorhodin production compared to the other enzymes (Fig. 8. 4).

$$\boldsymbol{\mu_i}\text{-}\boldsymbol{\sigma_i} \leq \boldsymbol{e_i} \tag{8.1}$$

$$x = (x\text{-mean}(x))/\text{var}(x) \tag{8.2}$$

$$y \approx x \cdot \beta \tag{8.3}$$

$$y = x^* \beta + \acute{\varepsilon} \text{ (residual)}$$

Table 8.1: Maximum (ub) glucose and l-glutamate exchange values.

Time	**Glucose Exchange**	**L-Glutamate Exchange**
21 h	4.528	11.462
29 h	0.779	1.973
33 h	0.551	1.395
37 h	0.338	1.116
41 h	0.327	1.078
45 h	0.316	1.043
49 h	0.223	0.803
53 h	0.22	0.793
57 h	0.217	0.784

Table 8.2: Constraints of stringent response-related enzymes (21 h).

Reactions	lb	ub
'S. coelicolor biomass function with AA replaced by tRNA-AA'	0.123	0.123
'draw_prot_Q9KZV6'	1.52E-06	INF
'draw_prot_P52560'	3.56E-07	INF
'draw_prot_Q9X8H1'	5.62E-07	INF
'draw_prot_O69970'	0	INF
'D-Glucose exchange (reversible)'	4.340	4.340
'L-Glutamate exchange (reversible)'	1.078	1.078

a **b**

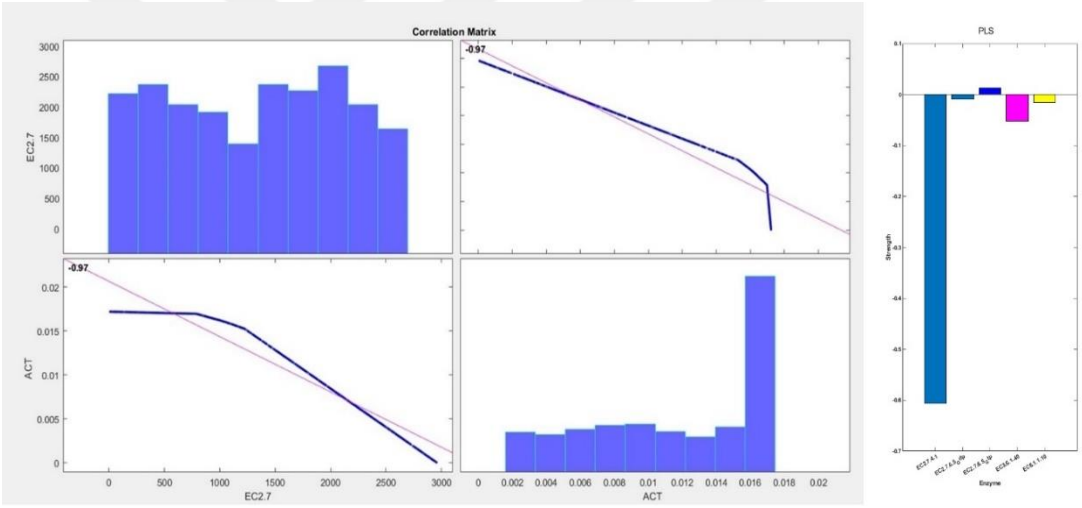

Figure 8.4: Results for ensemble modelling with a specified k_{cat} range for EC2.7.4.1. Ensemble modelling correlation graphs of EC2.7.4.1 when the ensemble model performed only for EC2.7.4.1 in a specific range (a). PLS analysis of ensemble model performed for five stringent response-related proteins when kcat for EC2.7.4.1 assigned in a specific range (b).

8.2. Constructing necSco-Δ*ppk* + pRA*lon*, necSco-Δ*ppk* Models: Identifying Actinorhodin Production-Related Pathways

To simulate SCOΔ*ppk*+pRA*lon* and ScoGEM-Δ*ppk* cells, we added a new constraint, 24 h transcriptomic data of SCO+pRA*lon* and SCO cells (PRJNA1077142) to ec-ScoGEM, respectively and silenced the *ppk* gene in the models. The fluxes of reconstructed models (nec-ScoGEM-Δ*ppk*+pRA*lon*, nec-ScoGEM-Δ*ppk*) were compared by performing FBA under 7 different glucose and l-glutamate intake conditions (model specified conditions given in Table 8.3). Significantly altered fluxes ($p<0.05$) were determined by the Mann-Whitney U test (also called Mann-Whitney Wilcoxon (MWW/MWU)) and fold changes were calculated for each enzyme in the model. A total of 28 significantly changed enzymes were identified and their relationship to the ACT cluster was determined using the STRING database (Fig 8.5). The outliers were eliminated and the relevant pathways of the remaining enzymes (25) were determined using the strepDB database (Fig 8.5). Statistical analyses showed that there was an 8.3-fold increase in *nuo* A-N operon (NADH dehydrogenase (complex-I; SCO4562-SCO4575)) flux, 4- fold increase in superoxide dismutase (Q7AKR0), 5-fold increase in P72392 in nec-ScoGEM-Δ*ppk*+pRA*lon*.

Table 8.3: Glucose and l-glutamate exchange values

Glucose Exchange	4.528/ 4.527/ 4.527/ 0.779/ 0.551/ 0.338/ 0.337
L-Glutamate Exchange	11.462/ 5.149/ 5.992/ 1.973/ 1.395/ 1.116/ 1.078

Furthermore, 7 fluxes for nec-ScoGEM-Δ*ppk*+pRA*lon* and 5 for nec-ScoGEM-Δ*ppk*+pRA were found to be inactive (flux=0) (Fig. 8.5). In the nec-ScoGEM-Δ*ppk*+pRA*lon* model, the flux of Q9L2C1 (activates the mevalonic acid pathway, which synthesizes the farnesyl-derived secondary metabolite from acetyl-CoA) was "0" and the flux of P72392 (responsible for activating the malonic acid pathway, which synthesizes the polyketide containing actinorhodin) was increased by a factor of 5, favouring the orientation towards the production of actinorhodin.

Enzymes exhibiting significantly high fluxes were grouped with the assistance of the STRING database (Fig. 8.5). 14 enzymes are related to the *nuo* complex. Seven of the remaining eleven enzymes were associated with secondary metabolite production, actinorhodin production, stringent response, or enzymes whose fluxes significantly increased in the nec-ScoGEM-Δ*ppk*+pRA*lon* model FBA. Among these enzymes, the Q9F2I9/methionine tRNA ligase is linked to the Q9ZBH7 enzyme which has a negligible negative effect on actinorhodin production. Its flux was determined as "0" in the FBA of nec-ScoGEM-Δ*ppk*+pRA*lon* model. This output also supports the hypothesis that the orientation towards the production of actinorhodin. The remaining enzymes listed as SCO5471, SCO5472, SCO2388, SCO2183, SCO1268, SCO1378 SCO3829, SCO3830, SCO3831, SCO5399. The enzymes SCO3829, SCO3830, and SCO3831 are members of the *bkd* gene cluster responsible for branched amino acid synthesis, a precursor of actinorhodin [Stirrett et al., 2009]**.** SCO5399, putative acetoacetyl-CoA thiolase, is an enzyme that has not yet been shown to be involved in ACT production. Although some studies have suggested that it is involved in leucine biosynthesis [Stirrett et al., 2009], it was not included in the ensemble modelling analysis because its flux in the FBA of the nec-ScoGEM-Δ*ppk*+pRA*lon* model was "0".

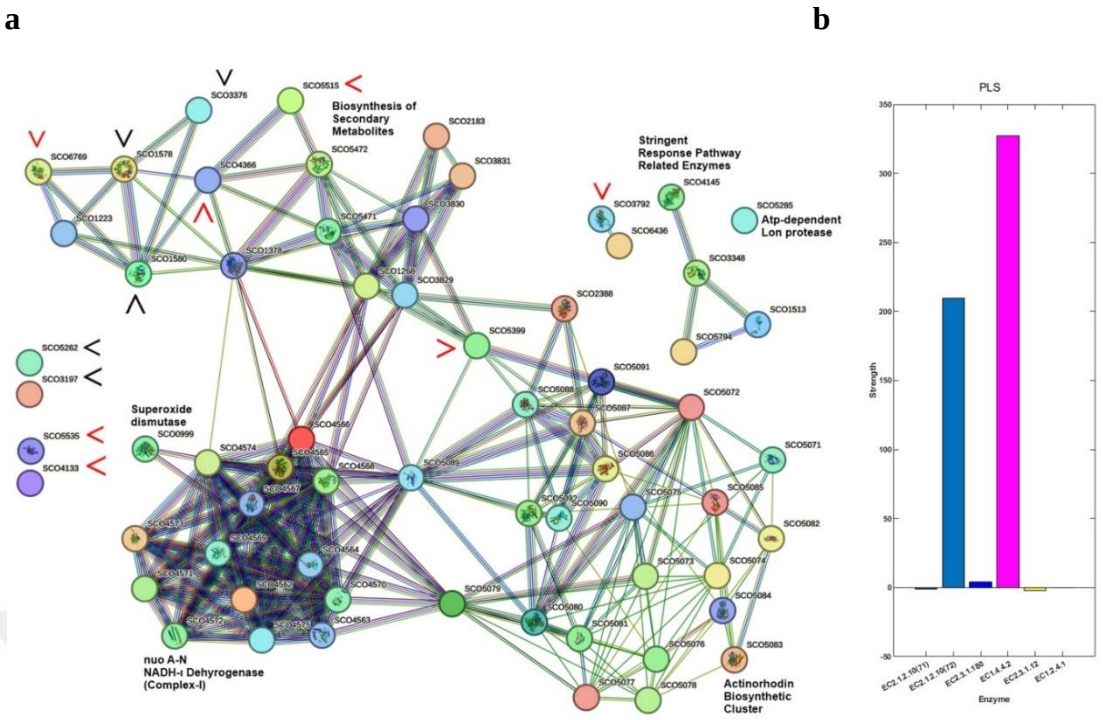

Figure 8.5: STRING & StrepDB database information of significantly ($p<0.05$) increased 25 enzymes (a) and stringent-response related enzymes. PLS analysis (b) of 6 enzymes associated with both secondary metabolite production and NADH-I. PLS analysis enzyme information: EC2.1.2.10(71)/Q6566, EC2.1.2.10(72)/Q6567, EC2.3.1.180/P72392, EC1.4.4.2/Q9AK84, EC2.3.1.12/Q9K3H2, EC1.2.4.1/Q9S2Q3. In nec-ScoGEM-Δ*ppk*+pRA*lon* model FBA, active fluxes (black) and inactive fluxes (red) were marked with the symbol "<".

The enzymes targeted in the ensemble modelling are P72392 (SCO2388)-Beta-ketoacyl-[acyl-carrier-protein] synthase III/ EC2.3.1.180, Q9AK84 (SCO1378)-Glycine dehydrogenase (decarboxylating)/ EC1.4.4.2, O86566 (SCO5471)-Glycine cleavage system H protein/ EC2.1.2.10(71), O86567 (SCO5472)-Aminomethyltransferase (glycine cleavage system T protein)/ EC2.1.2.10(72), Q9S2Q3 (SCO2183)-pyruvate dehydrogenase (acetyl-transferring)/ EC1.2.4.1, Q9K3H2 (SCO1268)-Dihydrolipoamide acetyltransferase component of pyruvate dehydrogenase complex enzyme/ EC2.3.1.12. The k_{cat} values of the enzymes were obtained from the BRENDA database and the ensemble modelling was carried out by following Tsigkinopoulou's method by considering parameters given in Table 8.2. According to PLS analysis P72392, Q9AK84 and O86567 enzymes positively affect ACT production (Fig. 8.5). Ensemble modelling results showed that the reactions that produce the ACT precursor molecule in nec-ScoGEM-Δ*ppk*+pRA*lon* are activated by

the integration of SCOpRA*lon* transcriptome data. This was the starting point of our study, which supports the idea that the integration of an extra copy of the *lon* gene into the SCOΔ*ppk* genome may have a positive outcome in ACT production.

8.3. Obtaining the SCO-Δ*ppk* + pRA*lon*, SCO-Δ*ppk* + pRA Strains

The kanamycin (*kn*) gene was amplified from pSK*desA*Kn plasmid by using the *kn* primers (Table 7.10). The *kn* gene was cloned into the *Eco*RV region of the pRA plasmid in *E. coli* DH5α and the *Eco*RI site of the pRA*lon* plasmid [Demir et al., 2019] (Fig. 8.6a). The recombinant plasmids were transferred into methylation-deficient ET12567/pUZ8002 strains. Recombinant *E. coli* strains ("DH5α+ pRA^{kn}", "DH5α+pRA^{kn}*lon*", "ET-pUZ+ pRA^{kn}", "ET-pUZ+ pRA^{kn}*lon*") were selected according to their kanamycin (DH5α) and apramycin (ET-pUZ) resistance. The presence of the *kn* gene in the pRA^{kn} and pRA^{kn}*lon* plasmids was demonstrated by *Nco*I restriction digestion (Fig. 8.6b). The recombinant plasmids were transferred to SCO-Δ*ppk* cells by performing conjugation between SCO-Δ*ppk* and ET-pUZ+ pRA^{kn} , ET-pUZ+ pRA^{kn}*lon* cells. Recombinant *Streptomyces* cells were selected according to their resistance to kanamycin, the growth of *E. coli* cells was prevented by nalidixic acid (NA). The presence of the *kn* and *lon* genes in the genomes of new recombinant strains (SCO-Δ*ppk*+ pRA^{kn} *lon*) was proved by Southern Blot Hybridization Analysis (Fig 8.7). As a result of the hybridization performed with the *kn* gene probe, a 7290 bp fragment containing the *lon* and *kn* genes and a 3893 bp fragment containing the *kn* gene were observed (Fig. 8.7a-lower panel). The presence of *kn* gene in the genome of SCO-Δ*ppk*+ pRA^{kn} cells was observed as a 2984 bp fragment (Figure 8.7b-lower panel). Unfortunately, the *lon* probe did not hybridize with any of the genomic fragments, but a 6381 bp fragment containing both *kn* and *lon* genes was observed on PCR-based southern blot analysis performed using the *lon* probe. Concerning the problems encountered during the study, we would like to point out that it is important to corroborate the PCR results with Southern blot hybridisation analysis, as pRA-proof primers can bind non-specifically in the genome (Fig 8.7-upper panel well 5/Δ*ppk* sample).

a

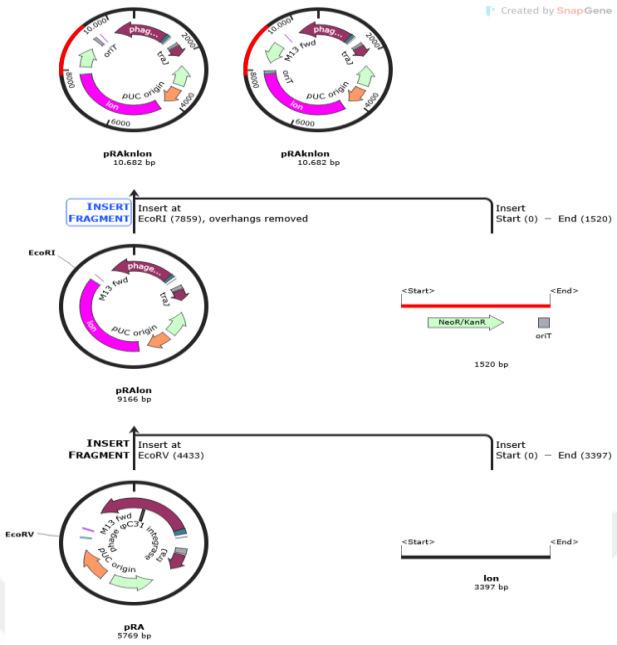

b

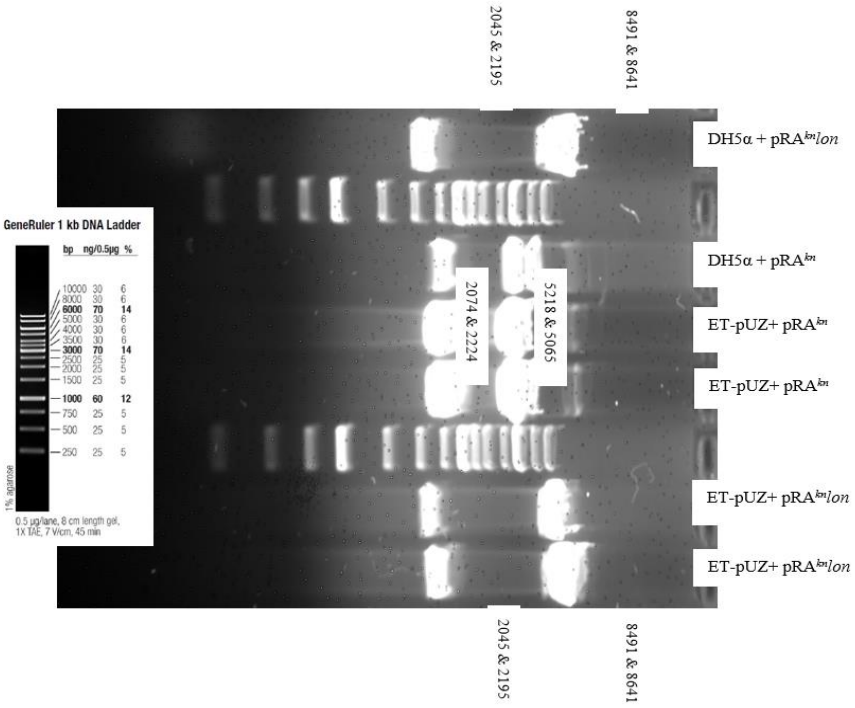

Figure 8.6: Evidence of the presence of *kn* gene in pRA^{kn} and pRA^{kn}*lon* plasmids transferred into *E. coli* DH5α and ET12567/pUZ8002 strains. *Nco*I has a restriction site on pRA, a restriction site on the *kn* gene, and no restriction site on the *lon* gene. The sizes of the fragments are shown as binary possibilities since the orientation of the *kn* gene is not known.

a **b**

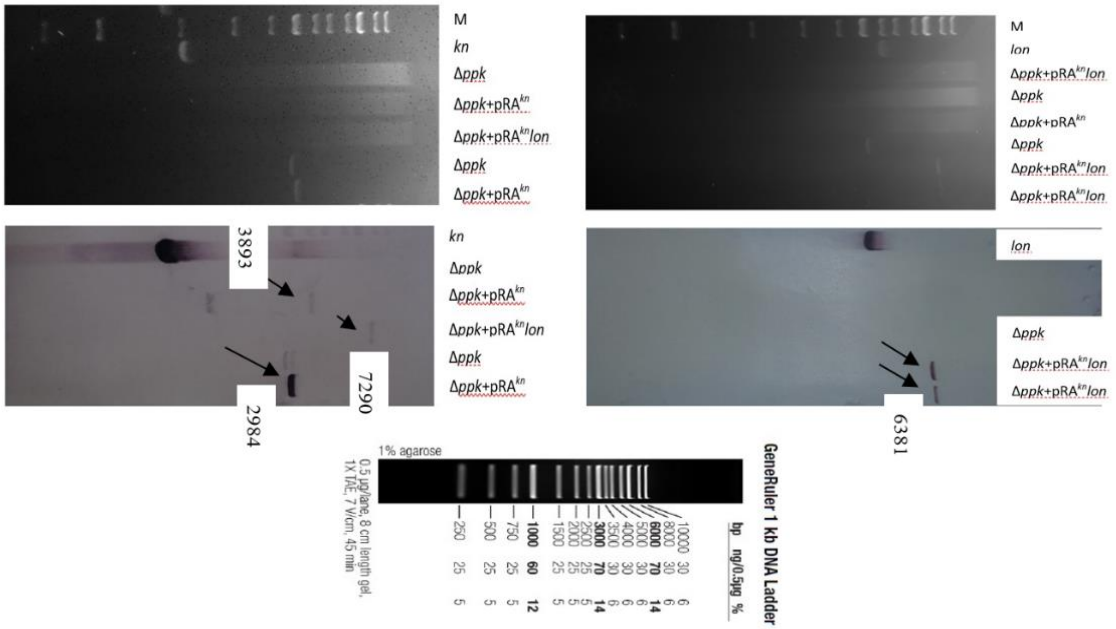

Figure 8.7: Southern blot hybridization analysis of SCO-Δ*ppk*+ pRA^{kn} and SCO-Δ*ppk*+ pRA^{kn} *lon* . Agarose gel images of genomic DNAs and PCR products (a-b upper panels). Fragments containing only *kn* gene (3893 bp and 2984) and "*kn* and *lon*" genes (7290) hybridized with *kn* probe (a-lower panel). Fragments containing "*kn* and *lon*" genes (6381) hybridized with *lon* probe (b-lower panel). The *kn* (1520 bp) and *lon* (3397 bp) genes used as controls (a&b first wells).

8.4. Quantitative Determination of the Presence of Extra *lon* gene in the SCO-Δ*ppk* + pRA*lon* Genome

To determine the expression of the extra *lon* gene in SCO-Δ*ppk*+pRA*lon*, qPCR analysis was performed. SCO-Δ*ppk*+ pRA*lon* and SCO-Δ*ppk* cells were grown in R2YE and samples were obtained for 60 and 72 hours. According to the qPCR results, *lon* gene expression in the SCO-Δ*ppk*+ pRA*lon* cells was found to be 1.4 and 1.6 times higher than the SCO-Δ*ppk* cells, at 60th and 72nd h of fermentation, respectively (Fig. 8.8).

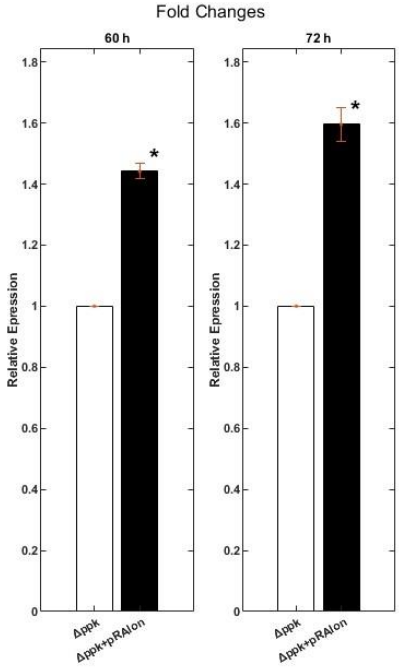

Figure 8.8: qPCR analysis results of SCO-Δ*ppk* and SCO-Δ*ppk*+ pRA*lon***.** Significant changes in *lon* expression ($p < 0.05$) were marked with "*". All cells were grown in R2YE at 30 ° C.

8.5. Determining Actinorhodin Production Profile of SCO, SCO-Δ*ppk*, SCO-Δ*ppk*+ pRA, SCO-Δ*ppk*+ pRA*lon* cells

To determine the actinorhodin (ACT) antibiotic production, SCO, SCO-Δ*ppk*, SCO-Δ*ppk*+ pRA, SCO-Δ*ppk*+ pRA*lon* cells were grown in R2YE media and samples harvested at 24-hour intervals. Significant changes in antibiotic production were determined by t-test analysis on MATLAB software. SCOΔ*ppk* + pRA*lon* showed a ~ 1.5 fold and 7.5 fold increase in actinorhodin production compared to SCOΔ*ppk* and SCOΔ*ppk* + pRA cells, respectively (Fig. 8.9a). The darkening of the bluish to dark blue colour observed in the dry pellet of SCO-Δ*ppk*+ pRA*lon* cells, presented in **Fig. 8.9b**, constitutes evidence of increased ACT production.

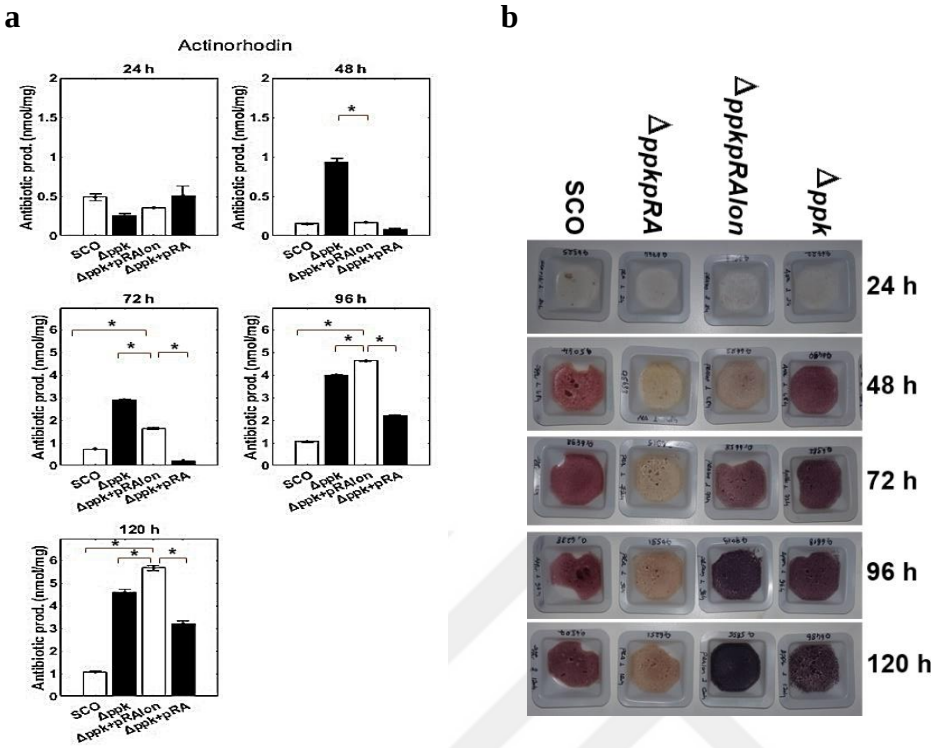

Figure 8.9: Changes in actinorhodin production. Significant changes in ACT production in SCOΔ*ppk*+pRA*lon* marked with "*" ($p<0.001$) (a). Visible colours of dried cells indicate changes in antibiotic production (b).

8.6. Superoxide Dismutase Analysis of Recombinant Cells

Our model simulations showed that the superoxide dismutase flux in nec-ScoGEM-Δ*ppk*+pRA*lon* increased 5-fold compared to that in nec-ScoGEM-Δ*ppk*. To validate these computational predictions, the SOD activity of the recombinant cells was experimentally measured after 72 hours of growth. These measurements were taken at two specific wavelengths, 560 nm and 540 nm, which are standard for assessing SOD activity. In this context, the SOD activity of the SCOΔ*ppk* + pRA*lon* strain demonstrated noteworthy enhancements. Specifically, the activity was found to be 1.085 times (8.4%), 1.11 times (10.5%), and 1.087 times (8.7%) higher compared to the baseline activities observed in the SCO, SCOΔ*ppk*, and SCOΔ*ppk* + pRA strains, respectively. This enhancement underscores the positive effect of the additional *lon* gene on SOD activity, aligning with and supporting the findings from the *in silico* predictions.However, it is important to note a discrepancy between the *in silico*

predictions and the in vitro results. While computational models predicted a 5-fold increase in SOD activity between the nec-ScoGEM-Δ*ppk*+ pRA*lon* and nec-ScoGEM-Δ*ppk* strains, empirical *in vitro* measurements revealed an increase of only 1.11-fold. This discrepancy underscores the complexity and limitations of computational predictions in biological research, emphasising the need for empirical validation.

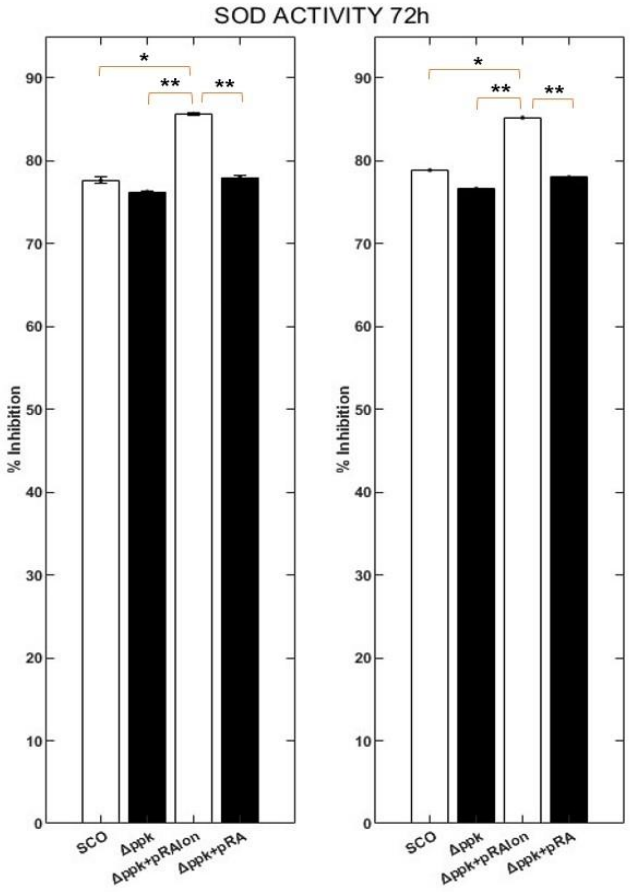

Figure 8.10: SOD activity assay results at 560 nm (left) and 540 nm (right). Significant changes in SOD activity in SCOΔppk+pRA*lon* were marked with "**" ($p<0.05$) and "*" ($p<0.5$). All cells were grown in R2YE at 30 °C. The starting wet inoculum weight for each cell was 0.005 g/ml.

8.7. Determining Morphological Changes of Recombinant Cells

Morphology of recombinant cells were analysed by using confocal laser scanning microscopy. The analyses showed that the *ppk*-deficient cells formed large colonies, except the SCOΔ*ppk*+pRA*lon* cells. Classical programmed cell death (PCD), whereby dead cells are typically observed to spread from the central region to the peripheral

sides, was observed in the SCO, SCO, SCOΔ*ppk* and SCOΔ*ppk*+pRA clumps. However, in the SCOΔ*ppk*+pRA*lon* clumps, the living cells were observed to be the predominant population. Moreover, SCOΔ*ppk*+pRA*lon* cells have formed elongated colonies and their hyphal protrusions are much more than those of other cells (Fig. 8.11). The approximate cell dry weights were determined as SCOΔ*ppk*+pRA*lon*, SCOΔ*ppk*+pRA and SCOΔ*ppk*, SCO from largest to smallest. Subsequently, a correlation was demonstrated between dry weights and actinorhodin production (Fig. 8.12).

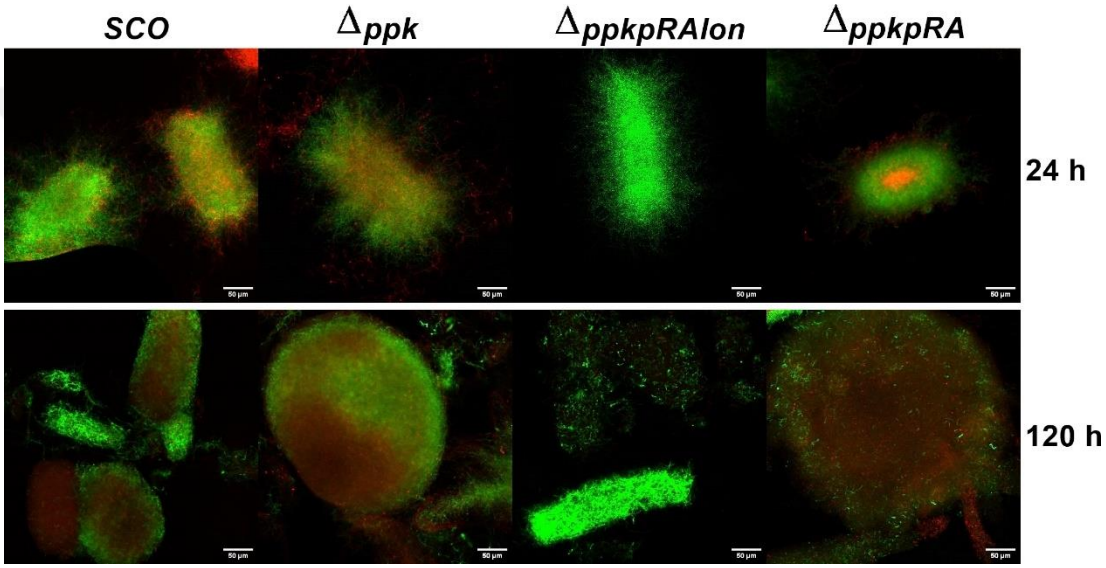

Figure 8.11. Confocal laser scanning microscope images at 50 μm magnitude. All cells were grown on R2YE at 30 ^{o}C. Starting wet inoculum weight for each cell was 0.025 g/ml.

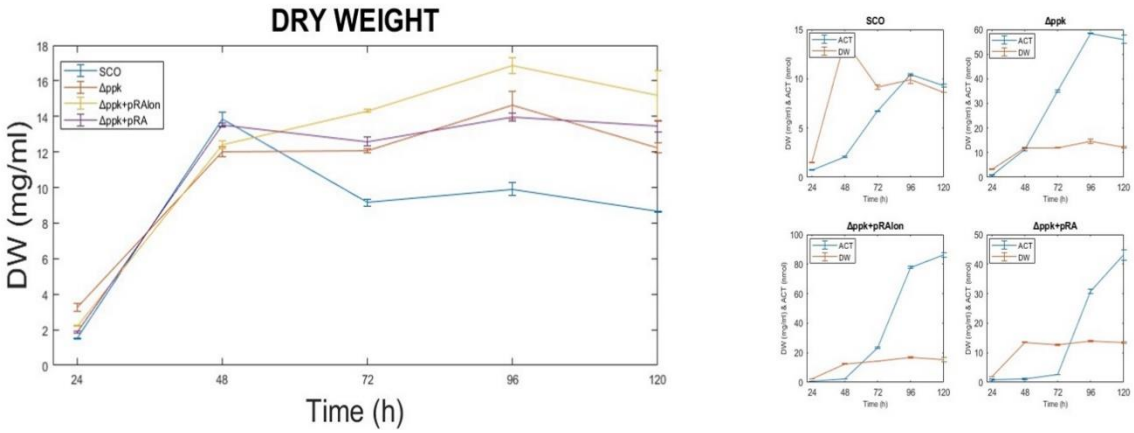

Figure 8.12: Growth and ACT production changes during the fermentation. All cells were grown in R2YE at 30 ºC. Starting inoculation concentration per cell was 0.5 g/ml.

Spore chain structures were examined by scanning electron microscope (SEM). No significant difference was observed in the cell spores. A delay in sporulation of SCOΔ*ppk*+pRA cells was observed on TBO agar (Fig. 8.13). In contrast, strong sporulation was observed in SCOΔ*ppk*+pRA*lon* cells (Fig. 13). Considering the live cell count results, colony formation abilities are listed as follows SCOΔ*ppk* ($3{,}72*10^8$ CFU/ml), SCO ($3{,}41*10^8$ CFU/ml), SCOΔ*ppk*+pRA*lon* ($0{,}0455*10^8$ CFU/ml) and SCOΔ*ppk*+pRA ($0{,}0042*10^8$ CFU/ml).

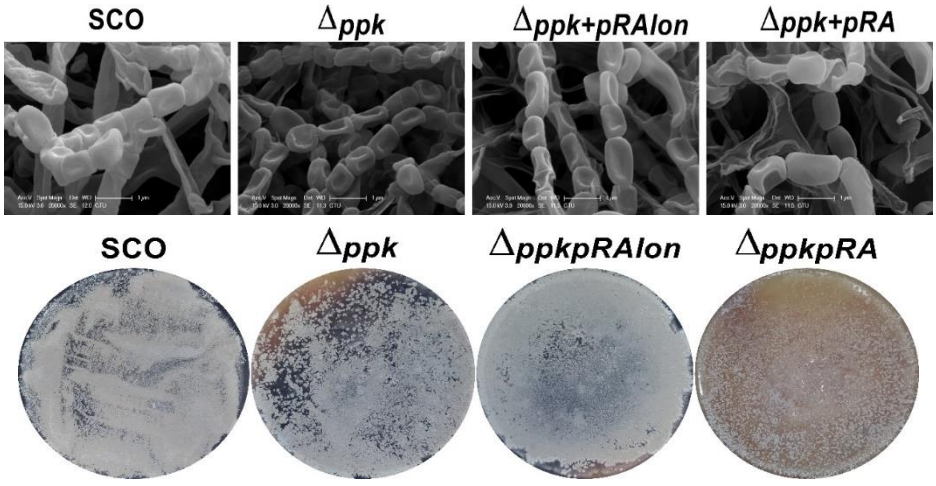

Figure 8.13: SEM images of SCO, SCOΔ*ppk*, SCOΔ*ppk*+pRA, SCOΔ*ppk*+pRA*lon* spore chains at 1 µm magnitude (a) and growth of mutant cells on TBO agar (b). All cells were grown on TBO agar at 30 ºC for 120 h. Starting inoculation concentration per cell was 0,004 g/ml.

8.8. Surprising Effect of Streptomycin Resistance Gene in *S. coelicolor* A3(2): Stimulating Primary Metabolism Instead of Secondary Metabolism

The initial plan for this study was to obtain SCOΔ*ppk*+pRA*lon* strain by using the streptomycin resistance gene (*aad*A) gene as a selective marker instead of *kn* resistance gene. This attempt was unsuccessful and we continued with the *kn* resistance gene, but since the expression of streptomycin resistance gene in *S. coelicolor* had very interesting effects, we decided to include these results in the thesis.

First, the *aad*A gene was amplified by using the DNA fragment, obtained by cleavage of the pIJ778 plasmid with *Eco*RI and *Hind*III, enzymes as a template. The primers (*aad*A) used in PCR were designed from the FRT regions on the plasmid. The 1411 bp PCR product (*aad*A gene) was isolated from the gel and cloned into the *Eco*RI site of pRA*lon* plasmid which has also apramycin resistance gene (*aac*(3)IV) as a selective marker (Fig. 8.14a). The recombinant *E. coli* DH5α+pRA$^{apr/aadA}$*lon* and *E. coli* ET12567/pUZ(8002)+ pRA$^{apr/aadA}$*lon* cells were selected according to their apramycin resistance. The pRA$^{apr/aadA}$*lon* plasmid was verified by digesting it with *Xba*I restriction enzyme and PCR analysis, which was performed with both *lon* and *aad*A primers (Table 7.10) (Fig. 8.14b&c). The pRA$^{apr/aadA}$*lon* plasmid was tranferred into SCO-Δ*ppk* cells by conjugation. *Streptomyces* recombinant cells were selected according to their resistance to streptomycin, and growth of *E. coli* cells was prevented by the presence of nalidixic acid (NA).

Surprisingly, the new recombinant cell SCO-Δ*ppk*+ pRA$^{apr/aadA}$*lon* showed different growth pattern from the wild-type cells (Fig. 8.15). No visible production of actinorhodin and undecylprodigiosin was observed in the solid culture (Fig. 8.15). It was unclear whether the observed outcome was a consequence of the expression of *lon* gene or not.

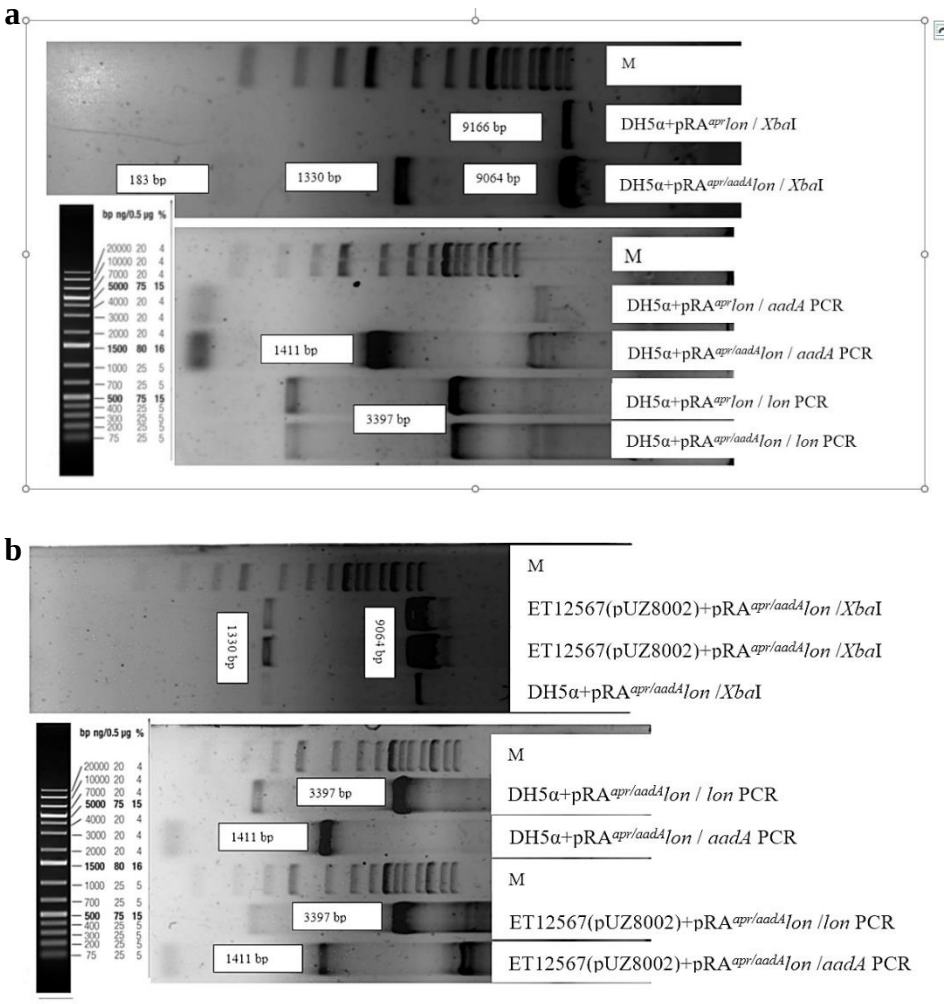

Figure 8.14: Verifying the pRA$^{apr/aadA}$*lon* plasmid. The *Xba*I restriction profile and PCR results were given for pRA$^{apr/aadA}$lon isolated from *E. coli* DH5α cells (a) and *E. coli* ET12567(pUZ8002) + pRA$^{apr/aadA}$on cells (b). The *Xba*I restriction profile of pRA$^{apr/aadA}$lon and pRA^{apr}*lon* (as illustrated in a and b upper panels) was demonstrated, with the second band (1330 bp) observed in the *Xba*I restriction belonging to the inner region of the *aadA* gene. The 183 bp band was not perfectly visualised because it was out of the marker sizes. The presence of the *lon* gene was demonstrated in both plasmids (a and b down panels). The PCRs were performed using *aadA-1* and *lon* primers, and Q5 High-Fidelity Enzyme DNA polymerase was utilised. The reaction conditions are presented in **Table 7.10**.

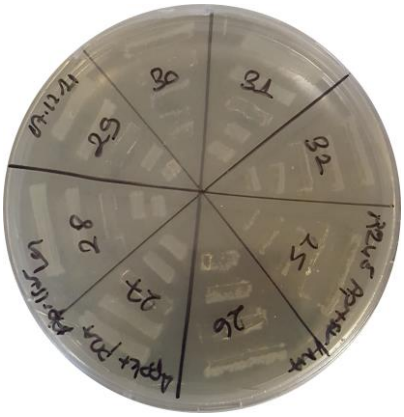

Figure 8.15: SCO-Δ*ppk* + pRA$^{apr/aadA}$*lon* growth profile in solid culture. Single recombinant colonies were grown in R2YE for 72 hours at 30 ºC.

To prove the presence of the *lon* gene in the SCO-Δ*ppk* + pRA$^{apr/aadA}$*lon* genome we performed southern blot hybridization analysis. Genomic DNA of SCO-Δ*ppk* + pRA$^{apr/aadA}$*lon* cell was isolated and digested with the *Nco*I and *Sph*I restriction endonucleases, which have a single cutting site on the pRA$^{apr/aadA}$*lon* plasmid. The size of the fragment containing the native *lon* gene was determined by determining the *Nco*I and *Sph*I restriction profile of StCB12 cosmid on the NEB cutter database. As a result of Southern blot hybridization analysis, it was observed that the *lon* probe was bound to a 9226 bp pRA$^{apr/aadA}$*lon* plasmid band containing *lon* and *aadA* gene fragments, and to a 7565 bp band containing the native *lon* gene fragment as expected (Fig. 8.16).

Figure 8.16: Southern blot analysis of SCO-Δ*ppk* + pRA$^{apr/aadA}$*lon*. The bands to which the *lon* probe is bound were marked with black arrows. The size of the *lon* gene used as a probe is 6000 bp.

8.8.1. Obtaining pRA$^{apr/aadA}$ Plasmid and SCO-Δ*ppk* + pRA$^{apr/aadA}$ Strain

The cells carrying the pRA$^{apr/aadA}$*lon* plasmid showed different growth characteristics from *Streptomyces* cells. To find out whether the expression of the *lon* gene was the

reason for this result we prepared the same plasmid without *lon* gene, pRA$^{apr/aadA}$. For this, the *aad*A gene was cloned into the *Eco*RV site of pRA^{apr} plasmid in *E. coli* DH5α and the recombinant plasmid was transferred to *E. coli* ET12567/pUZ(8002) cells. The presence of the *aad*A gene in the pRA$^{apr/aadA}$ plasmid was verified by digesting it with *Xba*I and PCR (Fig. 8.17). After verification, pRA$^{apr/aadA}$ plasmid was transferred to SCO-Δ*ppk* cells by conjugation. New recombinant cells were selected according to their resistance to streptomycin. Surprisingly, the recombinant cell obtained (SCO-Δ*ppk*+ pRA$^{apr/aadA}$) had a similar colony form to SCO-Δ*ppk*+ pRA$^{apr/aadA}$*lon* cells and they were similarly defective in antibiotic production (Fig. 8.18). This proved that the morphological and metabolic changes in the recombinant cell were not caused by the expression of the *lon* gene.

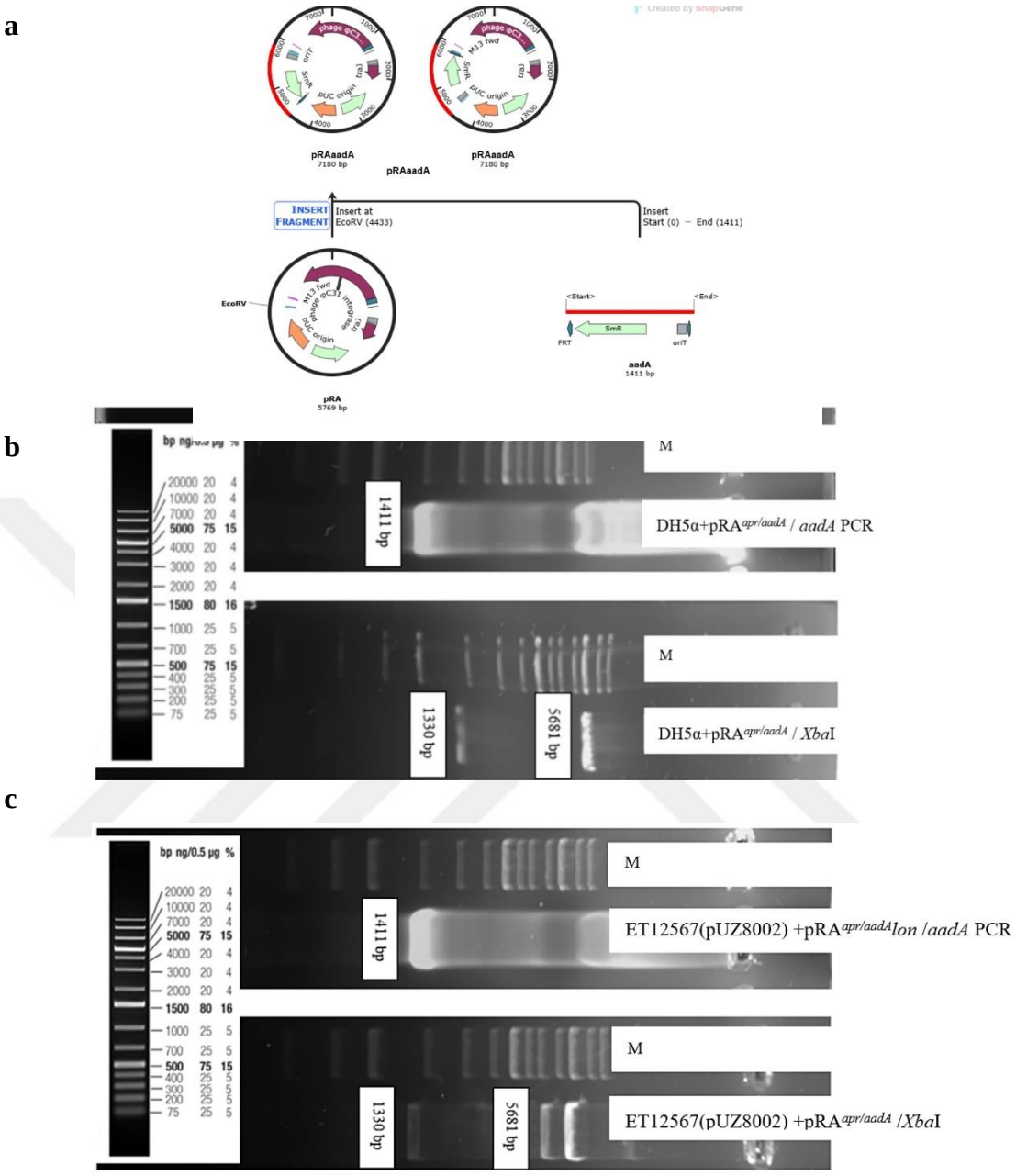

Figure 8.17: Verifying the pRA$^{apr/aadA}$ plasmid. Contructing pRA$^{apr/aadA}$ plasmid(a). *Xba*I restriction profile and PCR results were represented for *E. coli* DH5α+ pRA$^{apr/aadA}$ (b) and *E. coli* ET12567/pUZ8002+ pRA$^{apr/aadA}$ (b). The second band (1330 bp) observed in the *Xba*I digestion belongs to the inner region of the *aad*A gene. The 169 bp band was not perfectly visualised because it was out of the marker sizes. According to PCR results, the pRA$^{apr/aadA}$ plasmid transferred to both cells contains the *aad*A gene.

Figure 8.18: SCO-Δ*ppk* + pRA$^{apr/aadA}$ growth profile in solid culture. Single recombinant colonies were grown in R2YE for 72 hours at 30 ^{o}C.

To prove the presence of the *aadA* gene in the SCO-Δ*ppk* + pRA$^{apr/aadA}$ genome we performed southern blot hybridization analysis. Genomic DNA of SCO-Δ*ppk* + pRA$^{apr/aadA}$ was isolated and digested with the *Nco*I and *Sph*I. As a result of Southern blot hybridization, it was observed that the *aadA* probe was bound to the 5826 bp DNA band containing the *aad*A gene as expected (Fig. 8.19). The results indicated that the morphological and metabolic changes observed in SCO-Δ*ppk* + pRA$^{apr/aadA}$*lon* cells were not caused by the integration and expression of the *lon* gene. We hypothesized that the *aad*A gene might be causing these unexpected changes. Therefore, it was decided to transfer the pRA$^{apr/aadA}$ plasmid to the wild-type cells for further study.

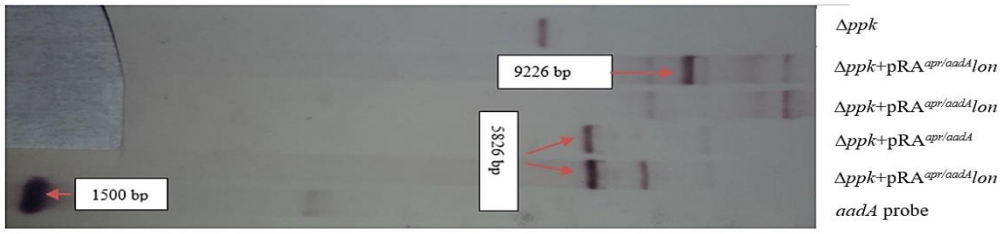

Figure 8.19: Southern blot analysis of SCO-Δ*ppk* + pRA$^{apr/aadA}$ and SCO-Δ*ppk* + pRA$^{apr/aadA}$*lon* . The bands to which the *aadA* probe is bound were marked with red arrows. The size of the *aadA* gene used as the probe is 1411 bp.

8.8.2. Obtaining SCO-pRA^{aadA} Strain

To determine whether the unusual growth and antibiotic production behaviours of SCO-Δ*ppk* + pRA$^{apr/aadA}$ and SCO-Δ*ppk* + pRA$^{apr/aadA}$*lon* strains were an effect of the

streptomycin resistance gene, we transferred the pRA$^{apr/aadA}$ into the wild-type strain. SCO+ pRA^{aadA} cells were generated by the same procedure used to generate recombinant SCO-Δ*ppk* cells. New recombinant cells were selected according to their resistance to streptomycin and were grown in R2YE.

Southern blot hybridisation with genomic DNA and PCR were performed to validate the presence of the *aad*A gene in SCO+ pRA^{aadA} cells. A 5530 bp fragment of genomic DNA containing the *aad*A gene was hybridised to the *aadA* probe on the Southern membrane as expected (Fig. 8.20a). Similarly, a 2875 bp PCR fragment containing the *aadA* gene was hybridised to the *aadA* probe (Fig. 8.20b).

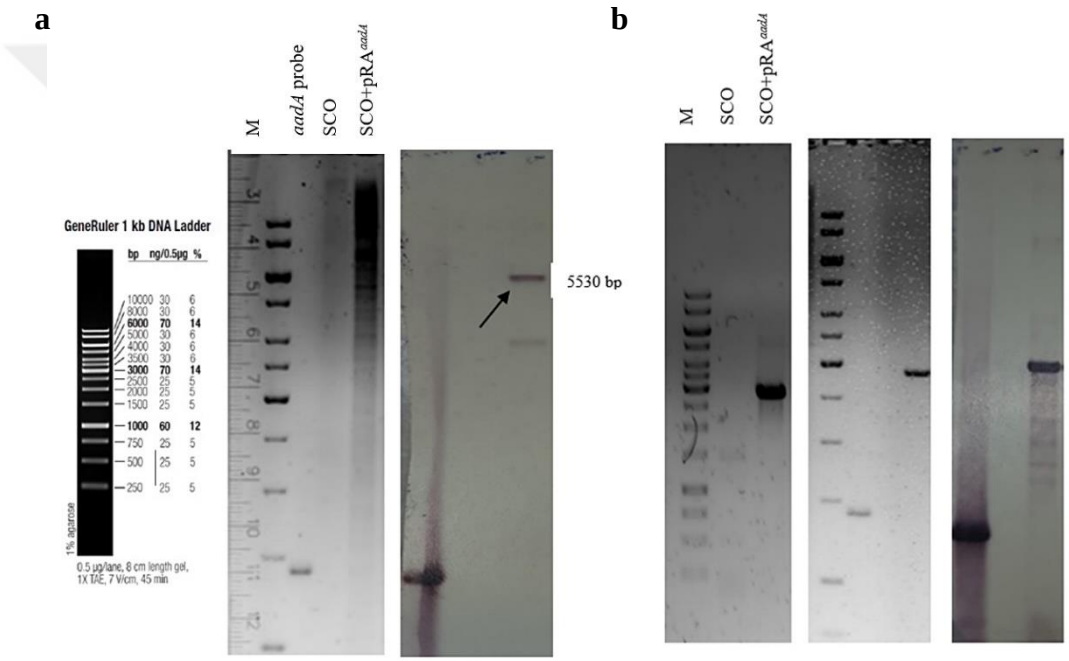

Figure 8.20: Verification of the presence of one copy of *aad*A gene in *S. coelicolor* A3(2) genome by Southern blot hybridisation (a), PCR (b-left panels), and Southern blot hybridisation results of PCR products (b-right panel). Agarose gel images of digested genomic DNAs and PCR products (a and b left panels). The size of the *aadA* gene used as the probe is 1411 bp.

The new recombinant cell was found to have dispersed colony formation and have the same growth profile as the streptomycin resistance gene expressing recombinant SCO-Δ*ppk* cells on R2YE (Fig. 8.21a and b). The results indicate that the changes in growth and antibiotic production are due to the presence of the *aad*A gene in the genome of

the recombinant cells and not to the expression of the *lon* gene or the absence of the *ppk* gene.

To determine the sporulation behaviour of SCO + pRA^{aadA}, the cells were observed on TBO agar for 10-12 days. It was observed that the recombinant cells could not sporulate on TBO and even failed to grow (Fig. 8.21b).

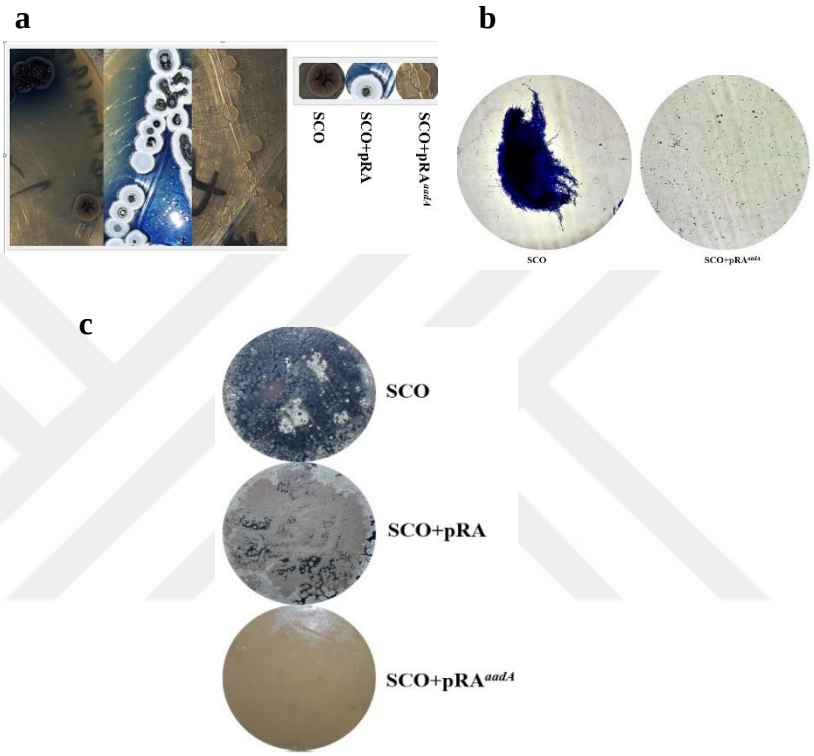

Figure 8.21: SCO + pRA^{aadA} growth in solid (a) and liquid culture (b). Single SCO + pRA$^{apr/aadA}$ colonies were grown in R2YE for 72 hours at 30 ^{o}C (a). 24 h cultures of wild-type and recombinant cells were stained with crystal violet and examined under a phase-contrast microscope at 20x magnification (b). Sporulation profile of SCO, SCO+pRA, SCO+pRA^{aadA} (c). The inoculum on TBO was 16 mg/ml of each cell.

8.8.3. Determining Releasing Compound(s) of SCO+pRA^{aadA}

8.8.3.1. Determining The Effect of Supernatant of SCO+pRA^{aadA} on the Growth of SCO

Given the perplexing morphology of the SCO+pRA^{aadA} colonies, we postulated that the peculiar behaviour of the SCO+pRA^{aadA} cells might be attributable to their production of extracellular metabolite(s) that could affect their growth. To test the

impact of the compounds released by the SCO+pRA^{aadA} cells on the colony formation of wild-type cell and its antibiotic production, the wild-type cells were treated with the supernatant of the 120-hour grown SCO+pRA^{aadA} cells. The supernatant of the SCO+pRA^{aadA} cells grown in R2YE for 120 hours at 30°C was filtered through a 0.22 μm filter (NEST vacuum filtration systems). The absence of any microorganisms in the filtrate was tested by inoculating 100-200 ml of filtrate onto the R2YE agar plate (without any antibiotics). 3 ml of supernatant was mixed with 0.05 g of SCO cells and inoculated onto a 15 ml R2YE agar plate. The results demonstrated that the supernatant treatment caused a great reduction in the number of viable cells and unexpectedly the colonies were transparent (Fig. 8.22). In addition, cells treated with the supernatant were unable to produce the colored antibiotics (blue and red).

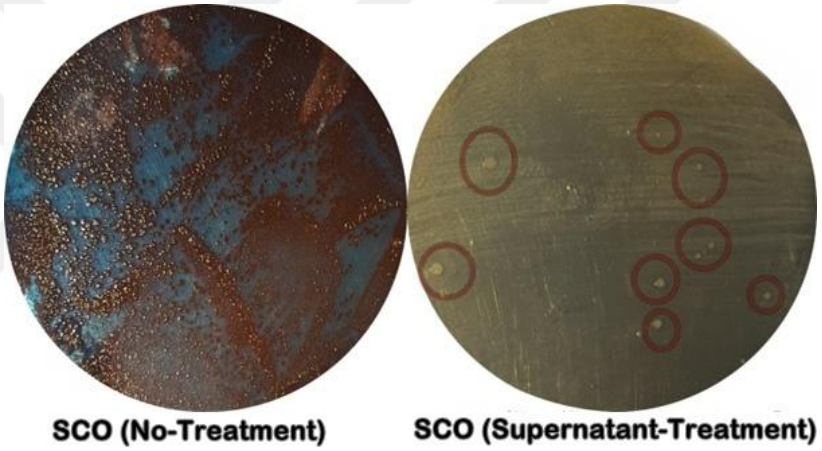

Figure 8.22: SCO cell growth after being treated with the supernatant of the 120-hour grown SCO+pRA^{aadA} cells . All cells were grown in R2YE at 30 ºC. 0.05 g of SCO was inoculated on to each plate.

8.8.3.2. HPLC Analysis of SCO+pRA^{aadA} Cells

To ascertain the metabolic changes in SCO+pRA^{aadA}, High-Performance Liquid Chromatography (HPLC) analysis was performed. SCO and SCO+pRA^{aadA} cells were cultured in R2YE for 48 hours, after which the resulting extracts were analysed. The results showed that the recombinant strain produced two metabolites that the wild-type strain did not produce (Fig. 8.23). The metabolite arriving at the 13.5th minute of flow was produced in significantly higher quantities compared to the metabolite arriving at the 15th minute (Fig. 8.23). While preliminary evidence suggests that these novel metabolites produced by the recombinant strain are associated with primary

metabolism, further identification and characterization is required. In the event that these metabolites are deemed to be of industrial significance, future studies should be conducted to investigate their production in high quantities.

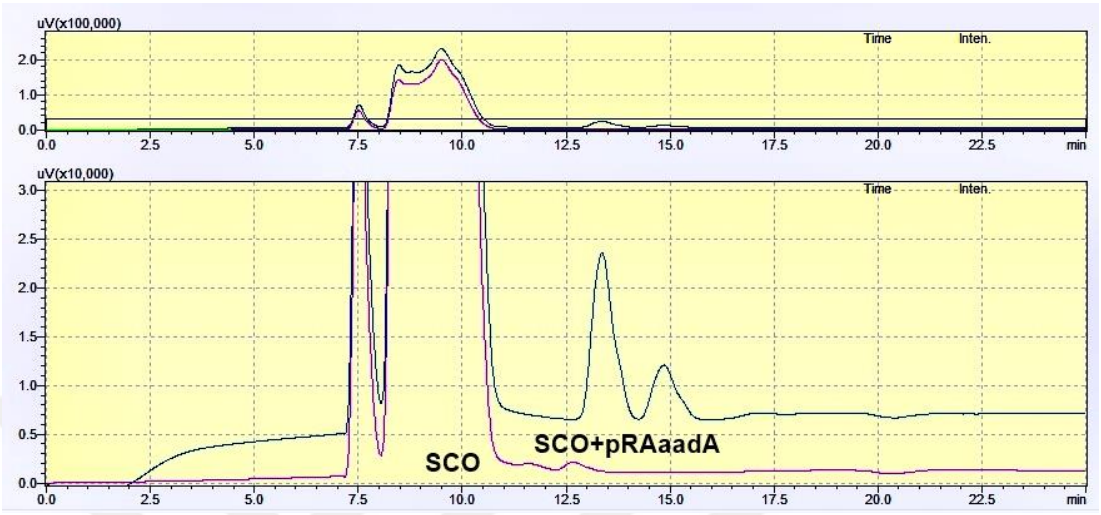

Figure 8.23: HPLC Analysis of the supernatant of SCO+pRA^{aadA} cells. All cells were grown in R2YE for 48 h at 30 ^{o}C.

9. DISCUSSION

The ATP-dependent Lon protease is a crucial intracellular protein that plays significant roles in bacterial survival and pathogenesis. This enzyme was first identified in *E. coli* cells, and its importance has been underscored by various studies over the years. A seminal study by Kuroda (2006) demonstrated the relationship between ATP-dependent Lon protease and the stringent response pathway in *E. coli*. The stringent response is a global regulatory system that permits bacteria to adapt to nutrient deprivation and other stress conditions by altering gene expression, protein synthesis, and metabolic activities. The stringent response pathway, influentially modulated by the ATP-dependent Lon protease, has been demonstrated to affect secondary metabolite production in *Streptomyces* species (Kuroda, 2006). Secondary metabolites are compounds that do not play a direct role in organisms' normal growth, development or reproduction; however, the production of these secondary metabolites has been a focus in research, because of their potential applications in medicine and biotechnology.

The present study concentrated mainly on a set of enzymes deemed critical to various metabolic processes, with particular reference to those involved in the stringent response and secondary metabolite production. The enzymes that were the subject of investigation included: Polyphosphate kinase, PPK, (Q9KZV6), an enzyme involved in the synthesis of polyphosphate, a polymer that plays a role in energy metabolism and stress response. RelA (P52560), a key enzyme in the stringent response, responsible for the synthesis of (p)ppGpp, which regulates the global adaptation to nutrient stress. Exopolyphosphatase, PPX, (Q9X8H1) which degrades polyphosphate, thereby balancing its levels and linking it to various cellular processes. Kinase/Phosphohydrolase/SpoT (O69970) is involved in the synthesis and hydrolysis of (p)ppGpp, functioning alongside with RelA in the stringent response. tRNA Synthetase (Q9ZBH7) plays a crucial role in protein synthesis by charging tRNAs with their corresponding amino acids. ATP-dependent Lon protease (Q9EVK2), an enzyme that plays a significant role in the degradation of misfolded or damaged proteins, thereby impacting the stringent response and overall cellular homeostasis. To enhance understanding and improve the production of secondary metabolites, a novel model was developed focusing on secondary metabolite production in the present study. This

model is referred to as necSco-GEM which represents an enhancement of the existing ecSco-GEM. The enhancement of secondary metabolite production was achieved by integrating 27 new reactions and 21 metabolites related to secondary metabolism into the existing ecSco-GEM framework.

In silico simulations performed using necSco-GEM have provided results that align with previous experimental findings. Notably, these results indicate that the enzyme PPK has a significant negative effect on the production of actinorhodin. These findings are consistent with prior studies conducted by Yalim Camci et al. (2012) highlighting PPK's inhibitory role in ACT production. This comprehensive study emphasises the intricate network of interactions between various enzymes and their collective influence on metabolic pathways, particularly those involved in secondary metabolite production. The development of the necSco-GEM model represents a significant step forward in our ability to predict and manipulate these metabolic processes, offering valuable insights for future research and potential applications in biotechnology and medicine.

The Lon protease gene (*lon*) has been proven to play a pivotal role in triggering antibiotic production in *S. coelicolor*, as demonstrated by Demir et al. (2019). To investigate the specific effects of *lon* overexpressing in a strain deficient in the *ppk* gene, two *in silico* strains were constructed: nec-ScoGEM-Δ*ppk*+pRA*lon* and nec-ScoGEM-Δ*ppk*. In both models, the *ppk* gene was knocked out to assess the impact of *lon* overexpressing in the absence of PPK activity. Ensemble modelling was applied to explore the potential effects of *lon* overexpressing on the production of actinorhodin (ACT). It was found that there were significant changes in metabolic fluxes associated with *lon* overexpression. This included an 8.3-fold increase in the *nuo A-N* operon (NADH dehydrogenase/complex-I) flux, indicating enhanced activity in the electron transport chain, which is crucial for cellular respiration and energy production. Additionally, a 5-fold increase was recorded in superoxide dismutase activity, an enzyme that plays a critical role in protecting cells from oxidative stress by converting superoxide radicals into hydrogen peroxide and oxygen. This increase suggests that *lon* overexpression may enhance the cellular defence mechanisms against reactive oxygen species. Furthermore, a 5-fold increase in Beta-ketoacyl-[acyl-carrier-protein] synthase III, an enzyme involved in fatty acid biosynthesis, was also observed. This enzyme catalyzes the initial step in the elongation process of fatty acid synthesis,

highlighting the potential shift in metabolic fluxes towards the biosynthesis of key cellular components. The findings highlight the intricate interplay between lon protease and diverse metabolic pathways in *S. coelicolor*. The substantial alterations in metabolic fluxes observed in the nec-ScoGEM-Δ*ppk*+pRA*lon* strain offer valuable insights into the mechanisms underlying antibiotic production and the broader metabolic adaptations associated with lon protease. These findings contribute to a more comprehensive understanding of the regulatory networks governing secondary metabolite production and offer potential avenues for optimising antibiotic yields in industrial and therapeutic applications.

In addition, we conducted an ensemble modelling investigation into the enzymes contributing to secondary metabolite production, with a particular focus on the *nuo A-N* operon and the production of actinorhodin. The implementation of ensemble modelling facilitates a comprehensive analysis through the integration of multiple models, thereby enabling the prediction of the collective behaviour of metabolic networks under diverse conditions. The results of this analysis highlighted several key enzymes that significantly influence ACT production in the nec-ScoGEM-Δ*ppk*+pRA*lon* model. Specifically, the following key findings were identified: Q9AK84 (SCO1378) - Glycine Dehydrogenase (Decarboxylating) / EC 1.4.4.2, O86567 (SCO5472) - Aminomethyltransferase (Glycine Cleavage System T Protein) / EC 2.1.2.10, P72392 (SCO2388) - Beta-Ketoacyl-[Acyl-Carrier-Protein] Synthase III. The results of the ensemble modelling revealed that these enzymes have a substantial positive effect on ACT production in the nec-ScoGEM-Δ*ppk*+pRA*lon* strain. The significant upregulation of these enzymes suggests their critical roles in enhancing the flux towards ACT biosynthesis. Specifically, the integration of these enzymes into the metabolic network appears to optimize the flow of precursors and energy, thereby boosting the overall production of ACT. These findings underscore the importance of the glycine cleavage system and the malonic acid pathway in regulating secondary metabolite production. By elucidating the specific contributions of these enzymes, researchers can develop targeted strategies to manipulate these pathways, thereby optimizing the yield of valuable secondary metabolites like ACT.

The findings of the Ensemble modelling suggest that the precursor reactions necessary for ACT production are significantly activated in the nec-ScoGEM-Δ*ppk*+pRA*lon* strain. To validate these *in silico* findings, an experiment was conducted in which an

additional copy of the *lon* gene was integrated into the SCOΔ*ppk* genome. The successful integration of the *lon* gene was confirmed using a Southern blot analysis. Following this genetic modification, the antibiotic production of the recombinant strain was examined. The results of these experiments were consistent with the *in silico* data, thereby demonstrating the accuracy of our computational predictions. Specifically, the strain SCOΔ*ppk*+pRA*lon* exhibited a ~1.5-fold increase in actinorhodin production compared to the SCOΔ*ppk* strain. Furthermore, a 7.5-fold increase in actinorhodin production was observed when the SCOΔ*ppk*+pRA*lon* strain was compared to the SCOΔ*ppk*+pRA cells.

Superoxide dismutase (SOD) is an enzyme that plays a crucial role in mitigating oxidative stress. The in silico finding of increased SOD activity in the recombinant cells was confirmed by in vitro experiments. Specifically, the fold change in SOD activity between the SCOΔ*ppk* and SCO-Δ*ppk*+pRA*lon* strains was calculated to be 5 in the *in silico* models, while the *in vitro* experiments showed a 1.1-fold increase.

The obtained observations provide compelling evidence that overexpressing the *lon* gene in the SCOΔ*ppk* significantly enhances both actinorhodin production and superoxide dismutase (SOD) activity. The congruence observed between the *in silico* models and the experimental data serves to emphasise the robustness of the approach employed, thus providing valuable insights concerning future research and biotechnological applications.

The bacterial electron transport chain (ETC) is a vital metabolic pathway. Proteins embedded in the cell membrane transfer electrons and generate a proton gradient. This gradient drives ATP synthesis, which is a crucial energy source for bacterial cells. The electron transport system (ETS) comprises a series of protein complexes, with the first being Complex I, also known as NADH: ubiquinone oxidoreductase or NADH dehydrogenase-I. This complex oxidises NADH, transferring two electrons (2e-) from NADH to coenzyme Q (ubiquinone), and concomitantly pumps four protons (4H+) out of the cell membrane per NADH molecule. This process of proton pumping generates a proton motive force across the membrane. Subsequent to Complex I, electrons are transferred sequentially to Complex Q, then to Complex III (cytochrome c reductase), and finally to Complex IV (cytochrome c oxidase). These complexes perpetuate the process of electron transfer and proton pumping, thereby contributing to the maintenance of the proton gradient. The final component of the electron transfer

system (ETS) is Complex V (ATP synthase), which utilises the proton gradient created by the preceding complexes to synthesise ATP from ADP and inorganic phosphate (Pi), thereby providing the cell with essential energy. In *S. coelicolor* A3(2), the expression of the SCO *nuo* operon (which encodes NADH-I) genes was observed to increase during the stationary phase[Brekasis & Paget, 2003]. This increase in expression facilitates the rapid conversion of reduced NADH into a proton motive force, thereby supplying energy to cells that are deprived of nutrients[Virolle, 2020,Zambrano & Kolter, 1993]. Nevertheless, elevated levels of NADH dehydrogenase/Complex I activity have also been demonstrated to result in increased oxidative stress within the cell, as posited by Virolle, (2020). This oxidative stress is a consequence of the elevated generation of reactive oxygen species (ROS) during electron transport. It is noteworthy that oxidative stress can stimulate the synthesis of actinorhodin (ACT), a secondary metabolite with antioxidant properties, which contributes to the mitigation of the deleterious effects of ROS [Virolle, 2020]. The modelling outcomes demonstrate that the nec-ScoGEM-Δ*ppk*+pRA*lon* strain exhibits a significant increase in the expression of the *nuo* A-N operon at 24 hours post-inoculation, a response not observed in the SCO wild-type strain. This increase, estimated at approximately eight-fold, has the potential to significantly impact various metabolic processes. In cases of NADH/NAD+ imbalance, serine, a component of the glycine cleavage system, is utilised for NADH production [Yang et al., 2020]. This finding corroborates the results of the modelling, which demonstrate an increase in the activity of beta-ketoacyl-[acyl-carrier-protein] synthase, an enzyme that is involved in the glycine cleavage system. In conclusion, it is hypothesised that the above metabolic processes are likely to result in increased oxidative stress within the cell. This oxidative stress, in turn, has been shown to induce the production of actinorhodin, using its antioxidant properties to protect the cell from damage. The up-regulation of key enzymes and operons involved in these pathways highlights the intricate relationship between oxidative stress, metabolic regulation and secondary metabolite production in *S. coelicolor*.

As demonstrated in previous studies the PhoR/PhoP regulon has been shown to positively control the *ppk*/*pptA*/*SLI*-4382 operon in *Streptomyces lividans* under phosphate (Pi) limitation [Shikura et al., 2021]. The enzyme PPK produces polyP in the presence of high ATP levels, and also generates ATP during energy starvation

[Ghorbel et al., 2006]. PolyP also serves as a crucial energy reserve that bacteria can mobilise during stress. The deficiency of PPK leads to a decrease in ATP levels, prompting the cell to shift towards oxidative metabolism to compensate for the energy shortfall [Esnault et al., 2017,Millan-Oropeza et al., 2020]. In oxidative metabolism, acetyl-CoA, a central metabolite, is diverted into the tricarboxylic acid (TCA) cycle, also known as the Krebs cycle. The TCA cycle is responsible for the generation of reduced cofactors such as NADH and $FADH_2$. These cofactors are subsequently reoxidized within the electron transport chain, a process that culminates in the production of ATP. However, this process also results in the generation of reactive oxygen species (ROS) and reactive nitrogen species (NOS), which can cause oxidative stress within the cell. Oxidative stress is characterised by an imbalance between the production of ROS and NOS and the antioxidant defences of the cell, potentially resulting in damage to cellular components such as DNA, proteins, and lipids. The production of ACT is triggered by oxidative stress, which is in turn caused by the presence of ROS and NOS [Lejeune et al., 2022]. The function of ACT is to neutralise these reactive species, thus protecting the cell from any subsequent oxidative damage. (Kusano & Ishihama (1997)(Ge et al., 2007; Lacour & Landini, 2004; Taverna & Sedgwick, 1996). A comprehensive analysis of the STRING database revealed no direct interaction between the *nuo* A-N operon, the glycine degradation system, or the ACT cluster and the enzymes associated with the stringent response (Fig. 8.5). This finding suggests that, although these pathways may not directly interact at the protein-protein interaction level, they are likely to be regulated by small regulatory molecules, which orchestrate complex cellular responses. It has been established that a high concentration of guanosine tetraphosphate (ppGpp) is capable of triggering the stringent response mechanism in *E. coli* [Chang et al., 2002]. This molecule is regarded as a global regulator, with the capacity to modulate a diverse spectrum of cellular processes, thus ensuring the adaptation of bacteria to conditions that are characterised by a paucity of nutrients, in addition to periods of stress. A critical effect of ppGpp is the synthesis of the rpoS subunit of RNA polymerase, which is essential for bacterial survival during the stationary phase [Gentry et al., 1993]. During this stage, RpoS modulates the expression of numerous genes associated with DNA repair, stationary metabolism, and secondary metabolite production [Ge et al., 2007,Lacour & Landini, 2004,Taverna & Sedgwick, 1996]. This regulatory process enables bacterial cells to effectively manage stress and preserve viability, thereby ensuring their adaptation and

survival in the stationary phase. Furthermore, polyP has been identified as a possible inducer of the stationary phase (Batt, 2014). In further support of this, a study by Kusano & Ishihama (1997)demonstrated that polyP possesses the capacity to modulate RNA polymerase activity, thereby influencing the transcription of genes that are essential for adaptation to the stationary phase. The precise function of polyP in *Streptomyces* species has yet to be fully elucidated; however, it is hypothesised to function similarly to polyP in *E. coli.* A more detailed investigation of the interactions between ppGpp, PPK/polyP, RpoS, and other related pathways in *Streptomyces* species would provide a more profound understanding of bacterial stress responses and metabolic regulation.

As demonstrated by (Chung et al., 1999) the sodF2 gene was identified in *S. coelicolor* in 1998. Subsequent studies have demonstrated the sodF2's capacity to enhance the production of secondary metabolites in *Streptomyces clavuligerus* and *Streptomyces lividans* [Kanth et al., 2011]. This finding is further substantiated by the documented interaction between SodF2 and ACT in *S. lividans*, where the expression of sodF2 resulted in a 1.6-fold increase in ACT production. The impact of superoxide dismutase (SOD) on *Streptomyces* mortality remains to be the subject of investigation. Nevertheless, based on the present state of understanding, a reasonable hypothesis is that the elimination of free radicals by SOD should have a beneficial effect on cell survival and reduce cell mortality. We can say that the SCOΔ*ppk*+pRA*lon* strain had a lower mortality rate in vegetative growth compared to other strains, including SCO, SCOΔ*ppk*, and SCOΔ*ppk*+pRA, although the number of viable spores was lower. This is attributed to the individual antioxidant effects of both actinorhodin (ACT) and superoxide dismutase (SOD). ACT itself is recognised for its antioxidant properties, which help neutralise reactive oxygen species (ROS) and protect cells from oxidative damage. When combined with the enhanced activity of SOD, the dual antioxidant effect could provide a synergistic protective mechanism, further reducing cell mortality in the recombinant strain during vegetative growth.

The present study proves that GEMs are reliable starting point for *in vitro Streptomyces* studies. Specifically, a simulation was conducted to explore the impact of an additional *lon* gene on the SCOΔ*ppk* recombinant cell, which is known to be deficient from polyP synthesising enzyme. This analysis enabled us to identify the pathways and enzymes that regulate ACT synthesis. Especially, NADH

dehydrogenase/complex I and beta-ketoacyl-[acyl-carrier-protein] synthase III were found to play an important role in ACT production. Similarly, the glycine cleavage system and superoxide dismutase have been shown to positively affect antibiotic production, probably by maintaining the balance in the respiratory system of the recombinant cell. This finding is significant as it is the first study to demonstrate the positive effects of the glycine cleavage system and superoxide dismutase on ACT production.

Streptomyces species are known to produce high levels of many secondary metabolites of medical and biotechnological importance. However, it has been recognized that *Streptomyces* species may be natural resources that can also produce primary metabolites of industrial importance. However, to date, research focusing on the primary metabolites of *Streptomyces* has been very limited. Although this study focused on the secondary metabolite production of *S. coelicolor* as the primary target, it opened a new area of research by showing that heterologous expression of the *aad*A gene triggers primary metabolism by shutting down secondary metabolism. Increasing the production of primary metabolites is of great importance for several industrial sectors, including pharmaceuticals, agriculture and food technology. This study is of particular importance as it demonstrates the unexplored potential of *Streptomyces* species as a natural source of primary metabolite production.

Table 7.10: Primers and PCR conditions

Primers	Sequence	Amplicon size	PCR Cycle			
lon-F *lon*-R	CGA TGA GCA GGT GCG GAG CG CTC CTA CAA CGT CGG CAT GAT	3397 bp	**Initial Denaturation**	**98 ºC**	**10 min**	
			Denaturation	98 ºC	10 sn	35 cycles
			Primer Annealing	60 ºC	30 sn	
			Extension	72 ºC	180 sn	
			Final Extension	72 ºC	2 min	
			Hold	4 ºC	60 min	
ppk-F *ppk*-R	ATAATTCCATATGATGAAGCCGACC GAGC ACTAGTTCAAGGTGTCGCTGTGC	2344 bp	**Initial Denaturation**	**98 ºC**	**10 min**	
			Denaturation	98 ºC	10 sn	35 cycles
			Primer Annealing	63 ºC	30 sn	
			Extension	72 ºC	45 sn	
			Final Extension	72 ºC	2 min	
			Hold	4 ºC	60 min	

Table 7.10: Primers and PCR conditions (continued).

Primers	Sequence	Amplicon size	PCR Cycle			
kn-F *kn*-R	GTGCTGACCCCGGATGAATGT AGCGGGGCAGGATAGGTGAAGTAG	1520 bp	**Initial Denaturation**	**98 ºC**	**5 min**	
			Denaturation	98 ºC	10 sn	35 cycles
			Primer Annealing	60 ºC	30 sn	
			Extension	72 ºC	40 sn	
			Final Extension	72 ºC	2 min	
			Hold	4 ºC	60 min	
*aad*A-F *aad*A-R	ATTCCGGGGATCCGTCGACC TGTAGGCTGGAGCTGCTTC	1411 bp	**Initial Denaturation**	**98 ºC**	**10 min**	
			Denaturation	98 ºC	10 sn	35 cycles
			Primer Annealing	60 ºC	30 sn	
			Extension	72 ºC	40 sn	
			Final Extension	72 ºC	2 min	
			Hold	4 ºC	60 min	

Table 7.10: Primers and PCR conditions (contiued).

Primers	Sequence	Amplicon size	PCR Cycle			
pRA-F pRA-R (Proof primers)	GTTTCGCCACCTCTGACTTG AACGCCCTTGAAGAGCTGTA **Caution:** We obtain ~ 1500 bp bant when we use *S. co* A3(2) genome so *S. co* A3(2)+pRA cannot be proved by using these primers.	1464 (start 4037 stop 5501) + insert bp	**Initial Denaturation**	**98 ºC**	**5 min**	
			Denaturation	98 ºC	10 sn	35 cycles
			Primer Annealing	65 ºC	30 sn	
			Extension	72 ºC	- sn depends on insert size	
			Final Extension	72 ºC	2 min	
			Hold	4 ºC	60 min	
lon probe-*F* *lon* probe-*R*	CGAGCTGGTGAAGGAGT CTTCTCGTCCTCCGTGT	1141 bp	**Initial Denaturation**	**98 ºC**	**10 min**	
			Denaturation	98 ºC	10 sn	35 cycles
			Primer Annealing	55 ºC	30 sn	
			Extension	72 ºC	45 sn	
			Final Extension	72 ºC	2 min	
			Hold	4 ºC	60 min	

Table 7.10: Primers and PCR conditions (continued).

Primers	Sequence	Amplicon size	PCR Cycle			
lon-F	CGAGCTGGTGAAGGAGTACA	161 bp	**Initial Denaturation**	**95 ºC**	**5 min**	
lon-R	*GCAGTTCGACCTTCTGCTC*					
HrdB-F	*TGCCTTCCTGGACCTCAT*	86 bp	**Denaturation**	95 ºC	15 sn	40 cycles
HrdB-R	*GAATTGTAGCCCTTGGTGTAG*		**Primer Annealing**	60 ºC	30 sn	
hrdB-F	CTCTTCCTGGACCTCATCCA	543 bp	**Extension**	60 ºC	40 sn	
hrdB-R	GTACACCTTGCCGATCTCGT					

REFERENCES

Akiyama, M., Crooke, E., & Kornberg, A.,(1993),"An exopolyphosphatase of *Escherichia coli*: The enzyme and its ppx gene in a polyphosphate operon",Journal of Biological Chemistry, 268(1), 633–639. https://doi.org/10.1016/s0021-9258(18)54198-3

Alam, M. T., Merlo, M. E., Hodgson, D. A., Wellington, E. M. H., Takano, E., & Breitling, R.,(2010),"Metabolic modeling and analysis of the metabolic switch in *Streptomyces coelicolor*",BMC Genomics, 11(1). https://doi.org/10.1186/1471-2164-11-202

Amara, A., Takano, E., & Breitling, R.,(2018),"Development and validation of an updated computational model of *Streptomyces coelicolor* primary and secondary metabolism",BMC Genomics, 19(1). https://doi.org/10.1186/s12864-018-4905-5

Andreeva, N., Ryazanova, L., Dmitriev, V., Kulakovskaya, T., & Kulaev, I.,(2013),"Adaptation of *Saccharomyces cerevisiae* to toxic manganese concentration triggers changes in inorganic polyphosphates",FEMS Yeast Research, 13(5), 463–470. https://doi.org/10.1111/1567-1364.12049

Andreeva, N., Ryazanova, L., Dmitriev, V., Kulakovskaya, T., & Kulaev, I.,(2014),"Cytoplasmic inorganic polyphosphate participates in the heavy metal tolerance of *Cryptococcus humicola*",Folia Microbiologica, 59(5), 381–389. https://doi.org/10.1007/s12223-014-0310-x

Barreiro, C., & Martínez-Castro, M.,(2019),"Regulation of the phosphate metabolism in *Streptomyces* genus: impact on the secondary metabolites",Appl Microbiol Biotechnol, 103(4), 1643-1658. doi: 10.1007/s00253-018-09600-2. https://doi.org/10.1007/s00253-018-09600-2

Bentley, S. D., Chater, K. F., Cerdeñ O-Tá Rraga, A.-M., Challis, G. L., Thomson, N. R., James, K. D., Harris, D. E., Quail, M. A., Kieser, H., Harper, D., Bateman, A., Brown, S., Chandra, G., Chen, C. W., Collins, M., Cronin, A., Fraser, A., Goble, A., Hidalgo, J., … Hopwood, D. A.,(2002),″ Complete genome sequence of the model actinomycete Streptomyces coelicolor A3(2)", Nature, 417(6885), 141-7. doi: 10.1038/417141a.

Bibb, M. J.,(2005),"Regulation of secondary metabolism in streptomycetes", Curr Opin Microbiol, 8(2), 208-15.https://doi.org/10.1016/j.mib.2005.02.016

Borodina, I., Krabben, P., & Nielsen, J.,(2005),"Genome-scale analysis of *Streptomyces coelicolor* A3(2) metabolism",Genome Research, 3(2), 820–829. https://doi.org/10.1101/gr.3364705.

Botos, I., Lountos, G. T., Wu, W., Cherry, S., Ghirlando, R., Kudzhaev, A. M., Rotanova, T. V., de Val, N., Tropea, J. E., Gustchina, A., & Wlodawer, A.,(2019),"Cryo-EM structure of substrate-free *E. coli* Lon protease provides insights into the dynamics of Lon machinery",Current Research in Structural Biology, 1, 13–20. https://doi.org/10.1016/j.crstbi.2019.10.001

Bowlin, M. Q., & Gray, M. J.,(2021),"Inorganic polyphosphate in host and microbe biology", Trends Microbiol, 29(11), 1013-1023. https://doi.org/10.1016/j.tim.2021.02.002

Breidenstein, E. B. M., Bains, M., & Hancock, R. E. W.,(2012),"Involvement of the lon protease in the SOS response triggered by ciprofloxacin in *Peudomonas aeruginosa* PAO1",Antimicrobial Agents and Chemotherapy, 56(6), 2879–2887. https://doi.org/10.1128/AAC.06014-11

Brekasis, D., & Paget, M. S. B.,(2003),"A novel sensor of NADH/NAD+ redox poise in *Streptomyces coelicolor* A3(2)",EMBO Journal, 22(18), 4856–4865. https://doi.org/10.1093/emboj/cdg453

Burby, P. E., & Simmons, L. A.,(2020),"Regulation of cell division in bacteria by monitoring genome integrity and DNA replication status",J Bacteriol, 202(2), e00408-19. https://doi.org/10.1128/JB.00408-19

Calmann, M. A., & Marinus, M. G.,(2003),"Regulated expression of the *Escherichia coli* dam gene",Journal of Bacteriology, 185(16), 5012–5014. https://doi.org/10.1128/JB.185.16.5012-5014.2003

Chang, D. E., Smalley, D. J., & Conway, T.,(2002),"Gene expression profiling of Escherichia coli growth transitions: An expanded stringent response model",Molecular Microbiology, 45(2), 289–306. https://doi.org/10.1046/j.1365-2958.2002.03001.x

Chung, C. H., & Goldberg, A. L.,(1981),"The product of the ion (capR) gene in *Escherichia coli* is the ATP-dependent protease, protease La (proteolytic enzymes/energy requirement/intracellular protein degradation)" ,Proc. NatL Acad. Sci. USA, 78 (8), 4931-4935. https://doi.org/10.1073/pnas.78.8.4931

Chung, H. J., Kim, E. J., Suh, B., Choi, J. H., & Roe, J. H.,(1999),"Duplicate genes for Fe-containing superoxide dismutase in *Streptomyces coelicolor* A3(2)",Gene, 231(1–2), 87–93. https://doi.org/10.1016/S0378-1119(99)00088-8

Clemmer, K. M., & Rather, P. N.,(2008),"The Lon protease regulates swarming motility and virulence gene expression in *Proteus mirabilis*",Journal of Medical Microbiology, 57(8), 931–937. https://doi.org/10.1099/jmm.0.47778-0

Demir, Z., Bayraktar, A., & Tunca, S.,(2019),"One Extra Copy of lon Gene Causes a Dramatic Increase in Actinorhodin Production by *Streptomyces coelicolor* A3(2)",Current Microbiology, 76(9), 1045–1054. https://doi.org/10.1007/s00284-019-01719-3

Dersch, L. M., Beckers, V., & Wittmann, C.,(2016),"Green pathways: Metabolic network analysis of plant systems",Metabolic Engineering, 34, 1-24. https://doi.org/10.1016/j.ymben.2015.12.001

Esnault, C., Dulermo, T., Smirnov, A., Askora, A., David, M., Deniset-Besseau, A., Holland, I. B., & Virolle, M. J.,(2017),"Strong antibiotic production is correlated with highly active oxidative metabolism in *Streptomyces coelicolor* M145",Scientific Reports, 7(1). https://doi.org/10.1038/s41598-017-00259-9

Fu, J., Zong, G., Zhang, P., Zhao, Z., Ma, J., Pang, X., & Cao, G.,(2017),"XdhR negatively regulates actinorhodin biosynthesis in *Streptomyces coelicolor* M145",FEMS Microbiol Lett., 364(22). https://doi.org/10.1093/femsle/fnx226

Ge, Y., Yang, S., Fang, Y., Yang, R., Mou, D., Cui, J., & Wen, L.,(2007),"RpoS as an intermediate in RsmA-dependent regulation of secondary antifungal metabolites biosynthesis in *Pseudomonas sp*. M18",FEMS Microbiology Letters, 268(1), 81–87. https://doi.org/10.1111/j.1574-6968.2006.00562.x

Gentry, D. R., Hernandez, V. J., Nguyen, L. H., Jensen, D. B., & Cashel, M.,(1993),"Synthesis of the stationary-phase sigma factor σ(s) is positively regulated by ppGpp",*Journal of Bacteriology*, *175*(24), 7982–7989. https://doi.org/10.1128/jb.175.24.7982-7989.1993

Ghorbel, S., Smirnov, A., Chouayekh, H., Sperandio, B., Esnault, C., Kormanec, J., & Virolle, M. J.,(2006),"Regulation of ppk expression and in vivo function of Ppk in *Streptomyces lividans* TK24",Journal of Bacteriology, 188(17), 6269–6276. https://doi.org/10.1128/JB.00202-06

Gramajo, H. C., Takano, E., & Bibb, M. J.,(1993a),"Stationary-phase production of the antibiotic actinorhodin in *Streptomyces coelicolor* A3(2) is transcriptionally regulated",Molecular Microbiology, 7(6), 837–845. https://doi.org/10.1111/j.1365-2958.1993.tb01174.x

Gramajo, H. C., Takano, E., & Bibb, M. J.,(1993b),"Stationary-phase production of the antibiotic actinorhodin in *Streptomyces coelicolor* A3(2) is transcriptionally regulated",Molecular Microbiology, 7(6), 837–845. https://doi.org/10.1111/j.1365-2958.1993.tb01174.x

Gur, E., Ottofueling, R., & Dougan, D. A.,(2013),"Machines of destruction – AAA+ proteases and the adaptors that control them",Subcellular Biochemistry, 66, 3–33. https://doi.org/10.1007/978-94-007-5940-4_1

Gust, B., Challis, G. L., Fowler, K., Kieser, T., & Chater, K. F.,(n.d.),"PCR-targeted Streptomyces gene replacement identifies a protein domain needed for biosynthesis of the sesquiterpene soil odor geosmin", Proc Natl Acad Sci U S A, 100(4), 1541-6. www.pnas.orgcgidoi10.1073pnas.0337542100

Gyun Kang, S., Jin, W., Bibb, M., & Joon Lee, K.,(1998),"Actinorhodin and undecylprodigiosin production in wild-type and relA mutant strains of *Streptomyces coelicolor* A3(2) grown in continuous culture", FEMS Microbiol Lett, 168(2), 221-6. doi: 10.1111/j.1574-6968.1998.tb13277.x.

Hanahan, D.,(1983),"Studies on Transformation of *Escherichia coli* with Plasmids",J Mol Biol., 166(4), 557-80. doi: 10.1016/s0022-2836(83)80284-8.

Harir, M., Bendif, H., Bellahcene, M., & Fortas and Rebecca Pogni, Z.,(2018a),"Streptomyces Secondary Metabolites",Basic Biology and Applications of Actinobacteria,IntechOpen. https://doi.org/10.5772/intechopen.79890

Harir, M., Bendif, H., Bellahcene, M., & Fortas and Rebecca Pogni, Z.,(2018b),"*Streptomyces* Secondary Metabolites",Basic Biology and Applications of Actinobacteria,IntechOpen. https://doi.org/10.5772/intechopen.79890

Jonas, K., Liu, J., Chien, P., & Laub, M. T.,(2013),"XProteotoxic stress induces a cell-cycle arrest by stimulating lon to degrade the replication initiator DnaA",Cell, 154(3). https://doi.org/10.1016/j.cell.2013.06.034

Kanth, B. K., Jnawali, H. N., Niraula, N. P., & Sohng, J. K.,(2011),"Superoxide dismutase (SOD) genes in Streptomyces peucetius: Effects of SODs on secondary metabolites production",Microbiological Research, 166(5), 391–402. https://doi.org/10.1016/j.micres.2010.07.003

Kell, D. B., & Goodacre, R.,(2014),"Metabolomics and systems pharmacology: Why and how to model the human metabolic network for drug discovery",Drug Discovery Today, 19, 171 - 182. https://doi.org/10.1016/j.drudis.2013.07.014

Khushboo, Kumar, P., Dubey, K. K., Usmani, Z., Sharma, M., & Gupta, V. K.,(2022),"Biotechnological and industrial applications of Streptomyces metabolites",Biofuels, 16.https://doi.org/10.1002/bbb.2294

Kim, M., Sang Yi, J., Kim, J., Kim, J. N., Kim, M. W., & Kim, B. G.,(2014),"Reconstruction of a high-quality metabolic model enables the identification of gene overexpression targets for enhanced antibiotic production in streptomyces coelicolor A3(2)",Biotechnology Journal, 9(9), 1185–1194. https://doi.org/10.1002/biot.201300539

Kong, D., Wang, X., Nie, J., & Niu, G.,(2019),"Regulation of Antibiotic Production by Signaling Molecules in *Streptomyces*",Front Microbiol., 10, 2927. https://doi.org/10.3389/fmicb.2019.02927

Kornberg, A., Rao, N. N., & Ault-Riché, D.,(1999),"Inorganıc Polyphosphate: A Molecule Of Many Functıons"., Annu Rev Biochem, 68, 89-125. doi: 10.1146/annurev.biochem.68.1.89.

Krysenko, S., & Wohlleben, W.,(2024a),"Role of Carbon, Nitrogen, Phosphate and Sulfur Metabolism in Secondary Metabolism Precursor Supply in *Streptomyces spp*.",Microorganisms, 12(8), 1571. https://doi.org/10.3390/microorganisms12081571

Krysenko, S., & Wohlleben, W.,(2024b),"Role of Carbon, Nitrogen, Phosphate and Sulfur Metabolism in Secondary Metabolism Precursor Supply in *Streptomyces spp*.",Microorganisms, 12(8), 1571. https://doi.org/10.3390/microorganisms12081571

Krysenko, S., & Wohlleben, W.,(2024c),"Role of Carbon, Nitrogen, Phosphate and Sulfur Metabolism in Secondary Metabolism Precursor Supply in *Streptomyces spp*.",Microorganisms, 12(8), 1571. https://doi.org/10.3390/microorganisms12081571

Kumar, V., Baweja, M., Singh, P. K., & Shukla, P.,(2016),"Recent developments in systems biology and metabolic engineering of plant–microbe interactions*", Frontiers in Plant Science, 7, 1421*.https://doi.org/10.3389/fpls.2016.01421

Kuroda, A.,(2006),"A polyphosphate-lon protease complex in the adaptation of *Escherichia coli* to amino acid starvation",Bioscience, Biotechnology and Biochemistry, 70(2), 325–331. https://doi.org/10.1271/bbb.70.325

Kuroda, A., Nomura, K., Ohtomo, R., Kato, J., Ikeda, T., Takiguchi, N., Ohtake, H., & Kornberg, A.,(2001),"Role of inorganic polyphosphate in promoting ribosomal protein degradation by the Lon protease in *E. coli*",Science, 293(5530), 705–708. https://doi.org/10.1126/science.1061315

Kusano, S., & Ishihama, A.,(1997),"Functional interaction of *Escherichia coli* RNA polymerase with inorganic polyphosphate",Genes to Cells, 2(7), 433–441. https://doi.org/10.1046/j.1365-2443.1997.13203301320330.x

Lacour, S., & Landini, P.,(2004),"σS-dependent gene expression at the onset of stationary phase in Escherichia coli: Function of σS-dependent genes and identification of their promoter sequences",Journal of Bacteriology, 186(21), 7186–7195. https://doi.org/10.1128/JB.186.21.7186-7195.2004

Lejeune, C., Sago, L., Cornu, D., Redeker, V., & Virolle, M. J.,(2022),"A Proteomic Analysis Indicates That Oxidative Stress Is the Common Feature Triggering Antibiotic Production in Streptomyces coelicolor and in the pptA Mutant of Streptomyces lividans",Frontiers in Microbiology, 12, 1–19. https://doi.org/10.3389/fmicb.2021.813993

Livak, K. J., & Schmittgen, T. D.,(2001),"Analysis of relative gene expression data using real-time quantitative PCR and the 2-ΔΔCT method",Methods, 25(4), 402–408. https://doi.org/10.1006/meth.2001.1262

Macneil, D. J., Gewain, K. M., Ruby, C. L., Dezeny, G., Gibbons, P. H., & Maeneil, T.,(1992),"Analysis of Streptomyces avermitilis genes required for avermectin biosynthesis utilizing a novel inte-gration vector (Recombinant DNA; polyketide; recombination; thiostrepton resistance; fermentation; restriction)", Gene, 111(1), 61-8. https://doi.org/10.1016/0378-1119(92)90603-M

Maisonneuve, E., & Gerdes, K.,(2014),"Molecular mechanisms underlying bacterial persisters", Cell, 157(3),539-48. https://doi.org/10.1016/j.cell.2014.02.050

Malpartida, F., & Hopwood, D. A.,(1986),"Physical and genetic characterisation of the gene cluster for the antibiotic actinorhodin in *Streptomyces coeIicolor* A3(2)" ,Mol Gen Genet, 205(1), 66-73. doi: 10.1007/BF02428033.

Manteca, Á., & Yagüe, P.,(2018),"Streptomyces differentiation in liquid cultures as a trigger of secondary metabolism", Antibiotics, 7(2), 41. https://doi.org/10.3390/antibiotics7020041

Millan-Oropeza, A., Henry, C., Lejeune, C., David, M., & Virolle, M. J.,(2020),"Expression of genes of the Pho regulon is altered in *Streptomyces coelicolor*",Scientific Reports, 10(1), 1–21. https://doi.org/10.1038/s41598-020-65087-w

Newman, D. J., Cragg, G. M., & Snader, K. M.,(2000),"The influence of natural products upon drug discovery",Natural Product Reports, 17(3), 215–234. https://doi.org/10.1039/a902202c

Nguyen, C. T., Dhakal, D., Pham, V. T. T., Nguyen, H. T., & Sohng, J. K.,(2020),"Recent advances in strategies for activation and discovery/characterization of cryptic biosynthetic gene clusters in streptomyces" ,Microorganisms, 8(4), 616. . https://doi.org/10.3390/microorganisms8040616

Ogawa, N., Tzeng, C.-M., Fraley, C. D., & Kornberg, A.,(2000),"Inorganic Polyphosphate in *Vibrio cholerae*: Genetic, Biochemical, and Physiologic Features",J Bacteriol, 182(23), 6687-93. doi: 10.1128/JB.182.23.6687-6693.2000.

Omnus, D. J., Fink, M. J., Kallazhi, A., Xandri Zaragoza, M., Leppert, A., Landreh, M., & Jonas, K.,(2023),"The heat shock protein LarA activates the Lon protease in response to proteotoxic stress",Nature Communications, 14(1). https://doi.org/10.1038/s41467-023-43385-x

Omura, S., & Shiomi, K.,(2007),"Discovery, chemistry, and chemical biology of microbiol products",Pure and Applied Chemistry, 79(4), 581–591. https://doi.org/10.1351/pac200779040581

Paget, M. S. B., Chamberlin, L., Atrih, A., Foster, S. J., & Buttner, M. J.,(1999),"Evidence that the Extracytoplasmic Function Sigma Factor E Is Required for Normal Cell Wall Structure in *Streptomyces coelicolor* A3(2)",J Bacteriol, 181(1), 204-11. doi: 10.1128/JB.181.1.204-211.1999.

Pérez-Redondo, R., Santamarta, I., Bovenberg, R., Martín, J. F., & Liras, P.,(2010),"The enigmatic lack of glucose utilization in Streptomyces clavuligerus is due to inefficient expression of the glucose permease gene",Microbiology, 156(5), 1527–1537. https://doi.org/10.1099/mic.0.035840-0

Rao, N. N., Liu, S., & Kornberg, A.,(1998),"Inorganic Polyphosphate in Escherichia coli: the Phosphate Regulon and the Stringent Response", Bacteriol, 180(8), 2186-93. doi: 10.1128/JB.180.8.2186-2193.1998.

Rashid, M. H., Rumbaugh, K., Passador, L., Davies, D. G., Hamood, A. N., Iglewski, B. H., & Kornberg, A.,(n.d.),"Polyphosphate kinase is essential for biofilm development, quorum sensing, and virulence of Pseudomonas aeruginosa",Proc Natl Acad Sci U S A, 97(17), 9636-41. doi: 10.1073/pnas.170283397.

Reusch, R. N.,(1989),"Poly-p-hydroxybutyrate/Calcium Polyphosphate Complexes in Eukaryotic Membranes", Proc Soc Exp Biol Med, 191(4), 377-81. doi: 10.3181/00379727-191-42936.

Romero-Rodríguez, A., Maldonado-Carmona, N., Ruiz-Villafán, B., Koirala, N., Rocha, D., & Sánchez, S.,(2018),"Interplay between carbon, nitrogen and phosphate utilization in the control of secondary metabolite production in Streptomyces",Antonie Van Leeuwenhoek, 111(5), 761-781. doi: 10.1007/s10482-018-1073-1.

Serrano, M., Hövel, S., Moran, C. P., Henriques, A. O., & Völker, U.,(2001a),"Forespore-specific transcription of the *lon*B gene during sporulation in Bacillus subtilis",Journal of Bacteriology, 183(10), 2995–3003. https://doi.org/10.1128/JB.183.10.2995-3003.2001

Serrano, M., Hövel, S., Moran, C. P., Henriques, A. O., & Völker, U.,(2001b),"Forespore-specific transcription of the *lonB* gene during sporulation in Bacillus subtilis",Journal of Bacteriology, 183(10), 2995–3003. https://doi.org/10.1128/JB.183.10.2995-3003.2001

Sharma, V., Kaur, R., & Salwan, R.,(2021),"Streptomyces: host for refactoring of diverse bioactive secondary metabolites",3 Biotech, 11(7), 340. https://doi.org/10.1007/s13205-021-02872-y

Shen, F., Sun, R., Yao, J., Li, J., Liu, Q., Price, N. D., Liu, C., & Wang, Z.,(2019),"Optram: In-silico strain design via integrative regulatory-metabolic network modeling",PLoS Computational Biology, 15(3). https://doi.org/10.1371/journal.pcbi.1006835

Shikura, N., Darbon, E., Esnault, C., Deniset-Besseau, A., Xu, D., Lejeune, C., Jacquet, E., Nhiri, N., Sago, L., Cornu, D., Werten, S., Martel, C., & Virolle, M. J.,(2021),"The phosin ppta plays a negative role in the regulation of antibiotic production in streptomyces lividans",Antibiotics, 10(3). https://doi.org/10.3390/antibiotics10030325

Sivapragasam, S., & Grove, A.,(2019),"The link between purine metabolism and production of antibiotics in streptomyces",Antibiotics, 8(2). https://doi.org/10.3390/antibiotics8020076

Stirrett, K., Denoya, C., & Westpheling, J.,(2009),"Branched-chain amino acid catabolism provides precursors for the Type II polyketide antibiotic, actinorhodin, via pathways that are nutrient dependent",Journal of Industrial Microbiology and Biotechnology, *36*(1), 129–137. https://doi.org/10.1007/s10295-008-0480-0

Sulheim, S., Kumelj, T., van Dissel, D., Salehzadeh-Yazdi, A., Du, C., van Wezel, G. P., Nieselt, K., Almaas, E., Wentzel, A., & Kerkhoven, E. J.,(2020),"Enzyme-Constrained Models and Omics Analysis of Streptomyces coelicolor Reveal Metabolic Changes that

Enhance Heterologous Production",IScience, 23(9). https://doi.org/10.1016/j.isci.2020.101525

Sulheim, S., Wentzel, A., & Almaas, E.,(2019),"*Predicting Strain Engineering Strategies Using iKS1317 : A Genome-Scale Metabolic Model of Streptomyces coelicolor"*, Biotechnology Journal, 1–10. https://doi.org/10.1002/biot.201800180

Taverna, P., & Sedgwick, B.,(1996),"Generation of an endogenous DNA-methylating agent by nitrosation in Escherichia coli",Journal of Bacteriology, 178(17), 5105–5111. https://doi.org/10.1128/jb.178.17.5105-5111.1996

Traxler, M. F., Summers, S. M., Nguyen, H. T., Zacharia, V. M., Hightower, G. A., Smith, J. T., & Conway, T.,(2008),"The global, ppGpp-mediated stringent response to amino acid starvation in Escherichia coli",Molecular Microbiology, 68(5), 1128–1148. https://doi.org/10.1111/j.1365-2958.2008.06229.x

Tsigkinopoulou, A., Hawari, A., Uttley, M., & Breitling, R.,(2018),"Defining informative priors for ensemble modeling in systems biology",Nature Protocols, 13(11), 2643–2663. https://doi.org/10.1038/s41596-018-0056-z

Tunca, S., Barreiro, C., Sola-Landa, A., Coque, J. J. R., & Martín, J. F.,(2007),"Transcriptional regulation of the desferrioxamine gene cluster of Streptomyces coelicolor is mediated by binding of DmdR1 to an iron box in the promoter of the desA gene",FEBS Journal, 274(4), 1110–1122. https://doi.org/10.1111/j.1742-4658.2007.05662.x

Virolle, M. J.,(2020),"A challenging view: Antibiotics play a role in the regulation of the energetic metabolism of the producing bacteria",Antibiotics, 9(2), 7–12. https://doi.org/10.3390/antibiotics9020083

Wainwright, M.,(1991),"Streptomycin: Discovery and Resultant Controversy", Hist Philos Life Sci, 13(1), 97-124.

Wang, H., Marcišauskas, S., Sánchez, B. J., Domenzain, I., Hermansson, D., Agren, R., Nielsen, J., & Kerkhoven, E. J.,(2018a),"RAVEN 2.0: A versatile toolbox for metabolic network reconstruction and a case study on Streptomyces coelicolor",PLoS Computational Biology, 14(10). https://doi.org/10.1371/journal.pcbi.1006541

Wang, H., Marcišauskas, S., Sánchez, B. J., Domenzain, I., Hermansson, D., Agren, R., Nielsen, J., & Kerkhoven, E. J.,(2018b),"RAVEN 2.0: A versatile toolbox for metabolic network reconstruction and a case study on Streptomyces coelicolor",PLoS Computational Biology, 14(10). https://doi.org/10.1371/journal.pcbi.1006541

Wentzel, A., Sletta, H., Consortium, S., Ellingsen, T. E., & Bruheim, P.,(2012),"Intracellular metabolite pool changes in response to nutrient depletion induced metabolic switching in Streptomyces coelicolor",Metabolites, 2(1), 178–194. https://doi.org/10.3390/metabo2010178

Xia, H., Zhan, X., Mao, X. M., & Li, Y. Q.,(2020),"The regulatory cascades of antibiotic production in Streptomyces",World J Microbiol Biotechnol, 36(1), 13. https://doi.org/10.1007/s11274-019-2789-4

Yalim Camci, I., Doruk, T., Avican, Ü., & Tunca Gedik, S.,(2012),"Deletion of polyphosphate kinase gene (ppk) has a stimulatory effect on actinorhodin production by streptomyces coelicolor A3(2)",Turkish Journal of Biology, 36(4), 373–380. https://doi.org/10.3906/biy-1110-19

Yan, Y., & Xia, H.,(2024),"The roles of SARP family regulators involved in secondary metabolism in Streptomyces",Front Microbiol, 15, 1368809. . https://doi.org/10.3389/fmicb.2024.1368809

Yang, L., Garcia Canaveras, J. C., Chen, Z., Wang, L., Liang, L., Jang, C., Mayr, J. A., Zhang, Z., Ghergurovich, J. M., Zhan, L., Joshi, S., Hu, Z., McReynolds, M. R., Su, X., White, E., Morscher, R. J., & Rabinowitz, J. D.,(2020),"Serine Catabolism Feeds NADH when Respiration Is Impaired",Cell Metabolism, 31(4), 809-821.e6. https://doi.org/10.1016/j.cmet.2020.02.017

Zambrano, M. M., & Kolter, R.,(1993),"Escherichia coli mutants lacking NADH dehydrogenase I have a competitive disadvantage in stationary phase",Journal of Bacteriology, 175(17), 5642–5647. https://doi.org/10.1128/jb.175.17.5642-5647.1993

Zhang, H., Ishige, K., & Kornberg, A.,(2002),"A polyphosphate kinase (PPK2) widely conserved in bacteria", Proceedings of the National Academy of Sciences of the United States of America, 99(26), 16678-16683.www.pnas.orgcgidoi10.1073pnas.262655199

BIOGRAPHY

Nagihan GENEL She completed her undergraduate education in 2017 at Gebze Technical University, Faculty of Basic Sciences, Department of Molecular Biology and Genetics. In 2019, she commenced her doctoral education at Gebze Technical University, under the supervision of Prof. Dr. Sedef TUNCA GEDIK.

PUBLICATIONS AND PRESENTATIONS FROM THE THESIS

Genel, N., & Tunca, S. (2024), “Combined effect of polyphosphate kinase and lon protease in *Streptomyces coelicolor* A3(2) antibiotic production”, Archives of Microbiology, 206 (10).

APPENDICES

APPENDIX-A: PRESENTATIONS FROM THE THESIS

1st International Congress on Biotech Solutions for Sustainability

Poster Title: Elucidation of The Network Between Stringent Response-Related Proteins and Antibiotic Production in *Streptomyces Coelicolor* A3(2) Through *in silico* and *in vitro* Studies

Poster Title: Heterologous Expression of Streptomycın Resistance Gene in *Streptomyces Coelicolor* A3(2) Caused Metabolic Change

APPENDIX-B: PATENTS

Title: Unique Method To Trigger ***** Productıon In *Streptomyces Coelicolor* A3(2)**.** International Application No. PCT/TR2023/****45, filed on September 12, 2023.